MODELLING ABOVE-GROUND CARBON STOCK OF TREES IN AGRO-ECOSYSTEM AND FOREST RESERVE UNDER REDD+ MECHANISMS

BEATRICE ASENSO BARNIEH

March, 2015

SUPERVISORS:
Ir. L. Van Leeuwen
Prof. A. Duker
Dr.T.A. Groen

MODELLING ABOVE-GROUND CARBON STOCK OF TREES IN AGRO-ECOSYSTEM AND FOREST RESERVE UNDER REDD+ MECHANISMS

BEATRICE ASENSO BARNIEH

Kumasi-Ghana, March, 2015

SUPERVISORS:
Ir. L. Van Leeuwen
Prof. A. Duker
Dr.T.A Groen

THESIS ASSESSMENT BOARD:
Dr. Y. A. Hussin (Chair)
Dr. B. Kumi-Boateng (External Examiner, KNUST)

ABSTRACT

Ghana is at the "readiness stage" of REDD+ project implementation. REDD+ mechanisms may affect agriculture in Ghana because, agriculture is one of the major drivers of deforestation and the main occupation in Ghana. Many scientists are of the view that, agricultural systems which conserve trees in the farms and incorporate tree planting fall within the REDD+ mechanisms of conservation, sustainable management of trees and carbon stock enhancement, and therefore farmers who practice such systems have to be compensated. However, in Ghana, farmers are not compensated when they conserve trees on their farmlands. As a result, some of the farmers deliberately fell matured trees from their farmlands, leading to a serious impact on the carbon stock of trees. Though the REDD+ mechanisms may offer an economic breakthrough for the farmers, the carbon stock potential of trees, a major requirement for the carbon financial credit has not been substantiated. Methods to monitor, report and verify (MRV) the changes in the carbon stock of trees, are usually not well developed. The aim of this research was to develop a method from Remote Sensing and Geographical Information Science techniques in combination with field measurements, to improve on a carbon stock simulation model, developed for Goaso Forest District and use the model to project the changes in the above-ground carbon stock of trees into the future, under Business as Usual (BAU) scenario, whereby the farmers expand their farms and fell trees from the Forest District, and a scenario whereby they are offered incentives to conserve the trees (REDD+). The deforestation rate and the effect of environmental drivers on deforestation and consequently on the carbon stock model were also analysed. The results indicated that, an annual net deforestation rate of 3% was recorded in Goaso Forest District from 2000-2012. The environmental drivers (elevation, distance to protected areas, roads, streams and towns) investigated in this research were all found to exhibit a significant effect on deforestation and consequently carbon stock, except the effect of distance to the protected areas, which recorded an insignificant effect on deforestation. The general trend was that, nearby distances favoured deforestation, whilst faraway distances inhibited it. The only exception from this trend was distance to town which was found to favour and exacerbate more deforestation in faraway distances. The research estimated that, the above-ground carbon (AGC) stock in Goaso agro-ecosystem is about 28.0 tons /hectare, out of the total AGC stock of 54.5 tons/hectare estimated for the whole Forest District. Signifying that, without the carbon stock in the agro-ecosystem, there would be only 26.5 tons of AGC stock per hectare in the Forest District. This demonstrates the importance of the AGC stock of trees in the agro-ecosystem to the Forest District. The carbon stock model also projected about 44.3 % decrease in the total AGC stock in the future under BAU scenario from 2001 to 2025 and a decrease of 16.4 % from 2015 to 2025 under BAU scenario as compared to 9.2 % and 1.4% decline in the forest carbon pool under REDD+ scenarios whereby the annual net deforestation rates were assumed to be reduced to 2% and 1% respectively. In contrast, the model predicted about 7% gain in the forest carbon pool from 2015-2025 under the REDD+ scenario with an assumption that there will be no deforestation but other conversions will continue. The conclusion from the research was that, both the agro-ecosystem and the forest reserve in Goaso Forest District have carbon stock potentials. Thus, the conservation of trees under REDD+ will lead to an increase in future AGC stock of trees in the Forest District. The AGC stock model was also seen as a major improvement on the existing model because, the average uncertainty in tons per hectare for the simulation over 25 years was very low (0.10 tons / hectare) as compared to the average uncertainty in tons per hectare (95.71 tons/hectare) for 12 years simulation recorded by the existing model.

Keywords: Forest, Carbon Stock, Modelling, REDD+, Agro-Ecosystem, Segmentation

Dedicated

To

Kobina Arko

And

Dr. James Asenso Barnieh

ACKNOWLEDGEMENTS

TABLE OF CONTENTS

LIST OF FIGURES

LIST OF TABLES

LIST OF EQUATIONS

LIST OF APPENDICES

LIST OF ACRONYMS

Acronyms	Meaning
AGB	Above-Ground Biomass
AGC	Above-Ground Carbon
BAU	Business as Usual
CPA	Crown Projection Area
DBH	Diameter at Breast Height
E/W	East/West
EGO	Environment for Geo-processing Objects
ESP	Estimation of a scale Parameter
FAO	Food and Agricultural Organization
GFD	Goaso Forest District
GIS	Geographical Information Science
GPS	Geographic Positioning System
GS	Gramm-Schmidt
HCS	Hyper-spherical Colour Sharpening
HIS	Intensity Hue and Saturation
HPF	High Pass Filter
IPCC	International Panel Conversion on Climate Change
ITC	Faculty of Geo-Information Science and Earth Observation
LAI	Leaf Area Index
LV	Local Variance
MRV	Monitoring, Reporting and Verification
N/S	North/South
NIR	Near Infra-Red
PCA	Principal Components Analysis
REDD+	Reduced Emissions due to Deforestation and Forest Degradation
ROC_LV	Rate of Change of Local Variance
R-PP	Readiness Preparation Proposal
RS	Remote Sensing
UNFCCC	United Nations' Framework Convention on Climate Change
UTM	Universal Transverse Mercator
VHR	Very High Resolution
WGS	World Geographical System

1. INTRODUCTION

1.1. Background

The interest in the world's forest has grown over the years, not because of the basic ecosystem services (food, shelter, water) it provides, but in response to the increasing awareness of the role it plays in the global carbon cycle. According to FAO (2010), healthy trees in the forest sequestrate about 289 Giga tons of carbon in their biomass. The assertion is that, sustainable management of forest through replanting and rehabilitation may increase carbon sequestration world-wide. Nevertheless, about 7.3 million hectares of the world's forests are destroyed by deforestation every year. Deforestation accounts for about 20% of the global greenhouse gas emissions (UN-REDD, 2009).

Reducing emissions from deforestation and forest degradation (REDD⁺) is recognized as a cost effective way of mitigating greenhouse gas emissions (UN-REDD, 2009). Against this background, the United Nations Framework Convention on Climate Change (UNFCCC), set up REDD⁺ to mitigate climate change by reducing carbon emissions due to deforestation and degradation in many countries (UN-REDD, 2009). However, the REDD⁺ mechanisms may indirectly affect agriculture, since agricultural expansion is one of the major drivers of deforestation and a major occupation in many countries (Gibbs et al., 2007; Houghton, 2005; Olander et al., 2012).

According to Horowitz (2010), agricultural systems, which incorporate tree planting or conservation fall within the REDD⁺ mechanisms of conservation, sustainable management of trees and carbon stock enhancement. Yet, conservation of trees is not attractive to small holder farmers because, the process of conservation does not translate into short term rise in income and social welfare (Gelens et al., 2010). Takimoto et al. (2008) emphasized that, without incentives and legal ownership rights, offering any part of the limited land for conservation, afforestation and reforestation will not be an option in many countries. Antle (2002) and Jindal et al.(2012) are also of the view that, farmers who conserve or plant trees on their farmlands need to be compensated. Since this may reduce the income they generate from food production which is their main source of livelihood.

Nonetheless, farmers in Ghana for example, are not compensated or offered any kind of incentives from legal logging of trees on their farmlands by the government. In view of this, some farmers deliberately engage the services of chainsaw operators to illegally fell matured trees from their farmlands or use fire or "ring barking" to gradually remove the trees to avoid and minimize damages as well as trees competition with their crops (Gelens et al., 2010). Though, the REDD⁺ carbon financial incentives, may help small holder farmers who conserve trees on their farmlands to achieve financial independence, many countries (Funder, 2009), including Ghana, do not have the technological capacity (methods, software programs, satellite data, technical experts), to ensure that these small holder farmers benefit from the REDD⁺ carbon financial credit (Ghana REDD⁺ R-PP, 2010). It is obvious that, the conservation of trees under REDD⁺ mechanisms may lead to an accrued gain in carbon stock in the future, but the amount or how much is not known. According to Qureshi et al. (2012), correct assessment of the amount of carbon stock in trees may help REDD⁺ member countries to identify and target priority areas of management intervention and farmers to also benefit from the carbon financial credit.

Ghana is among the member countries preparing the grounds to implement the REDD+ mechanisms. The country's "readiness preparation proposal (R-PP)" to benefit from the REDD+ carbon financial incentive was accepted in 2010. The R-PP is a starting point in the REDD+ capacity building, and presents a comprehensive overview of the current situation, the challenges and the steps towards the national REDD+ strategy development. The challenge for Ghana now is the identification of REDD+ priority areas, monitoring, reporting, and verification (MRV) of changes in carbon stock under different scenarios. It is explicit in the R-PP that, the country requires technical capacity building (methods, software programs, VHR satellite data, human resources and so on) to be able to monitor, report and verify the amount of carbon stock in trees (Ghana REDD+ R-PP, 2010).

In order for farmers to be considered for REDD+ carbon financial incentives, the contribution of trees in the agro-ecosystem to the country's carbon pool must be monitored, reported, verified and included in the estimates from the forest reserve because, the REDD+ member countries are only eligible for carbon credit payment, following an accurate carbon stock monitoring, reporting as well as verification (MRV) of the reduced emissions (Ghana REDD+ R-PP, 2010). Therefore, a method for assessing and modelling the current and future carbon stock of trees in both the forest reserve and the agro-ecosystem (off-forest reserve) in the country under different scenarios is crucial to unravel the amount of AGC stock being lost through deforestation.

1.2.   Guidelines for carbon stock measurement and reporting

The International Panel Conversion on Climate Change IPCC (2003), Good Practice Guidance for Land Use, Land Use Change and Forestry Inventory Methods, for carbon emissions reporting, highlighted on the possible carbon pools to be measured for carbon emissions reporting under REDD+, namely; above-ground biomass (AGB), below-ground biomass, dead wood, litter and soil carbon. It is proposed that, only the carbon pools which are continuously changing and can be monitored cost effectively must be measured. Carbon pool from AGB of trees (AGC) is an example of carbon stock which is continuously changing, highly affected by deforestation and can be measured cost effectively as compared to the other carbon pools. AGC also accounts for the largest carbon pool (60-90%) of the total carbon stock estimated from trees. Furthermore, reduction in carbon emissions from other pools such as litter, soil and so on, have not yet been considered for carbon financial incentives under REDD+ (CIFOR, 2009).

The IPCC's guidance permits forest carbon stock inventories at different levels of complexities, often referred to as "tiers". Three main tiers are proposed for carbon inventories and reporting under REDD+. The tier one uses carbon stock default values provided at the continental scale, which is stratified by the ecological biome with a very high level of uncertainty. The tier two, uses some country specific data from a look up table for the assessment of the carbon stock dynamics. The uncertainty associated with this tier is high to medium. The tier three on the other hand, uses advanced methods and detailed country specific data including national inventories, measurement systems repeated through time with low uncertainty level. Generally, inventories with higher tiers are more accurate and less uncertain (IPCC, 2003).

Two approaches are available under the tier3. One option is to create two carbon maps for two different years and estimate the differences between the two carbon maps or compare the two carbon maps over time. This approach is only feasible when historical data on carbon stock estimates are available for the past years. Another option is to combine land cover change maps over a period of time with carbon stock maps or carbon stock estimates. This means that, the tier three requires Remote Sensing (RS) and Geographical Information Science (GIS) techniques in order to be able to estimate changes in AGC stock. According to Rossillo-Calle et al. (2007), electromagnetic response from RS image can be combined with structural parameters from trees for AGC stock estimation. The approach has been more successful in boreal and

temperate forests and in "young stands" with less density of biomass (Rosenqvist et al., 2003), but has not been more promising in the tropical areas due to the complex ecosystem (canopy structure), which causes the RS signals to be saturated. Also, the use of optical RS in the tropics is limited by cloud cover.

However, current methods such as Radar System can penetrate through clouds and can operate both day and night (Asner, 2001). According to Leckie et al. (2003), the invention of VHR satellites, such as IKONOS, Quick Bird, OrbView-3, GeoEye and Worldview-1 and 2 have offered the opportunity to extract very detailed information at the individual tree level. This has offered more hope for extraction of forest parameters for accurate AGC stock estimation. VHR imageries facilitate individual tree crown delineation, species identification, estimation of crown density and forest stand polygon delineation. Worldview-2 for instance, has high spectral diversity. Its new bands; Red Edge, NIR1, NIR2 can be used to identify trees in the tropics even at the specie level. Many segmentation algorithms and software programs (e.g. eCognition) for Object based Analysis (OBIA) are now available for extraction of biophysical parameters from trees.

1.3.   Approaches to monitor changes in AGC stock at the national level

Monitoring changes in AGC stock repeatedly at the national level, requires deforestation rates, estimated from land cover maps of different years to be combined with AGC stock estimates. It is often recommended that, the deforestation rate (land cover change rate) is estimated from the same strata from which the carbon stock sampling was done, by employing "wall to wall" mapping or by targeting sampling using the same stratified sampling method as the carbon stock. The major strength of this approach is that, it offers the opportunity for carbon stock estimates to be used to model emissions in the past, present and the future (Gibbs et al., 2007). RS approach can be used to assess and estimate land cover changes due to deforestation (deforestation rate). Deforestation rate estimated from RS satellite data has been found to be more reliable, consistent and more accurate than the rates estimated from census data (Houghton, 2005). Nonetheless, it was argued by Houghton (2005) that, this method has not been used often in the tropics.

According to Gibbs et al. (2007), RS methods alone may not be able to model changes in carbon stock and therefore it must be combined with process models. Process models can map deforestation risk areas in addition to carbon value quantification. They offer the opportunity to establish a link between drivers and the rate of deforestation. Aguilar-Amuchastegui and Forrest (2013) noted that, it is possible to simulate and compare multiple land use scenarios with models and re-run the scenarios again with respect to changes in drivers. Modelling under different scenario facilitates creative ways of thinking that enables stakeholders to modify established patterns of assessing situations and future planning actions in order to ensure that, they are in the best position to cope with the future as in the case of tropical forest with forest fringe communities (Wollenberg et al., 2000).

Schoemaker (1993), explained that, scenarios are more suitable when uncertainties are high as in the case of carbon stock estimation. Several land use change models are now available and they have provided opportunities to develop a scenario and project the future role of land cover change in earth system functioning. According to Veldkamp and Lambin (2001), a land use change scenario modelling, done in a "spatially–explicit integrated and multi-scale manner", serves as a technique for projecting alternative scenarios into the future and to also undertake experiments that increase our understandings of the major processes in land use changes. A mentioned was made to the fact that, part of the complexities in the land use system can be represented by land use change models to allow testing of the sensitivity of land use patterns to changes in the variables under study. Veldkamp and Lambin (2001) stressed that, through scenario building, the robustness of the integrated socio-ecological systems can be tested.

Two main scenarios are vital under the carbon compliance market. Business as Usual (BAU) assumes that, historical trends continue in to the future in the absence of policy intervention and socio-economic changes. Interventional or Management scenario, assumes that historical trends are intervened to alter the rate or pattern of change. Examples of such Interventional scenarios are: REDD⁺ Projects, Forest Investment Programme, Carbon Voluntary Markets, Policy Changes, Land Use Intensification Programmes, Cultural Practices and so on (Mckenzie et al., 2012).

Many tools are available for modelling carbon stocks of trees under REDD⁺ mechanisms. Examples of such tools are: Land Use Change Modeller, Dinamica EGO, GEOMOD, MAXENT, Clue S, Invest Scenario Generator, AFOLU Carbon Calculator and many more. Aguilar-Amuchastegui and Forrest (2013) gave an overview of the various tools and how they are operated as well as their pros and cons. Among the software programs which are freely available, Dinamica EGO (Environment for Geo-processing Objects), an open source modelling platform has been found to model future carbon stock under different scenarios more accurately than all the others (Aguilar-Amuchastegui & Forrest, 2013).

1.4.   Research Problem and Justification

Despite the fact that, many studies have stressed on the important roles trees in the agro-ecosystem and the forest reserve may play in mitigating greenhouse gases, the role played by trees in the agro-ecosystem has not received International recognition (Albrecht & Kandji, 2003; Takimoto et al., 2008). This is attributed to the lack of sufficient data on carbon stock dynamics in the agro-ecosystem to support climate change decisions. Specific information on the amount of carbon stock in the agro-ecosystem is often not available in many countries because, the quantification of the carbon stock potential of trees in the agro-ecosystem has not been undertaken (Takimoto et al., 2008). Many of the studies (Baral, 2011; Basuki et al., 2009; Bayat et al., 2012; Samalca et al., 2007; Karna, 2012), conducted to substantiate the carbon stock potential of trees did not include the estimates from the agro-ecosystem in their analysis. This is because, methods to measure carbon stock in the agro-ecosystem are usually not well developed (Takimoto et al., 2008).

Methods for accurate carbon stock assessment and modelling, which takes into an account, the contribution of carbon stock of trees in the agro-ecosystem and the carbon stock estimates of trees in the forest reserve are crucial in Ghana because, according to the Ghana's R-PP, the development of a historically adjusted reference emission scenario in the country is at the embryonic stage. This will involve quantifying historical emissions and removals and then developing future trajectories based on economic development and agricultural scenario data. Also, methods for accurate carbon stock assessment and modelling may provide the requisite information and data required for the implementation of REDD⁺ mechanisms in the country, since REDD⁺ member countries are only eligible for carbon financial credit payment, following an accurate carbon stock monitoring, reporting as well as verification (MRV) of the reduced emissions (Ghana REDD+ R-PP, 2010).

Houghton (2005), highlighted that, a comparison of carbon stock estimates against ground truth data is needed in the tropics for the validation of carbon stock estimates. Nevertheless, ground truth data to validate the contribution of carbon stock of trees in climate change mitigations are few on the global front (Takimoto et al., 2008). Bosetti and Lubowski (2010) mentioned the availability of field data for monitoring and assessment of carbon stock as the main challenge confronting the implementation of REDD⁺ mechanisms in developing countries. Rosenqvist et al. (2003) also stressed that, the establishment of a national carbon stock baseline dataset and the assessment of changes in carbon stock, may provide the information and data needed to fulfil the implicit requirement for carbon stock monitoring under the article 3 of the Kyoto protocol of the UNFCCC. This requires that carbon stock estimates are combined with deforestation rate estimated from land cover maps of different years as well as drivers of deforestation (environmental or

socio-economic variables) to allow the carbon stock estimates to be used to model emissions in the past, present and the future (Gibbs et al., 2007).

According to Maeda et al. (2011), models offer opportunities to simulate land cover changes as well as deforestation rates to discover the underlying causes and determinants of the changes. They emphasized that, models present the platform to anticipate the impact of changes and also to foresee the appropriate measures to control such changes and mitigate the effects. Qureshi et al. (2012) also explained that, correct modelling of carbon stock may help REDD⁺ member countries to identify and target priority areas of management intervention and the farmers to also benefit from the REDD⁺ carbon financial credit.

Over the years, many studies (Maeda et al., 2011; Soares-Filho et al., 2009; Soares-Filho et al., 2007; Soares-Filho et al., 2006; Soares-Filho et al., 2004; Soares-Filho et al., 2003; Soares-filho et al. 2002; Veldkamp & Lambin, 2001) have used models to investigate deforestation so as to understand the drivers and dynamics of forest conversion into other land uses and the environmental side-effect associated with them. Dinamica Ego software program is among the various spatial model software programs which have been used over the years to model the future scenarios (Maeda et al., 2011; Soares-filho et al., 2002; Soares-Filho et al., 2009). The aforementioned authors all dwelled on Remote Sensing (RS) and Geographical Information Science (GIS) applications in combination with field measurements (ground truth data) to facilitate modelling under different scenarios.

Though, RS and GIS techniques are appropriate for estimating AGC stock in inaccessible areas (Gibbs et al., 2007), not many studies have focused on this in Ghana. In a situation whereby RS and GIS applications have been used to study the land use systems in Ghana, the focus has always been on the forest reserve only, even though the agro-ecosystem (off-forest reserve) constitutes a greater part (70%) of the forest pool in Ghana (Bih, 2006). An attempt to use RS and GIS applications in Goaso focused on land use change detection and tree density measurement. This study, which was undertaken by Gelens et al. (2010) under the auspices of the Tropenbos International Ghana Programme was able to map and detect changes in the various land cover types using RS and GIS applications in combination with field measurements.

However, the study did not look into the carbon stock modelling in the whole Forest District [forest reserve and the agro-ecosystem] (Gelens et al., 2010). In 2012, Mutanga estimated the carbon stock of trees on farmlands in Ejisu Juabeng District of Ghana, but did not ascertain the amount of carbon stock which was available in the past and the expected amount in the future as required by the REDD⁺ mechanisms (Mutanga, 2012). Carbon stock dynamic model, which can model past and future changes in carbon stock under different scenarios and satisfies the requirement of the "Good Practice for Monitoring, Reporting and Verification (MRV)" for REDD⁺ is required in Ghana (Ghana REDD⁺ R-PP, 2010).

Therefore, this research improved on an unpublished method for modelling past and future carbon stock of trees under different scenarios, developed for Goaso Forest District. This method, which was developed by Groen (Personal Communication, 2014), used the tier 1 of the IPCC (2003), Good Practice Guidance for AGC stock reporting. But the uncertainty surrounding this tier, is very high. However, Ghana has indicated in the REDD⁺ readiness proposal to use at least the tier two in carbon emissions reporting (Ghana REDD⁺ R-PP, 2010). Therefore, the model was improved by using the IPCC tier3 (IPCC, 2003). Historical data on AGC estimates are not available in Ghana and hence the option one of the tier 3 was not feasible. Landsat-7 (2000-2012) imageries and WorldView-2 image were available for the adoption of the option 2 of the IPCC tier 3. These data facilitated the current AGC stock assessment and future modelling under BAU scenario, whereby deforestation continues into the future and REDD⁺ scenario, whereby farmers are offered financial incentives to halt deforestation and conserve trees. Ground truth AGC stock estimate of trees in the agro-ecosystem was also included in the analysis of the current AGC stock estimates for the

whole study area (forest reserve and the agro-ecosystem) because, this may serve as a basis for small holder farmers to be considered for REDD+ carbon financial incentives.

The model improvement was implemented by harnessing on the pixel based land cover classification ability of ARCGIS software program (Bakker et al., 2009), carbon stock estimation ability of the eCognition software program (Definiens, 2009; Leckie et al., 2003) and the heuristic ability of the Dinamica EGO software program (Soares-Filho et al., 2009). The research was undertaken in Goaso Forest District (GFD) because, the model developed by Groen was based on this Forest District. It is also one of the potential high forest zones in Ghana, which can serve as a priority area for REDD+ pilot project implementation due to the dramatic agricultural expansion in the District. The new developments in the Forest District, mentioned earlier, made it a representative area and also a very good case for this research (Gelens et al., 2010).

1.5.   Main Objective

To assess the current AGC stock in woody biomass and improve on a method for modelling future changes in the AGC stock based on two scenarios (BAU and REDD+).

1.5.1.   Specific Objectives

1.   To estimate the AGC stock of trees per hectare from VHR satellite image in the whole GFD and only the agro-ecosystem.

2.   To estimate the annual net deforestation/change rate from 2000-2012 in GFD.

3.   To analyze the effect of drivers (explanatory/environmental variables) on deforestation and consequently carbon stock in GFD.

4.   To model the effect of the BAU and REDD+ scenarios on the future AGC stock.

1.6.   Research Questions

1.   What are the AGC stock estimates of trees per hectare in the whole GFD and the agro-ecosystem only?

2.   What are the annual deforestation/change rates from 2000-2012 in GFD?

3.   What are the effects of the drivers (explanatory/environmental variables) in GFD on deforestation and consequently carbon stock?

4.   What are the expected effects of the BAU and REDD+ scenarios on the future AGC stock in GFD?

2. LITERATURE REVIEW

2.1. Definitions

2.1.1. Forest Land

Forest land is categorized by FRA (2010), as all land with woody vegetation, covering more than 0.5 hectares, with tree height higher than 5m, and a canopy cover more than 10% or the trees are capable of reaching these threshold "in situ". Land predominantly under agricultural activities and urban land use are not included.

2.1.2. Canopy Cover/ Crown Projection Area (CPA)

Canopy cover is defined by FRA (2010) as the percentage of ground, covered by vertical projection of the outermost perimeter of the natural spread of the foliage of plants which cannot exceed 100%. It is calculated by measuring the maximum crown diameter assuming a circular crown projection (Kuuluvainen, 1991).

2.1.3. Deforestation

IPCC (2006) defines deforestation as "the direct human-induced conversion of forested land to non-forested land".

2.1.4. Cropland

According to IPCC (2003), cropland is characterised by arable and tillage land and agroforestry system whereby, vegetation falls below the threshold for forest classification which is consistent with the selection of national definition.

2.1.5. Fallow land

Fallow land is an uncultivated land capable of regenerating into forest land. A land must be uncultivated for many years, between 6-10 years before it can be classified as a fallow land (Gelens et al., 2010).

2.1.6. Above-ground biomass

Above-ground biomass (AGB) is defined as all living biomass above the soil, including stems, foliage, branches, stumps, barks and seeds. About 45%-50% of AGB is equivalent to the above-ground carbon (AGC). Biomass of living roots are classified as below-ground biomass (FRA, 2010).

2.1.7. Allometric equations

According to Kettering et al. (2001), allometric equations are the quantitative relationship between measurable tree variables like DBH and height to other variables, which are too difficult to be assessed such as above-ground biomass, above-ground carbon, and standing volume and so on. Brown (2002) established that the relationship between an allometric equation and measured DBH can provide a reliable estimate of the total biomass for broad range of forest categories and ecological zones.

2.1.8. Uncertainties in carbon stock estimates

Uncertainties in carbon estimates refer to the inaccuracies and errors involved in carbon stock estimation. This is estimated by calculating the mean of the carbon estimate, plus or minus two standard deviation away from the mean (IPCC, 2003).

2.2. REDD[+] mechanisms

The United Nations' Framework Convention on Climate Change (UNFCCC), endorsement of the forest rich countries call, to include economic incentives in the Kyoto Protocol, marked the genesis of REDD[+] mechanisms in many countries. The REDD[+] mechanisms are aimed at offering financial incentives to motivate countries to freely reduce national deforestation rates and associated carbon emissions below a baseline, be it historical or future. Countries can therefore trade their emissions reduction for carbon credit on the International Market. It is expected that, the reduction in carbon emissions due to deforestation and forest degradation may lead to climate change mitigation, conservation of biodiversity, and protection of ecosystem services and goods (Gibbs et al., 2007; Olander et al., 2012).

2.3. Approaches for above-ground biomass and carbon stock measurement

A myriad of approaches and data sources are available for AGB and AGC stock measurements. According to IPCC (2003), AGC= 0.47*(AGB). A cursory review of literature shows that, the methods for the AGB estimation can be categorized based on the sources of data used (Lu, 2006). AGB estimation from field measurement may involve destructive sampling or direct measurements and the use of allometric equations (Jia & Akiyama, 2005; Liddell et al., 2007; Miksys et al., 2007). Though, destructive sampling may improve the accuracy of the forest carbon stock estimation, it may be expensive and time consuming over a large areas (Gibbs et al., 2007).

Allometric equation on the other hand, uses regression relationship between measured destructive harvest sample and an independent variables such as diameter at breast height (DBH), crown diameter, tree height and tree density to estimate forest AGB (Fehrmann & Kleinn, 2006; Muukkonen & Heiskanen, 2007). Chave et al. (2005) and Brown (2002) indicated that, DBH alone may account for about 95% of the variation in AGB and hence it is not worthwhile to use specie specific allometric equations for AGB estimation. They stressed that; generalised allometric equations may be effective in tropical forest AGB estimation, provided the ecological zones and the forest types are taken into consideration.

However, they cautioned that, estimates from allometric equations must be validated with sampling of 2 to 3 large trees especially, in Africa where there are limited ground based dataset for developing allometric equations. AGB is therefore estimated from allometric equation by applying an expansion factor to extrapolate the results over a large area. In some instances, correlations between AGB and look-up tables are coupled to estimate AGB in other pools (Gibbs et al., 2007). According to Houghton et al. (2001), 20% of the forest AGB is equivalent to root biomass. Likewise, AGB in dead wood or litter has been found to be equivalent to 10-20% of AGB in matured forest.

RS data can also offer opportunities for forest AGB measurement. It is seen as an alternative to the traditional methods for estimating biomass or changes in carbon stock. RS approach has gained an International recognition due to its capacity to clearly capture spatial information and the possibility of allowing monitoring and evaluation of carbon stock to be repeated in areas which are inaccessible and also in a cost effective manner. However, RS instruments are unable to measure carbon stock directly and therefore ground based data are needed in addition to RS data. Over the years, research focus has been directed towards the development of relationship between structural parameters such as tree height, DBH, CPA, basal area, biomass and many other parameters extracted from trees in the forest or plantation and the electromagnetic response from RS image (Rossillo - Calle et al., 2007).

Recent global scale mapping relies on multi-spectral optical RS data. Optical RS is a passive sensing system, which uses the visible and near-infrared reflectance from solar radiation reflected from the earth surface. Optical remote sensors can relate field measurements of AGB to the observation from satellite sensitivity of the optical reflectance and canopy structure variations (Goetz et al., 2009). In many cases, biomass is

estimated by using a direct relationship between spectral response and multiple regression analysis (Roy & Ravan, 1996). K nearest neighbour (Tomppo et al., 2002), neural network as well as indirect relationship between parameters extracted from RS data such as leaf area index (LAI), crown closure and height or shadow fractions have also been used to estimate biomass and carbon stock (Feng et al., 2007; Leboeuf et al., 2007; Luther et al., 2006; Suganuma et al., 2006; Zheng et al., 2007). Satellite based RS approach has the strength of providing "wall to wall observation of carbon stock proxies" (Drake et al., 2003).

Information, derived from Synthetic Aperture Radar (SAR), Light Detection and Ranging (LIDAR), Optical and synergetic measurements of multi-sensors can also be combined with ground based measurements for carbon stock estimation (Goetz et al., 2009). The use of RADAR for AGC stock estimation has been fruitful since it operates in the microwave region and therefore can penetrate through clouds (Patenaude et al., 2005). However, this approach is also limited due to data saturation problems in tropical forest (Gibbs et al., 2007). Though, the LIDAR system can estimate carbon stock accurately, it is very expensive and limited in spatial extent (Rosenqvist et al., 2003).

Many options are now available to delineate individual tree crowns from VHR images for carbon stock estimation (Bunting et al., 2010). For instance, the eCognition software program has opened the way for object based information extraction from VHR images (Wei et al., 2005). On top of providing the opportunity to delineate individual tree crowns, VHR images also provide the platform to differentiate the species (Ke et al., 2010). The relationship between CPA and tree diameter at breast height (DBH) has been established (Shimano, 1997). Therefore AGC stock can be estimated from the relationship between CPA and AGC stock estimated from field measured DBH (Muukkonen & Heiskanen, 2007). This approach has been found to improve the accuracy of AGB and AGC stock estimation (Zheng et al., 2004). Table 1, is an overview of the benefits and limitations of the available methods to estimate national level forest carbon stocks as it was put forward by Gibbs et al. (2007).

Table 1: Benefits and limitations of the available methods to estimate national level forest carbon stocks

Method	Description	Benefits	Limitations	Uncertainty
Biome averages	Estimates of average forest carbon stocks for broad forest categories based on a variety of input data sources	• Immediately available at no cost • Data refinements could increase accuracy • Globally consistent	• Fairly generalized • Data sources not properly sampled to describe large areas	High
Forest inventory	Relates ground-based measurements of tree diameters or volume to forest carbon stocks using allometric relationships	• Generic relationships readily available • Low-tech method widely understood • Can be relatively inexpensive as field-labor is largest cost	• Generic relationships not appropriate for all regions • Can be expensive and slow • Challenging to produce globally consistent results	Low
Optical remote sensors	• Uses visible and infrared wavelengths to measure spectral indices and correlate to ground-based forest carbon measurements • Ex: Landsat, MODIS	• Satellite data routinely collected and freely available at global scale • Globally consistent	• Limited ability to develop good models for tropical forests • Spectral indices saturate at relatively low C stocks • Can be technically demanding	High
Very high-res. airborne optical remote sensors	• Uses very high-resolution (~10–20 cm) images to measure tree height and crown area and allometry to estimate carbon stocks • Ex: Aerial photos, 3D digital aerial imagery	• Reduces time and cost of collecting forest inventory data • Reasonable accuracy • Excellent ground verification for deforestation baseline	• Only covers small areas (10 000s ha) • Can be expensive and technically demanding • No allometric relations based on crown area are available	Low to medium
Radar remote sensors	• Uses microwave or radar signal to measure forest vertical structure • Ex: ALOS PALSAR, ERS-1, JERS-1, Envisat)	• Satellite data are generally free • New systems launched in 2005 expected to provide improved data • Can be accurate for young or sparse forest	• Less accurate in complex canopies of mature forests because signal saturates • Mountainous terrain also increases errors • Can be expensive and technically demanding	Medium
Laser remote sensors	• LiDAR uses laser light to estimates forest height/vertical structure • Ex: Carbon 3-D satellite system combines Vegetation canopy LiDAR (VCL) with horizontal imager	• Accurately estimates full spatial variability of forest carbon stocks • Potential for satellite-based system to estimate global forest carbon stocks	• Airplane-mounted sensors only option • Satellite system not yet funded • Requires extensive field data for calibration • Can be expensive and technically demanding	Low to medium

Source: (Gibbs et al., 2007a)

2.4. Pixel based image classification

A process whereby pixels are assigned to "nominal or thematic" classes is termed as pixel based image classification in RS and GIS platforms. In the process of image classification, a multi-band image is inputted into an image classification software program (ARCGIS, ERDAS etc.) which produces a raster cell with a thematic code. The classification relies on different spectral characteristics of different materials of the earth. Five main steps are involved in the image classification process. The first step involves acquisition and processing of RS image to be classified. Followed by the definition of the clusters in the feature space (a graph depicting the feature vectors). Two main approaches (supervised and unsupervised) are employed in the definition of the clusters. The supervised cluster definition approach allows the user to define the clusters during training of sample data. In contrast, unsupervised cluster definition is executed automatically by a clustering algorithm.

After the clusters are defined in the feature space, a classification algorithm (Box classifier, Minimum distance to mean, Maximum likelihood, Interactive classifier, Iso data classifier and so on) is used to assign pixels to classes. The actual classification is then ran by assigning each "multi-band pixel" in the image to a predefined class based on the digital numbers of the pixels leading to a classified image. The quality of the classified image (accuracy assessment) is assessed by a comparison between a reference or ground truth data and image classification results. An error matrix or a confusion matrix is produced as an output (Bakker et al., 2009).

2.5. Object based image analysis in eCognition software program

The emergence of very high resolution satellite images such as WorldView-2 with spatial resolution of less than one metre, Quickbird, Ikonos , Geoeye and many more (Blaschke, 2010), have increased the use of optical satellites systems in many areas (Gibbs et al., 2007). As a result, many techniques have been developed to facilitate the extraction of important features from an image (Blaschke, 2010). Object based Image Analysis (OBIA) technique is now in existence to better extract object features such as Crown Projection Area (CPA) from VHR images since it is impossible to extract such features from pixel based image classification algorithm owing to the fact that, object features of interest are bigger than pixels (Ardila et al., 2011).

According to Ardila et al. (2011), spectral geometric and contextual characteristics of objects are employed by OBIA to generate homogenous objects which provide more information than a single pixel. OBIA has been successful in improving the accuracy of forest biomass estimation. It is now possible to group objects with similar properties in an image with OBIA (Lamonaca et al., 2008). Morales et al. (2008) established that, segmentation techniques are effective in separating tree crowns from objects of similar size and reflectance. Features of trees extracted from image object can be related to ground based field measurements in a regression model for AGB and AGC stock estimation (Gibbs et al., 2007). Many Segmentation algorithms are now available for object based image classification.

2.5.1. Segmentation algorithms

According to Möller et al. (2007), segmentation is a spatial clustering technique, which results in non-overlapping subdivided segments or units. During image segmentation, original image is partitioned into homogenous regions by the process of subdivision, merging and reshaping operation of the image objects (Liu & Yang, 1994). Image segmentation serves as a fundamental and crucial step in object-based image classification, mainly because object-based classification result is influenced by the output of the segmentation process (Gao et al., 2011).

Different segmentation techniques are available and can be categorized either as boundary based/edge based or region based algorithms. Another way of classifying these algorithms is by grouping them as either top-down strategy or bottom-up strategy. Top-down strategy involves cutting bigger objects into smallest pieces. Examples are chessboard, quad tree, contrast filter and contrast split segmentation. Bottom-up strategy on the other hand, involves merging of small pieces to obtain bigger objects based on homogeneity criteria often termed as region based. Multi-resolution segmentation is an example. This algorithm extracts information from the image by grouping similar pixels spatially and spectrally into homogenous areas to produce an image object (Definiens, 2009).

2.5.1.1. Multi-resolution segmentation

Multi-resolution segmentation algorithm in eCognition software program is applied to subdivide an image into non-overlapping segments (Möller et al., 2007). Multi-resolution image segmentation is vital since it is the building block of the object based classification employed in the individual tree crown delineation.

The segmentation permits the identification of homogenous areas to allow grouping of specific objects (Kim et al., 2010). It also necessitates the extraction of information from the image by grouping similar pixels to form homogenous image object (Blaschke, 2010).

Multi-resolution segmentation algorithm reduces the average heterogeneity and increases the homogeneity in a given number of image objects. This is important because, image objects produced by heterogeneous data are smaller than homogeneous data. The homogeneity of the object is influenced by colour, smoothness, shape, and compactness. For instance, the value of the shape field controls the relationship between shape and colour criteria, the colour criteria increases when the shape is decreased (Saha, 2008). This is an indication of how much spectral values of the image layers affect the heterogeneity of the segmented objects.

More spatial uniformity and less spectral uniformity are introduced into the image segments when the value of the shape field is increased. The compactness homogeneity criterion on the other hand is employed when different image objects are compact and can be separated from non-compact objects by weak spectral contrast. A higher value of compactness creates compact segments (Definiens, 2009). The multi-resolution segmentation involves the following steps:

A. Image fusion

According to Pohl and Van Genderen (1998), image fusion which is the combination of two or more different images to form a new image can be grouped into three main levels in RS, namely; pixel data level, feature level and decision level. At the pixel level, fusion of optical image is done to improve spatial resolution, retain the spectral conformity of the original multi-spectral data, and also to enhance the structural and textural details. Zhang (2010) termed this process as pan-sharpening. According to him, pan sharpening is a pixel level fusion technique that combines lower resolution colour pixels with higher resolution panchromatic pixels in order to produce a high resolution colour image. Intensity Hue and Saturation (IHS), Principal Components Analysis (PCA), High Pass Filter (HPF), Gramm-Schmidt (GS) and Watershed Transformation are some of the image fusion techniques which are often used for pan-sharpening.

B. Filtering

Filtering is an image enhancement technique which involves the altering of spatial features of an image (Leica Geosystems, 2011). Filtering is often conducted to enhance the edges of pixels or features (trees) in the scenes before the segmentation process.

C. Estimation of Scale Parameter (ESP)

The multi-resolution image segmentation process involves a lot of subjective decisions (trial and errors). Therefore, in order to introduce objectivity into the segmentation process, ESP tool is used to select the best scale parameter at which the image is to be segmented and the size of the object prior to the segmentation process. The ESP tool operates in a bottom up approach. It generates image objects at multiple scales iteratively. It is based on the principle of Local Variance (LV) of object's heterogeneity at multiple scales within an image, thereby calculating the local variances for each scale. The variation in heterogeneity can be investigated by plotting the LV against the scale parameter (Dragut et al., 2010). A scale parameter refers to the maximum allowed heterogeneity for the resulting object of the image. It determines the presence or absence of an object. Objects appear differently when a scale parameter is altered. Land cover classification for instance requires a bigger scale than tree crowns identification (Benz et al., 2004). The value of the scale parameter can be adjusted to produce the required size of an object.

Dragut et al. (2010), after discovering that, the threshold of the LV alone cannot predict the scale parameter of the segmentation, introduced the Rate of Change of Local Variance (ROC_LV), whose peaks determine the scale at which the image can be segmented in addition to the LV curve. A graph of the LV against each scale or average object size can be plotted as well as rate of change of the local variance. The rate of change of the local variance is inversely proportional to the scale parameter, whereas the local variance is directly proportional to the scale parameter.

D. Watershed transformation

According to Wang et al. (2004), watershed algorithm facilitates splitting of overlapping tree crowns into individual tree crown based on threshold conditions. Image to be processed is seen as topographic surface by this algorithm. Three basic notions are applied. These are local maxima, catchment basins and watershed lines (Chen et al., 2004). Wang et al. (2004) emphasized that, when a grey scale image is inverted, the local maxima turn up to be the local minima with holes perforated at the local minima. The catchment basins which correspond to the tree crowns can be found in between the local maxima and minima.

Wang et al. (2004), further explained that, the watershed lines in the inverted image are the local maxima. This makes the image assumes the shape of watershed catchment. Therefore, each valley collects water from the local minima until water spills over the watershed into adjacent valley when water is introduced in the system. Closed contours represent watersheds surrounding areas which separate the whole area into different basins and form the desired boundaries of each object and hence, when this transformation is applied to forest, clusters of trees are considered as the catchment and the under flooding water scenarios. The trees which represent valleys touch each other and therefore such trees can be separated into individual trees.

Chen et al. (2004) accentuated that, after executing the process, the algorithm calculates an inverted distance map based on the inverted distances for each pixel to the image object so as to determine the maximum distance from the edge. The point farther away from the image object border is assumed to be the local maxima. The distance from each point in the object to the local maxima are estimated by the algorithm. All the pixels within the specified threshold of the local maxima are merged as one new segment. The process continues until splitting of image objects into smaller units satisfies the specified threshold condition.

E. Morphology

According to Shafri et al. (2011), morphology is the study of shape and size of objects. Morphological operations are performed to smooth the borders of the image in order to give shape to the objects. Two morphological operations are available in the eCognition software program. These operations are pixel based morphological operation, which removes pixels from an image which is completely separated from an image object called "open image object algorithm". On the contrary, "close image object algorithm" adds isolated pixels in the surroundings to an image object. Definiens (2011) defined closing as the complementary area to the surrounding area of an image object that can accommodate a mask completely.

2.6. Regression analysis

Over the years, regression analysis has played an important role in modelling the relationship between field measurement and RS data. The rationale behind, is to determine the relationship between a response (dependent variable) and one or more explanatory variables (independent variables). The two variables are proportional to each other. Change in one variable causes a change in another variable (Husch et al., 2003). According to Hemery et al. (2005), there is a strong linear relationship between trees with DBH range of 20-50cm and CPA. Dawkins (1963) also shared the same sentiments and added that, for the common range of forest tree sizes between 20cm and 50cm DBH, there will be a negligible distortion of the linear relationship between DBH and CPA.

Nevertheless, Hemery et al. (2005), stressed on the reduction in the rate of growth in CPA due to the effect of senility and competition for DBH with range exceeding 50cm. Whereas, CPA of trees in open and less dense forest continue to grow without the effect of competition from the nearby trees.

2.7. Overview of the Dinamica EGO software program.

The Dinamica EGO software program, is a cellular automata model which serves as a spatial simulation model of landscape dynamics. It has a multi-scale vicinity-based transitional (change) functions, which incorporate "spatial feedback approach to a stochastic multi-step simulation engine". The software applies weight of evidence or logistic regression to calculate spatial dynamic transition probabilities (Soares-Filho et al., 2002). The "EGO" in the software's name stands for Environment for Geo-processing Objects. The software is designed to develop both simple static spatial model and complex dynamic model (Soares-Filho et al., 2009).

According to Soares-Filho et al. (2003), the operations in the software involve "nested iterations, dynamic feedbacks, multi-region approach manipulation, and algebraic combinations of data in several formats, such as maps, tables, matrices and constants, decision processing for bifurcating and joining pipelines and a series of complex spatial algorithms for the analysis and simulation of space-time phenomena". The software, is the home of spatial analysis algorithms, often used in GIS environment as well as algorithms, designed for spatial simulations such as "transition functions, calibration and validation methods". These algorithms are termed as "functors" in the software program and they are arranged in sequence to allow data flow in graphical format. Models can be created in the software platform by "dragging and connecting the functors" via their ports which represent connectors to the data types, ranging from maps, tables, matrices, mathematical expressions and constants.

2.7.1. Building a land-use and a land-cover simulation model in Dinamica EGO software program

The Dinamica EGO software program can be used to develop a space-time model whereby the state or an attribute of a certain geographical location is driven by a set of drivers and changes over a time span. The modelling process, involves calibration, running, and validation. The following steps can either be ran as a separate model or be combined as single model in the software:

2.7.1.1. Transition rate calculation (deforestation rate)

Deforestation rate (change rate) is described as "transition rate" in Dinamica EGO software platform. Therefore, deforestation rate and "transition rate" may be used interchangeably in this thesis. Transition rate is defined in the software as the, "system that changes over discrete time increments, in which the values of any variable in any given period is the sum of fixed percentages of all the variables in the previous time step". The rate can be fed into a Land Use Change Model as a fixed parameter or updated from the feedback of the model (Soares-Filho et al., 2009).

According to Soares-Filho et al. (2009), two different matrices can be produced as a result of transition rate calculation. A single step matrix, one of the matrices, encompasses a time period represented as a single step. Whereas, multiple-step matrix corresponds to a time step unit per year, month or day, determined by dividing the time period by a number of time steps. Net quantity of change, which is the percentage of land that will change to another state, is fixed by the transition rate (change rate).

2.7.1.2. Calculating ranges to categorize gray-tone variables

The weight of evidence method ("A Bayesian method in which the effect of a spatial variable on a transition/change is calculated independently of a combined effect") works with categorical data only and hence, quantitative data (Distance maps, altitude, and slope) must be categorized. To ensure preservation of data, the weight of evidence ranges are calculated based on the data structure. Details of it can be found in

Agterberg and Bonham-Carter (1990) and Soares-Filho et al. (2009). The categorization employed in Dinamica EGO software program, selects the number of intervals and their buffer sizes so as to preserve the data structure. Land cover maps of different years and a set of co-registered map layers (raster cubes) are inputs for the weight of evidence ranges calculation. The output from the categorization, can be used as input data in calculation of the "Weight of Evidence Coefficients".

2.7.1.3. Calculating weights of evidence coefficients

Dinamica EGO software program uses weight of evidence method adapted from Agterberg and Bonham-Carter (1990) to convert historical land cover maps and drivers of change into transition probability maps (Kamusoko et al., 2011). According to Soares-Filho et al. (2002), a transition probability shows the most favourable areas for a change. The influence of each driver on the spatial probability of transition is denoted by the weight of evidence.

The weight of evidence coefficient calculation uses the same input data as the weight of evidence ranges calculation. The output data from the calculation of the weight of evidence ranges (weight of evidence skeleton) are also used in addition as an input data for the weight of evidence coefficient calculation. After the model is ran, the weight of evidence coefficient is calculated automatically. The model produces as an output, a log file with six columns. The first column displays the weight of evidence ranges, the second demonstrates the buffer size in cells, the third depicts the number of transitions (change) occurring within each buffer, the fourth shows the coefficients obtained from the model, the fifth column also shows the contrast measure and the last, the results from the statistical significance test (Soares-Filho et al., 2009).

The weight of evidence contrast measures the effect of the environmental variables on deforestation or land cover change. A positive weight of evidence contrast means, there is a significant effect which favours deforestation, a negative weight of evidence contrast also demonstrate a significant effect which inhibit deforestation, whilst weight of evidence of zero or near zero depicts that the variable under study does not exert effect on deforestation or the effect of the variable on deforestation at a particular range is insignificant (Soares-Filho et al., 2009). A graph of the weight of evidence contrast against the ranges can be plotted from the output log file.

2.7.1.4. Setting up and running simulation model with "expander and patcher"

Two or more categorical maps, annual deforestation rates, weight of evidence coefficients, statistic variables are the major input data into the simulation model. The model can be simulated in annual steps or a single step. The major functions which play a role in the simulation are "mux categorical map" which enables dynamic update of the input land cover maps, "calc weight of evidence probability map" which calculates a transition/change probability map for each transition specified by adding the weight of evidence, "calc change matrix" which receives the transition matrix. The "calc change matrix" calculates crude rates of the quantities to be changed by multiplying the transition rate by the number of available cells specified for a change. The "expander and patcher", two complementary transition functions from local cellular automata rule, designed to reproduce spatial patterns of change are used by Dinamica EGO software program as a "transition engine".

The "expander function" is responsible for the expansion and contraction of the previous patches of a certain class, whilst the "patcher function" is designed to generate or form new patches through "seeding mechanisms". The patcher searches for cells around a selected location for a joint transition. The process is initiated by selecting the core cell of the new patch and subsequently a specified number of cells around this core cell. The two functions allow the formation of patches of change in a variety of sizes and shapes. The number of iterations can be set by the "repeat" function (Soares Filho., 2009). Dinamica EGO software program allows modelling of the effect of a complex scenarios such as REDD+ on a transition rate. Economic, social and political scenarios can be integrated into the model. The effect of these underlying

factors on deforestation can be analysed in Dinamica Ego software program. The software can act as a heuristic device, useful for assessing the short term and long term impact of socio-economic, political and environmental framework on greenhouse gas emissions (Sampaio et al., 2007; Schneider et al., 2006). A flow chart depicting the steps in the modelling process is shown in Figure 1.
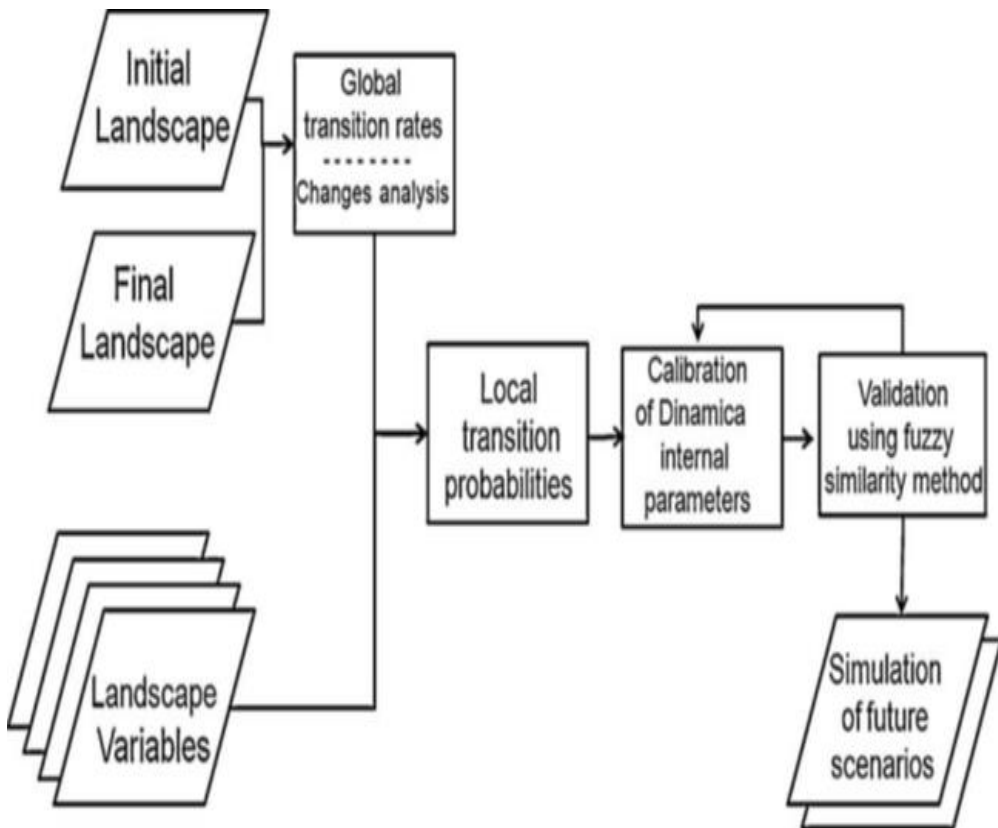
Figure 1: The major steps undertaken in Dinamica EGO software program

Source: Soares-Filho et al., 2002

3.   MATERIALS AND METHODS

3.1.   Satellite data and their uses

Landsat-7 2000 and 2012 with 30m spatial resolution were used to create initial and final land cover maps respectively for deforestation rate estimation. The two images had already been geo-referenced into the UTM 30N projection, WGS1984 spheroid datum. The focus of this research was to estimate the carbon stock in trees only and hence it was essential to delineate trees from the different land cover types for the carbon stock measurement. This task could not be accomplished by the Landsat imageries. This is because, research has shown that, Landsat imageries cannot be used to estimate AGC stock accurately. It often leads to uncertainty in the carbon stock estimates (Thenkabail et al., 2004). In the tropical forest, Landsat imageries are not effective in estimating carbon stock in dense canopy closure and have the tendency to underestimate carbon stock results (Waring & Running, 2010). Therefore, a VHR Worldview-2 image (2012) with 4 spectral bands of 2m multi-spatial resolution and a panchromatic band of 0.5m spatial resolution were pan-sharpened and used for tree crown delineation and AGC stock estimation. Google earth image and Topographic map of Ghana also aided in the land cover classification. Other ancillary data such as forest inventories of trees also facilitated the identification of trees on the field. Table 2 and Table 3 give details of the field instruments and software programs used for this research.

Table 2: Field instruments

S.N	Instruments	Purposes
1	IPAC, GPS	Geospatial Location of Sample Plots
2	Clinometer Haga	Tree Height Measurement
3	Calliper 100cm	DBH Measurement
4	Clinometer Suunto	Aspect and Slope Measurement
5	Spherical Densiometer	Crown Density Measurement
6	Compass	Bearing and Direction Measurement
7	Measuring tape (30 and 50m), Diameter tape (5m)	Radius of Sample Plots and DBH Measurement
8	Digital camera	Taking Photos of Trees

Table 3: Software programs

S.N	Software Programs	Purposes
1	ArcGIS version 10	GIS Analysis
2	eCognition Developer 8,	Object Based Image Analysis
3	ESP tool	Estimation of Scale Parameter
4	Dinamica EGO	Carbon Stock Dynamics Modelling
5	ERDAS IMAGINE 2010	Image Processing
6	Microsoft Excel 2013	Statistical Analysis
7	Microsoft Power Point 2013	Presentation
8	Microsoft Visio 2013	Flow Chart and Conceptual Diagram
9	Microsoft Word 2013	Writing Thesis
10	Mendeley	Referencing

3.2. The study area

3.2.1. Description of the study area

The study was undertaken in Goaso Forest District (GFD). GFD is located between the latitude 6° 47"48" and 7°06'44" N and longitude 2°17" 53" and 2°38'46" W in the southern part of Ghana, specifically, Brong Ahafo Region. GFD covers a total area of 2,188km². The area is one of the forest rich zones in Ghana. It lies within the moist semi deciduous tropical zone. The climate is humid with an estimated annual rainfall ranging between 1250-1750mm. The rainfall pattern is bimodal. The major rainfall is from April to July and the minor rainfall is from September to October. The average monthly rainfall ranges between 1250mm and 1750mm. The relative humidity in the dry season is between 70% and 75% and between 75% and 80% in the wet season. The topography is undulating lowland and with an elevation of 100-300m above the sea level. The type of soil commonly found in the area is forest ochrosol which is reddish in colour and well drained in the upper horizons and brownish in the middle horizons. The soil is more fertile and supports the growth of many crops. The nutrients are often leached since most of them are located at the upper part and are prone to soil erosion (Bih, 2006; Gelens et al., 2010). Figure 2 is a map of the study area.
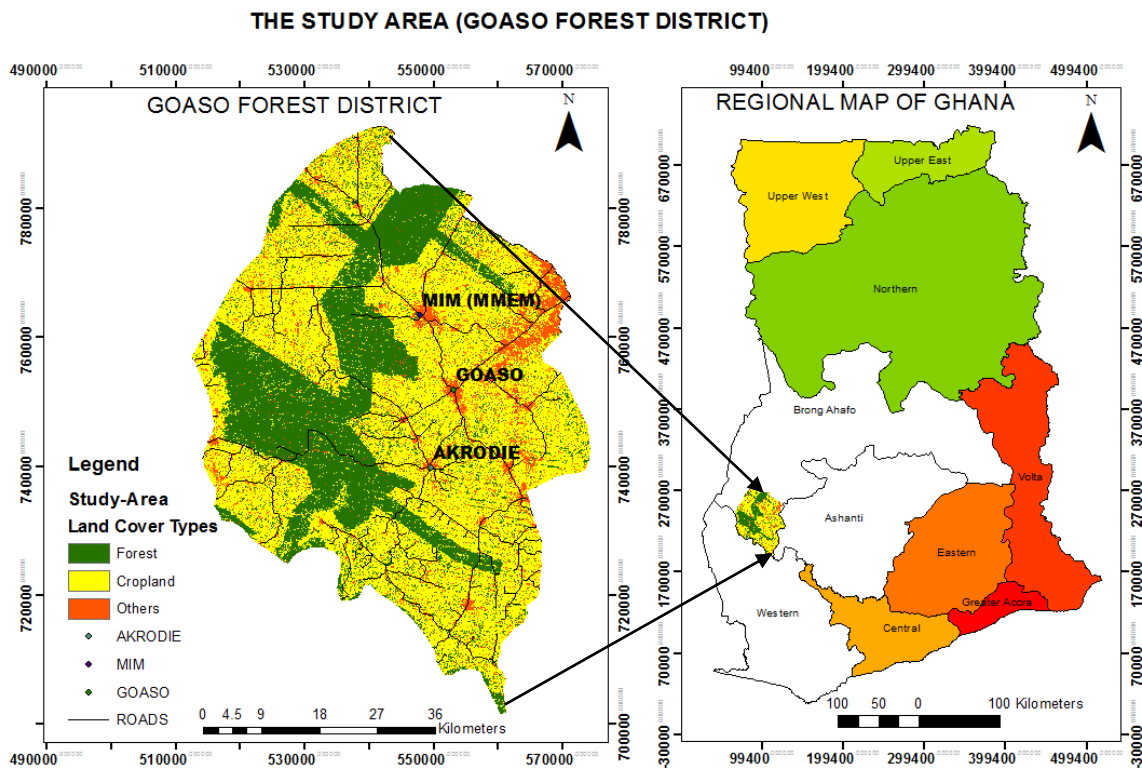
Figure 2: Map of the study area

3.2.2. Land tenure system

The Complex land tenure system in Goaso deserves to be mentioned in the scientific literature. Traditional heads (chiefs) are the custodian owners of all the lands in the Goaso Forest District. Parcels of land for farming are leased out to the farmers for farming within a period of time or are given to them for farming in the form of "share cropping". Trees in the agro-ecosystem (off-forest reserve) are seen as public assets and therefore 75% of the royalties from timber logging goes to the Government and the remaining 25% to the Chiefs. The farmers do not receive any form of incentives. On some few cases, they are given small token when the crops are damaged by legal logging or not at all. The farmers have responded to this by felling any matured trees and samplings of timber trees even before they reach maturity. Fallow period has also been drastically reduced from 10 years to 4 years due to the scarcity of land for farming (Gelens et al., 2010).

3.2.3. Land use system

The land outside the forest reserve (off-forest reserve) has suffered a severe agricultural expansion and illegal logging of trees and intensive land use. The condition was declared as degraded in 1995. However, it is common to find trees on agricultural land, particularly, in shaded cocoa farms, secondary forest in abandoned agricultural land, along the stream, and sacred groves. The major land cover types in the area are: crop (annual and perennial), tree crop (Cocoa, oil palm), forest, tree fallow, shrub fallow, and grassland. The forest fringe communities depend mainly on the resources found in the off-forest reserve such as food, medicine, firewood as their source of livelihood. The main occupation in the area is farming. Approximately 70% of the population are employed in this sector. Food crops such as maize, cocoyam, cassava, and plantain are mostly cultivated in the area (Bih, 2006; Gelens et al., 2010).

3.3. Methodology

The methodology employed in this research involved four major steps. These are: Pixel based classification of the Landsat Imageries in ARCGIS, AGC stock estimation from field measurement, AGC stock estimation from Worldview-2 satellite image in eCognition software program and future AGC stock modelling in Dinamica EGO software program. The research estimated AGC stock from a regression model between Crown Projection Area (CPA), extracted from a Very High Resolution (VHR) Worldview-2 satellite image in eCognition software program and an AGC stock, estimated from the relationship between DBH and site specific allometric equation. The deforestation rate from 2000-2012 was also estimated. The effect of environmental drivers on deforestation was then ascertained to facilitate modelling of the changes in carbon stock of trees in Dinamica Ego software program, under a scenario whereby farmers expand their farms and remove trees from the agro-ecosystem and the forest reserve, that is the Business as Usual (BAU) scenario, and a management scenario, whereby farmers were assumed to be offered carbon financial incentives to maintain, conserve and protect trees (REDD+). Figure 3 is a flow chart of the methodology.
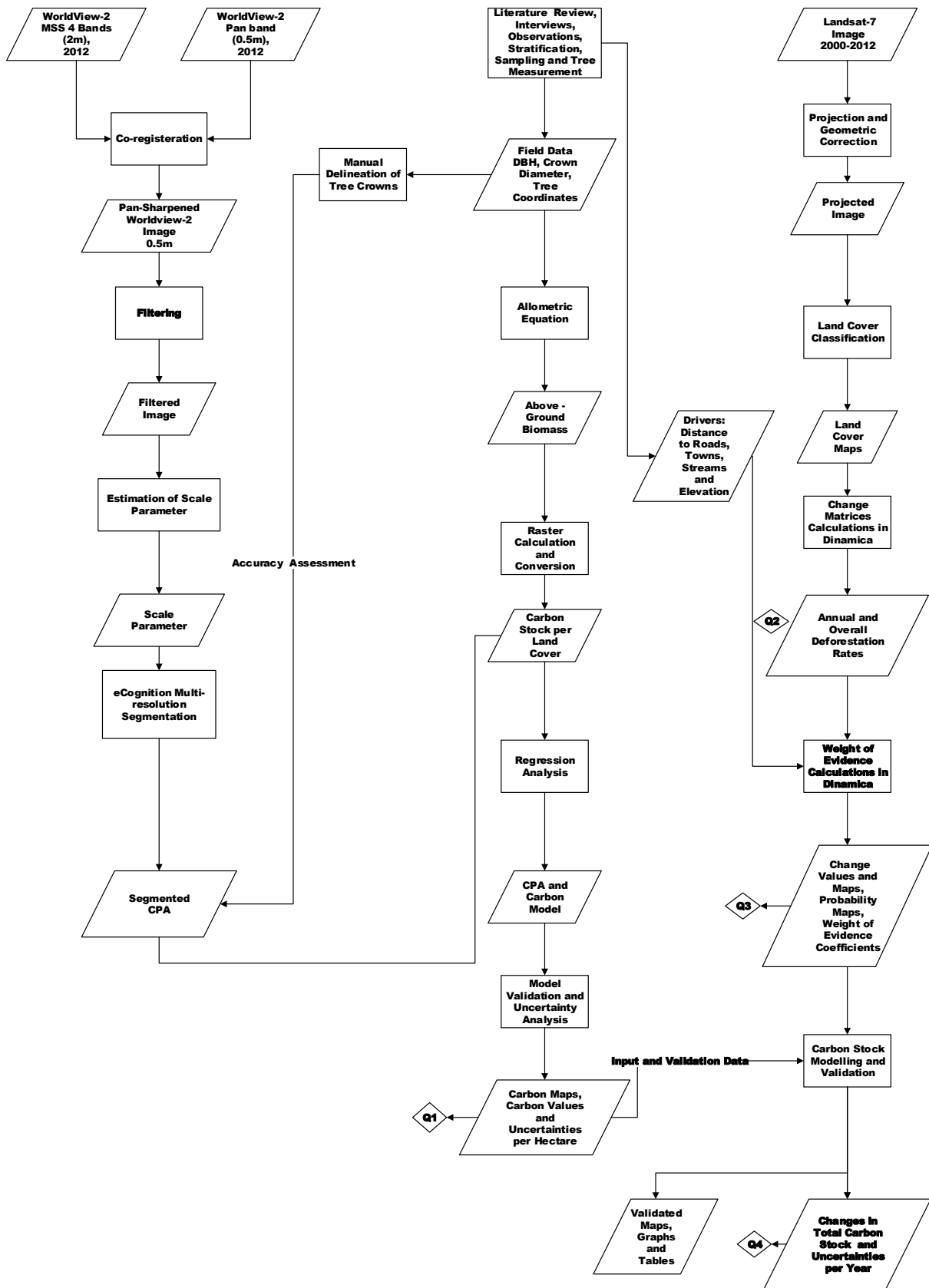
Figure 3: Flow chart of the methodology

3.4. Pre field work

A work plan, detailing all the activities to be done on the field was developed using Microsoft Word. Also, recording sheet for field inventory, data collection and observations to be made in the field was developed using Microsoft Excel.

3.4.1. Image processing and sampling design

A multi-spectral Worldview-2 image with four bands was pan-sharpened with panchromatic Worldview-2 band. The image had already been geo-referenced and co-registered with the UTM 30N projection, WGS 1984 spheroid datum. The study area was therefore stratified into four major strata (cropland, forest, fallow and cocoa). According to Husch et al. (2003), stratification of the study area yields more accurate estimates of the tree parameter than simple random sampling. Stratification ensures homogenous strata (CIFOR, 2009). The centre of the sample plots were distributed in the stratified area of interest on the image. The shape file of the sample plots was overlaid on the Worldview-2 image. Circular plots covering an area of 500m² and with a buffer of radius, 12.62m on a flat terrain were laid on plots found on forest stratum (Husch et al., 2003). However, on croplands, fallow lands and cocoa plantations with less tree density, squared plots of 625m² were laid (Altrell & Vuorinen, 2002). Due to the limited time which was available for the field study, 83 sample plots were laid. Twenty-seven (27), 31, 7 and 18 of the sample plots were distributed on cocoa plantation, cropland, fallow and forest respectively.

3.5. Field work

3.5.1. Data collection

The Worldview-2 image which was saved in a jpeg format was converted into enhanced compression wavelet format together with the sample plots. The image and the sample plots were loaded and saved on the IPAC and printed at the same time to facilitate navigation and measurement on the field. The study centre point of the first plot was found by the nearest well defined point on the maps using the IPAC, GPS as a back-up, compass and the printed map. The distance and the bearing to the plot centre from this known point were found by the compass, the maps, and a protractor. The sample plots were laid by placing a stick at the centre of the sample plots. The slope correction table was used to define the appropriate radius of the sample plot especially on sloping grounds. The slope measurement was done in the direction of maximum slope whilst ensuring the use of a correct scale. Areas with slope less than 5% were considered flat.

The aspect was measured with a compass in N/S and E/W direction for all the square plots to prevent introduction of bias into the sampling process. The coordinates of all the sample plots and the natural trees to be measured were taken. The trees were demarcated and marked with a chalk visible from the centre of the plots. The diameter tape was used to measure the DBH of the individual natural trees with diameter greater than 10cm at a height above 130cm. The assumption was that, trees with diameter less than 10cm contribute less to the total biomass estimation (Brown, 2002). The crown diameters of some of the trees were measured with a tape under the crown on the ground and towards the plot centres perpendicular to the tape direction whilst the edges of the crowns were gauged.

3.6. Post field work

The field data were processed in Microsoft Excel. The tree crowns in the sample plots were digitized by overlaying the shape file of the sample plots on the Worldview-2 image in ARCGIS software program. This allowed an information exchange between field measurements and Crown Projection Area (CPA) extracted from the Worldview-2 image. They were also used as training data for accuracy assessment. The following land cover types were observed on the field: forest, fallow, grassland, shrubland, oil palm plantation, cocoa

plantation, cropland and settlement. These land cover types were merged into 3 classes (forest/trees, cropland, others) after field data collection using the method of interactive supervised classification in ARCGIS environment. The rationale behind the merging was that, the areas covered by some of the land cover types (shrubland, grassland, oil palm) were small. Besides, the tree densities on some of them (settlement, grassland, shrubland, and oil palm plantation) were discovered to be minimal. On top of the training samples collected from the field, Google earth and Worldview-2 images also aided the classification process.

3.6.1. Above ground carbon stock estimation per stratum from the field data

Several allometric equations have been developed for tropical rainforest (Basuki, 2012; Brown, 2002; Keller et al., 2001). Though, specie specific allometric equations are available for some tree species in Ghana, allometric equations for the calculation of the total AGB involving DBH only were not available for many of the tree species identified from the field. Allometric equations, involving DBH, developed for some trees species (*Ceiba pentandra, Nauclea diderrichii and Daniellia thurifera*) in Ghana were found to be the same and therefore were used to represent the allometric equations of all the tree species identified on the field since, according to Chave et al., (2005) and Brown (2002), DBH alone explains about 95% of the variation in AGB. AGB was therefore calculated using field measured DBH of the trees from the allometric equation below:

Equation 1: Allometric Equation

Above Ground Biomass = 0.16502*DBH^ (2.3351)

> **Where,**
>
> **0.16502 = the allometric parameter**
>
> **^2.3351 = the average wood density**

The allometric equation is published at "GloballomeTree" website. The AGC stock was therefore estimated from AGB by multiplying the individual results by 0.47.

3.6.2. CPA extraction from the Worldview-2 image

Crown Projection Area (CPA) of trees, delineated or extracted from VHR satellite has been found to provide a reliable estimate of AGB and subsequently AGC stock when it is combined in a regression relationship with AGB or AGC stock, estimated from the relationship between field measured DBH and allometric equation (Muukkonen & Heiskanen, 2007). Therefore, the image segmentation algorithm in eCognition software program was used to extract the CPA of trees from Worldview-2 image. This research used multi-resolution segmentation as well as contrast split segmentation for the CPA extraction. The multi-resolution segmentation was used to segment the image whilst the contrast split segmentation was also used for separating vegetation from non-vegetation areas. The whole segmentation processes are summarised in Figure 4.
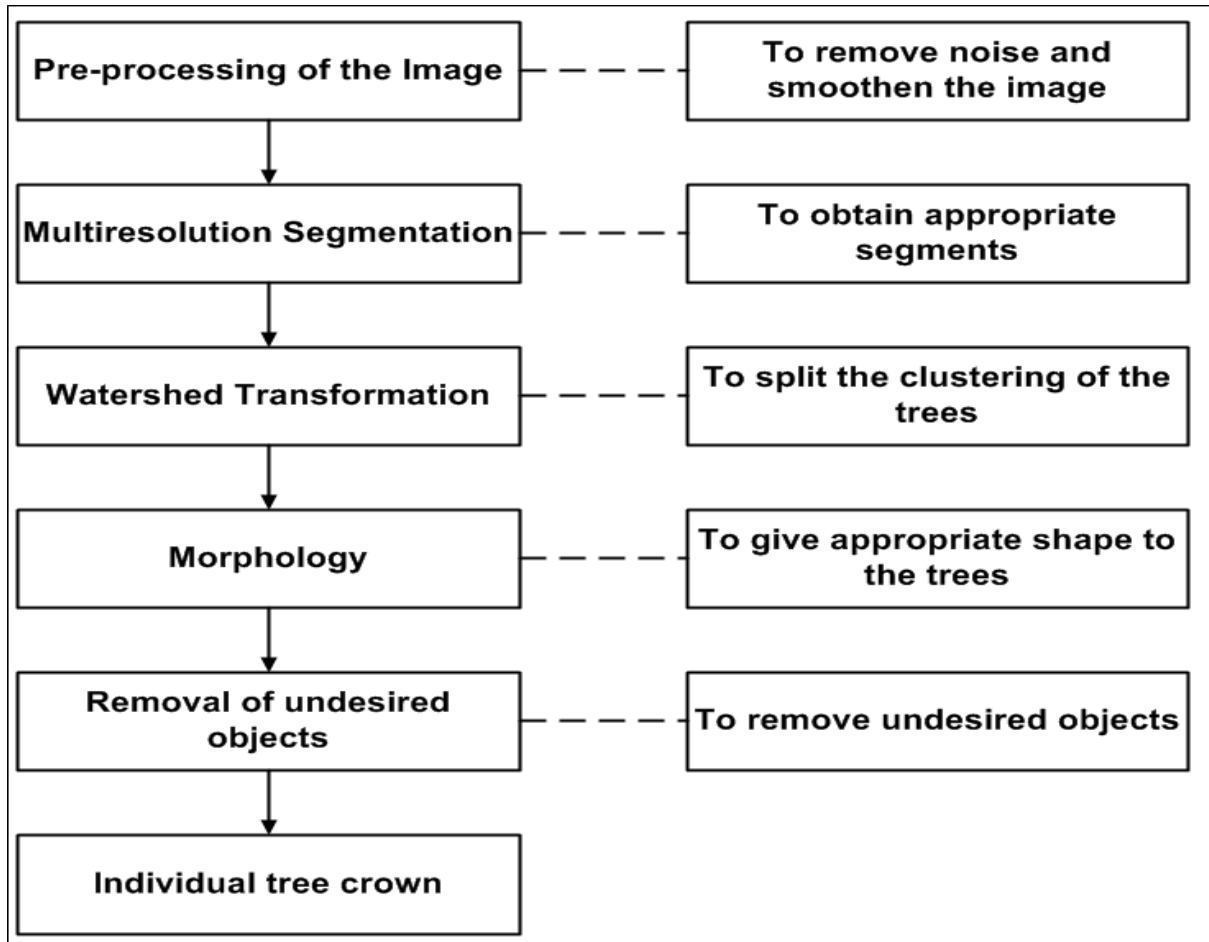
Figure 4: The segmentation processes

Source: Barel, 2011

3.6.2.1.   Pre-processing

A.   Image fusion / Pan-sharpening

This research employed hyper-spherical colour sharpening (HCS) technique, which is one of the latest pan-sharpening algorithms developed purposely for Worldview-2 imageries for the pan-sharpening. The 2m multi-spectral Worldview-2 image band was therefore pan-sharpened with 0.5m panchromatic Worldview-2 band to produce a pan-sharpened image of 0.5m spatial resolution, with all the multi-spectral information retained (Leica Geosystems, 2011). The HCS was used because; it accepts any number of bands and can also handle spectral and spatial recovery over a large variety of scenes. Padwick et al. (2010) compared HCS, IHS, GS and PCA, and discovered that, HCS maintains the best balance between spectral and spatial quality. The pan-sharpening was done in ERDAS software program.

B.   Filtering

The panchromatic image was filtered with a 3×3 low pass convolution filter. The convolution filter estimates the averages of small sets of pixels within the window size to produce an image, whose features are more enhanced. According to Definiens (2011), the convolution filter removes noise and also intensity of variation due to the internal structure of the trees.

C.   Estimation of a Scale Parameter (ESP)

The image segmentation process involves a lot of subjective decisions (trial and error). Therefore, in order to introduce objectivity into the segmentation process, ESP tool was used to select the best scale parameter at which the image was to be segmented and the size of the object prior to the multi-resolution segmentation process. The scale parameter for the segmentation rule set which had already been developed in the ESP tool was loaded into the eCognition software program to obtain the optimal scale parameter for the multi-resolution image segmentation. In this research, a scale parameter of 45 was used for the segmentation.

3.6.2.2.   Multi-resolution segmentation

The aim of the multi-resolution segmentation was to subdivide the image into non-overlapping segments (Möller et al., 2007). Segmentation of the image was vital since it is the building block of the object based classification employed in the individual tree crown delineation or extraction from the other land covers. Segmentation permits the identification of homogenous areas to allow grouping of specific objects (Kim et al., 2010). It also necessitates the extraction of information from the image by grouping similar pixels to form homogenous image object (Blaschke, 2010). This algorithm was adopted because, it reduces the average heterogeneity and increases the homogeneity in a given number of image objects.

The shape homogeneity criterion was set to 0.8 to produce uniform shapes with little emphasis on the uniformity. The compactness homogeneity criterion on the other hand, is employed when different image objects are compact and can be separated from non-compact objects by weak spectral contrast. A higher value of compactness creates compact segments (Definiens, 2009). Therefore the default value of 0.5 was chosen for this segmentation to obtain a balance between compact and non-compact segments. Plants exhibit high reflectance in the near infra-red region of the spectrum and hence they are easily separated from each other objects in this band. Therefore, 4 was assigned to the image layer weight field since the image layer weight shows the level at which the bands in the image influence the segmentation process (Definiens, 2009).

A.   Identification of trees

GFD is a complex ecosystem with different land cover types. It is composed of settlements, bare land, cocoa, oil palm plantation, trees, shrubland, and grassland. The image was also covered with shadows and clouds. Also, due to the nature of the forest (closed canopies), intermingling crowns were common. Therefore it was essential to mask and remove all the undesirable materials from the image to allow accurate tree crowns delineation.

I.   *Masking of shadows, clouds and settlements*

Brightness values of the pixels were used as criteria to mask out clouds and shadows from the image. Pixels with very high and low brightness values were masked out as clouds and shadows respectively. Objects with brightness values less than or equal to 320 were classified as shadows. The remaining objects were separated by contrast split segmentation and classified as vegetation and non-vegetation. This was possible by the use of Difference Vegetative Indices of the objects. Simple ratio was chosen over the other vegetation indices because, the contrast in reflectance between vegetation and non-vegetation (buildings, cloud) areas were more distinct within the near infrared and red band. A simple ratio is a division of the near infrared band and the red band reflectance. Vegetation has higher values in these regions of the spectrum. It is one of the greenness vegetation indices which measures the total quantity and vigour of green vegetation (Sims & Gamon, 2002). The Equation 2, in the next page was used to calculate the simple ratio.

Equation 2: Simple Ratio

$$\text{Simple Ratio} = \frac{\text{Near Infrared Band}}{\text{Red Band}}$$

The ratio ranges from 0-30. Non vegetative objects were found to have a simple ratio less than or equal to 3.5 and hence they were classified as such. Whilst the remaining objects with simple ratio greater than 3.5 were classified as vegetation (Tucker, 1979). After the separation, the objects which were classified as shadows and non-vegetation were merged.

II. Watershed transformation

The results from the segmentation and the basic classification depicted some large segments. These large segments were assumed to be some clusters of trees with intermingling crowns (Wang et al., 2004). Because of the nature of the forest canopy (closed) in the study area. Watershed transformation was used to split these clusters since the aim of the whole segmentation process was to delineate the individual tree crown but not clusters. The size of the largest tree crown observed in the field was used as the maximum crown size to split clusters of tree crowns. On the field, the maximum crown size was observed to be 36m. This is equivalent to 72 pixels in the image and therefore 72 was entered in the "length factor field" of the watershed transformation algorithm.

Chen et al. (2004) emphasized that, after executing the process, the algorithm calculates an inverted distance map based on the inverted distances for each pixel to the image object so as to determine the maximum distance from the edge. The point farther away from the image object border is assumed to be the local maxima. The distance from each point in the object to the local maxima are estimated by the algorithm. All the pixels within the specified threshold of the local maxima are merged as one new segment. The process continues until splitting of image objects into smaller units satisfies the specified threshold condition.

III. Morphology

This research applied "open image object algorithm" to smooth the edges of the segmented tree crowns since it was found to be faster as compared to the "close image object algorithm" when it was applied on the whole segmented image. Stemming from the fact that, tree crowns are round, a circular mask of pixel size 10 was created. The mask in eCognition software program is seen as a structuring element.

IV. Refining the shape of the tree crowns

There is an expansion of cocoa plantation in the study area. In view of this, it was essential to ensure that, the segmentation result was not affected by the tree crowns of the cocoa plantation. Therefore, further morphological operation was applied to remove undesirable objects from the segmented image. Cocoa trees have intermingling crowns and small crown diameter and therefore some of the small and elongated objects, presumed to be cocoa plantations were removed from the segmented image.

The size of the maximum crown diameter of cocoa tree and minimum crown diameter of the other trees as well as geometric shape of the image objects were used as threshold conditions to remove crowns of cocoa trees from the image. Objects with roundness greater than or equal to 0.7 and pixel length of 20 which is equivalent to 10m were removed from the segmented image. The rule set developed for the entire processes is shown in Figure 5.

- Segmentation
  - 14:31.828   45 [shape:0.8 compct.:0.5] creating 'New Level'
- Shadow Masking
  - 0.094   unclassified with Brightness <= 320 at New Level: Shadow
  - 05.954   Shadow at New Level: merge region
- Contrast Split Segmentation
  - 0.125   with Simple Ratio > 3.5 and Simple Ratio <= 3.5 at New Level: edge ratio spl
  - 0.078   unclassified with Simple Ratio <= 3.5 at New Level: Others
  - 0.297   Others at New Level: merge region
  - 0.063   unclassified with Simple Ratio > 3.5 at New Level: Trees
- Morphology
  - 04:05.828   Trees at New Level: watershed transformation (72)
  - 01:03.796   Trees at New Level: opening: Trees
- Remove Undesirable Objects
  - 04.750   Trees with Length <= 20 Pxl and Area <= 20 Pxl at New Level: remove object
  - 10.515   Trees with Roundness >= 0.7 at New Level: remove objects (merge by shape
- Export Results
  - 01:48.438   Trees at New Level: export object shapes to Thesis_SEG_Length_20_Round_

◄◄ ◄ ► ►► \Main/

Figure 5: The segmentation rule set

3.6.2.3.   Validation of the segmented image

Validation of the segmentation results is required for the assessment of the quality of the segmented image. The segmented tree crowns must reflect true tree crowns in reality (Clinton et al., 2010). The segmented image was validated by using a reference polygon obtained from manual digitization of the tree crowns. The coordinates of the trees measured on the field which were identified on the image were manually digitized and saved to serve as reference polygons for the validation of the segmentation. The area of intersection between the manually digitized reference polygons and the polygons obtained from the automatic segmentation of the image was assessed.

Best scores were assigned for reference polygons with one to one matching with the automated segments (Zhan et al., 2005). Polygons were assigned one to one matching if the area of intersection was above 50%. The relative area approach developed by Möller et al. (2007) was also used. This approach is based on visual interpretation and judgment of the degree of fit of the segmented objects with reference objects. Best scores were assigned with segmented objects, completely covered by the reference objects.

3.6.3. Regression modelling and uncertainty analysis

DBH of the trees in this research were sampled from both dense and open forest, as well as croplands, the possibility of the relationship between the field calculated AGC stock and the CPA deviating from the linear relationship was high. The linear relationship between the carbon, calculated from the field and the CPA, extracted from the Worldview-2 image, predicted some negative carbon values. Though this may be expected, since the developed model is valid for trees with DBH, equal to or greater than 10cm only, and also due to the fact that young trees with DBH less than 10cm were not measured on the field, negative carbon values are not acceptable in reality. Therefore, other relationships were explored to ensure that only positive carbon stock values were predicted by the model.

Power function was observed from the DBH allometric relationship **(Above Ground Biomass = 0.16502*DBH^ (2.3351))**, which indicated that, the regression relationship between the carbon, calculated from the DBH and the CPA was also likely to exhibit a power relationship as observed by Shimano (1997). According to Shimano(1997), CPA grows with the second power relationship with the DBH and the increase rate of CPA slows as DBH increases with transformation. Therefore, the CPA was transformed to the second power (CPA^2) to address this challenge. A linear regression model was then developed between the transformed CPA (CPA^2) and the AGC stock, calculated from the field. Giving rise to a linear equation below:

Equation 3 : CPA^2 linear equation

Above ground carbon = βo +βi*CPA^2

Where,

βo is the intercept

βi is the slope or the coefficient of the CPA^2

The equation from this relationship predicted only positive carbon values and hence it was adopted to calculate the AGB from the Worldview-2 image and subsequently AGC stock. The aim of this research was not to test the relationship between the two variables (AGC stock from DBH and CPA), but to develop a robust equation (model) from the variables which can be used to estimate the carbon stock from the segmented image. Therefore, only tree crowns which were classified accurately and demonstrated one to one matching were selected for the model development and validation.

This was necessary because, according to Pouliot et al. (2002), unidentified and misclassified trees are not suitable for model development and evaluation. Over segmented and under segmented tree crowns were removed before the model development. Outliers were also removed since according to Mora et al. (2010), a good and a robust model must have a few outliers. 70% of the data were used for the model development and 30% were also used for validation.

The quality of the model was assessed by the R^2 and standard error. R^2 explains the variation in the predicted AGC stock values and the calculated AGC stock values. Uncertainty involved in the carbon estimates per land cover type was then estimated by calculating the mean $\pm$ 2×standard deviation away from the mean (IPCC, 2003). The equation 4 was used to calculate the uncertainty involved in the AGC stock estimation.

Equation 4: Uncertainty

Uncertainty = Mean $\pm$ 2 × Standard Deviation (IPCC, rule)

3.6.4.   Modelling changes in the AGC stock in Dinamica EGO software program

Modelling future carbon stock requires a software program with heuristic ability (Sampaio et al., 2007; Schneider et al., 2006). However, the eCognition software program, which was used to estimate the current AGC stock does not have a heuristic ability for future scenario creation. Therefore, the future AGC stock modelling was implemented in Dinamica EGO software program because, it has a heuristic ability. The "patcher isometry index" which is a heuristic parameter in Dinamica EGO software program act as a heuristic function for future scenario creation (Soares-Filho et al., 2002).

3.6.4.1.   Input data

Two historical land cover maps: initial (2000) and final (2012), carbon density in tons per hectare in excel csv format (area statistics), annual change rate (transition matrix) also in excel csv format, environmental raster cubes (digital elevation model , distance to road, distance to town, distance to streams, distance to protected forest resampled to the same spatial resolution) were used as input data into the carbon stock dynamic model (Yi et al., 2012). The environmental variables were selected based on the finding from the literature review (Gelens et al., 2010) and field observation.

3.6.4.2.   Data selection and preparation for the model development

Historical land cover maps were represented by the Landsat-7 land cover maps (2000-2012). The dates for the two images were chosen based on the availability of the images, the ongoing agricultural expansion (Gelens et al., 2010) and at the same time the introduction of agroforestry in Ghana (Kalame et al., 2011) between the two periods. The 2012 image was chosen to represent the current land cover map due to the absence of cloud on the image. Also, all the images covering the study area from 2012 upwards, which were freely available were covered by clouds. Each of the two images was classified into three classes (forest/trees, cropland, and others). These three classes were developed to monitor the rate at which the trees in the GFD were being converted to croplands and other land cover types. The assumption was that, the AGC stock in croplands and the class "others" were 0, since only the AGC stock of trees were measured on the field and estimated from the Worldview-2 image. The classification was done by using, pixel based "Interactive Supervised Classification Algorithm" in ARGIS environment. Approximately, 50% of the ground control points collected from the field were used as the training samples and 50% were used as ground truth data for the accuracy assessment.

The deforestation (change) rates also referred to as global transition rates were then calculated from the initial (2000) and final (2012) land cover maps in Dinamica Ego by using "two categorical maps" and "determine the transition matrix" functions. The "determine transition matrix function" calculates the change rates without taking into an account the spatial distribution of such changes. The total amount of changes for each type of land cover given in the simulation period were therefore calculated (Soares-Filho et al., 2002). Multiple change rates (annual) and single change rates (combined change rate from 2000-2012) were produced as outputs.

3.6.4.3.   Calculation of transition probabilities

After the change rates and the role of each land cover maps were clearly defined, the continuous variables such as distance to roads were categorized and weight of evidence ranges were calculated. The weight of evidence skeleton produced as an output from the categorization was used as an input for the weight of evidence coefficient calculation. The local transition probabilities were also calculated by the software for each grid cell by considering the driving factors of the study area (the environmental variables). These probabilities are termed as local transition probabilities and it is different from global transition rate since the later does not take the spatial distribution of the changes into an account. Methods such as logistic regression and neural networks can be used to estimate the transition probabilities in Dinamica EGO software. However, the 2009 version of the software which was used for this study uses Weight of Evidence

(WoE) method explained earlier in Chapter 2 of this thesis (Soares-Filho et al., 2002, 2009). Equation 5 is used by the software to estimate the spatial probability of a transition.

Equation 5: Probability of a transition

$$P_{x,y}\{T/V_1 \cap V_2 \cap \cdots \cap V_n\} = \frac{O\{T\} \times e^{\sum_{i=1}^{n} W_{x,y}^+}}{1 + O\{T\} \times \sum_{j=1}^{t} e^{\sum_{i=1}^{n} W_{x,y}^+}},$$

where P_{xy} is the probability of the transition or change occurring in each cell with coordinates x, y; T is the land cover transition/change; Vi is a cell with all the possible environmental variables (explanatory variables) *i* designated to explain the transition T; and O {T} is the odds of a transition which is represented by the ratio between an estimated transition probability and the complementary probability of non-occurrence transition which is given by the equation below:

Equation 6: Odds of a transition

$$O\{T\} = \frac{P\{T\}}{P\{\overline{T}\}},$$

Where P{T} is the probability of a transition T occurring which is described by the number of cells where the relevant land cover transition took place, divided by the total number of cells covering the study area; $P(\overline{T})$ is the probability of a transition T not occurring determined by the number of cells where the relevant land cover transition is absent which is divided by the total number of cells in the study area; and $W_{x,y}^+$ is the weight of evidence for an estimated environmental variable range illustrated by the equation below:

Equation 7: Weight of Evidence

$$W+ = \log_e \frac{P\{Vi/T\}}{P\{Vi/\overline{T}\}},$$

Where $P\{V_i/T\}$ is the probability of variable Vi occurring in the presence of transition T, defined as the number of cells where both Vi and T are located, divided by the total number of cells where T is located; whereas $P\{V_i/\overline{T}\}$ is the probability of variable Vi occurring in the absence of transition T which is defined as the number of cells where both Vi and $\overline{T}$ are located divided by the total number of cells where T is not located.

Therefore, the W+ value is a representative of the relationship between an estimated land cover transition and a specified variable. Higher value of W+ is an indication of a greater probability that a particular transition occurred. Contrary, negative W+ indicates a lower probability that an estimated transition occurred in the presence of the corresponding variable range. Dinamica Ego produces a spatially explicit probability maps and weight of evidence log file, in which each cell is assigned the probability for an estimated transition based on the W+ values of each range for every variable investigated. The weight of evidence log file gives the details of the weight of evidence contrast, weight of evidence coefficient, buffer size, the results of the statistical significant test, the weight of evidence ranges, and the number of transition executed.

3.6.4.4. Calibration of the Dinamica–EGO software program internal parameters

Stochastic algorithm is used by the Dinamica Ego software program for allocating land cover change. The "expander and patcher transition algorithms" are responsible for the land cover change allocation. The expansion of the previously existing patches of a particular class is executed by the "expander function", whilst the "patcher function" is designed to produce new patches through seed formation mechanisms (Soares-Filho et al., 2002). The algorithms scan the initial land cover map to sort out the cells with the highest probabilities and arrange them in a data array. Cells are therefore randomly selected from the top to the bottom of the data array.

The internal stochastic selection mechanisms can be controlled by loosening and tightening the degree of the randomization. Finally the land cover map is again scanned to execute the selected transitions. The percentage of changes executed by the two algorithms are the first parameters to be calibrated in the simulation. The mean and variance of new patch sizes were also adjusted. This was done individually for the "expander and patcher" functions. Patcher isometry index which is a heuristic parameter also forms part of the internal parameters of the model. Compact patches are produced by high isometry index whilst fragmented patches are generated by low isometry values (Soares-Filho et al., 2009).

3.6.4.5. Future Scenario Creation

After the model has been calibrated by changing the internal parameters of the "patcher and expander functions" as well as the input parameters simultaneously, the simulation was ran under BAU and REDD⁺ scenarios. The BAU scenario was simulated by applying exploratory approach. This approach is a sequence of emerging events (Alcamo & Ribeiro, 2001). The annual transition rate (deforestation rate) from the year 2000-2012 obtained from the transition matrix calculation was used to represent the change rate under BAU scenario whereby farmers remove trees from the Forest District. Deforestation rate under the BAU was assumed to be static and not affected by any external policy. REDD⁺ scenario was made to represent the targeted future whereby farmers are offered carbon financial incentives to conserve trees in the Forest District. Therefore, the Ghana REDD⁺'s mission of reducing deforestation rate by 100% in the future was adopted and hence the net annual deforestation rate which was obtained from the multiple transition calculation was assumed to be reduced from 3% under BAU scenario, to 2%, 1% and 0% under three different and independent REDD⁺ scenarios from 2015 to 2025.

The carbon stock/carbon density and the uncertainty values in tons per hectare, estimated from the 2012 Worldview-2 image in the eCognition software were used as baseline carbon stock and uncertainty values (area statistics) for the simulation. This is because, Dinamica Ego software program does not have the algorithm to extract the carbon stock values from the VHR images. The number of iterations was set to run 25 times under BAU scenario (from 2000-2025), with the initial (2000) carbon stock and uncertainty values calibrated as 0.

The "calculate weight of evidence algorithm" applies the principles of Bayesian's rule to estimate the conditional probability by taking constraints into consideration (Soares-Filho et al., 2009). The "patcher and expander functions" allocate the changes accordingly, taking into account the average size and the shape of the patches and whether new patches should emerge (patcher) or existing ones should expand (expander). The "calculate carbon density function" therefore calculates the carbon density per year, whilst the "calculate uncertainty value function" calculates the uncertainty values per year.

The simulated land cover maps (2001-2025), carbon stock and uncertainty values (2001-2025), probability maps (2001-2025), weight of evidence coefficients, and area statistics were produced as outputs. The BAU scenario was rerun again by representing the initial and final land cover maps by the simulated 2015 land cover map, obtained from the BAU simulation and was used to project the AGC stock from 2015 to 2025 under BAU scenario. The results were compared with the results obtained from the 2001-2025 simulation,

ran by using the actual and original land cover maps (2000-2012). After the results from the 2015 simulated land cover map and the one obtained from the actual land cover maps were verified to be the same, the 2015 simulated land cover map was again used to represent the initial and final land cover maps under the three different REDD+ scenarios whereby the annual net deforestation rate was assumed to be reduced from 3% to 2%, 1% and 0% from 2015 to 2025. The simulated 2015 land cover map was used because, the original 2015 land cover map for the study area was unavailable. Figure 6 is an illustration of the carbon stock model implemented in the Dinamica EGO software program.
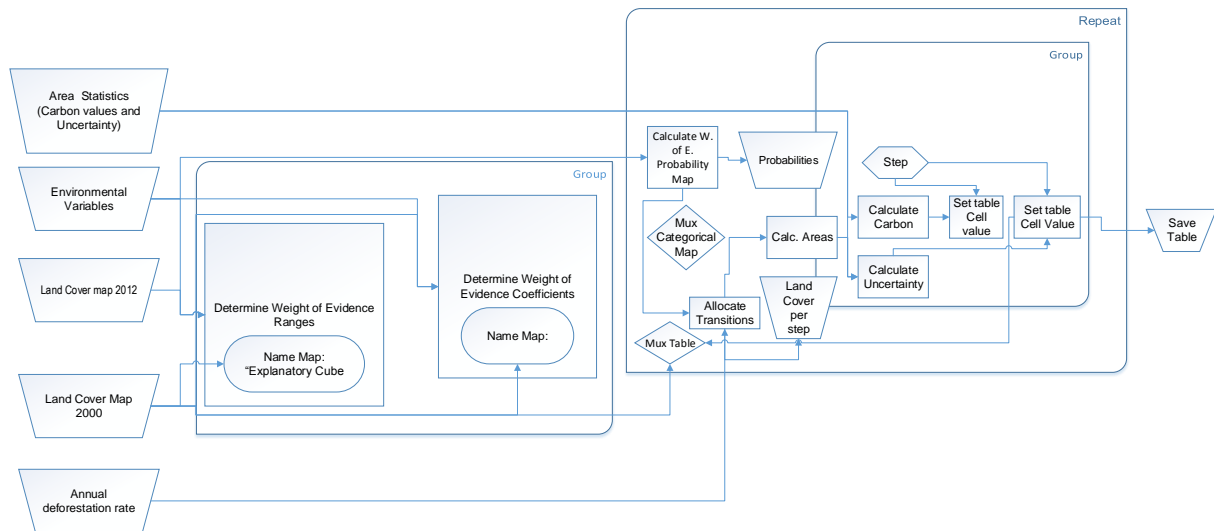
Figure 6: Carbon stock modelling in Dinamica EGO software program

3.6.5. Validating the carbon stock model in Dinamica EGO software program

According to Soares-Filho et al. (2009), "maps which do not match exactly cells by cells" may exhibit similar spatial patterns and agreement within certain cell vicinity. Over the years, different comparison methods have been developed to alleviate these problems. One of such comparison methods is the multiple resolution fitting procedure, introduced by Costanza (1989). This comparison method is based on a map fit within an increasing window sizes. A method to differentiate errors due to location and quantity was also developed by Pontius (2002). Hierarchical fuzzy pattern matching method, developed by Power et al. (2001) has also been used for validation.

The comparison method employed in Dinamica Ego is a modified form of Kfuzzy method by Hagen (2003), which is similar to Kappa statistic and fuzzy similarity of a location and category within a cell neighbourhood context. This method, known as; "Calc Reciprocal Similarity" in Dinamica Ego software program makes use of an exponential decay function with distance, to weigh the cell state distribution around a central cell (Soares-Filho et al., 2009).

Initial land cover map (2000), final land cover map (2012) and the simulated land cover map (2012) were used as input data for the validation. The validation method uses the initial and the final land cover maps in addition to the simulated map (2012) instead of only the final land cover map which in this case was the 2012 land cover map and the simulated 2012 map. This is because, according to Soares-Filho et al. (2009), simulated maps tend to look like the initial land cover map (2000 land cover map), and therefore this validation method evaluates the spatial fit between change maps to get rid of the spatial inheritance that might have arisen between the initial land cover map and the simulated map.

The output map from this validation shows changed cells. A "two way similarity" is calculated from the first map to the second map and from the second map to the first map. Soares-Filho et al. (2009) recommended that, minimum similarity values should be chosen as the validation results because random maps tend to give rise to an artificially high fit when univocally compared. This is attributed to the fact that, changes are spread over the entire area of a random map.

The following, were produced as an output from the validation: Two similarity maps (maps showing the degree of spatial match from first to the second input map and vice versa), the similarity varies from 0 (no match) to 1 (a perfect match). Minimum similarity index (the similarity obtained by comparing the simulated changes against the actual ones) as well as two values of similarity (first and second mean index for a given window size, comparing the first mean map to the second mean map and vice versa).

Owing to the fact that, the results from this study may be used in decision making, the validity of the model was critical. Therefore, "multiple window similarity" approach was also used to measure the spatial fitness between the simulated changed map (2012) and the actual 2012 changed map. "A constant decay function within a variable window" was employed in this method (Soares-Filho et al., 2009).

The first part of this method was not different from the "Calc Reciprocal Similarity", in that, they have the same input data. The model fitness was assessed with reference to the location of changes only because; a fixed quantity of transition matrix was received by the simulation. The method also takes into an account the cell resolution of the input map. Half of the input map resolution was the window search radius. A window size of 11*11, starting from 1 to 11 by an increment of two, ranging from 1*1, 3*3, 5*5, and 7*7 to 11*11 was set. This was essential because, according to Soares-Filho et al. (2009), the window size must be odd. After the validation, a graph showing the model fitness per spatial resolution was drawn from the multiple minimum similarity values in percentage and the resolution of the window search radius in meters.

4. RESULTS AND DISCUSSION

4.1. Above-ground carbon stock estimation per stratum from the field measurements

The research revealed four major strata (cocoa, cropland, fallow, and forest), in the study area for the purpose of the field measurement. These strata constituted the major land cover types with a considerable tree density in GFD. The remaining land cover types (oil palm plantation, grassland, shrubland, water, bare land, settlement) were classified as the class "Others". The Table 4 is an overview of the trees and DBH distribution from the field measurements. Table 5 also gives details on AGC stock per stratum estimated from the field measurement.

Table 4: Tree and DBH distribution

Strata	Number of plots	Number of trees	Number of trees/ha	Sum of DBH/cm	Average DBH/cm
Cocoa	27	82	49	5842.10	71.25
Cropland	31	86	44	4411.30	51.90
Fallow	7	18	41	1410.00	78.33
Forest	18	321	357	8476.00	26.41
Overall	83	507	102	20139.40	39.57

Table 5: Above-ground carbon stock per stratum estimated from the DBH of the sampled trees

Strata	Total area/sqrm	Total Area/ha	Sum of AGC stock kg/stratum	AGC stock tons/ha	Average AGC stock in tons / plot
Cocoa	16875	1.6875	193037.04	114.39	71.49
Cropland	19375	1.9375	140067.01	72.29	45.16
Fallow	4375	0.4375	76729.01	175.38	10.96
Forest	9000	0.9000	128419.06	142.69	7.13
Overall	49625	4.9625	538252.12	108.46	6.48

Forest recorded more trees per hectare than all the other land cover types. The number of trees recorded in the forest stratum alone constituted about 63.31% of the total number of trees sampled in the study area. This is because, the impact of human activities such as illegal logging on farmlands (cocoa, cropland) hinder the growth of young trees (Gelens et al., 2010). Furthermore, policies to protect trees outside the forest reserve are not strict and uniform in Ghana (Wiggins et al., 2004). Meanwhile, the forest is a reserve and under the strict protection by the government.

Despite the fact that, the forest recorded the highest tree density per hectare, the average DBH of the trees in the forest was the lowest among all the other land cover types (strata). This may be attributed to the fact that, the sizes of the trees in the forest were found to be smaller as compared to the trees found on the other strata (fallow, cocoa and cropland). Selective logging of matured trees in the forest reserve may also have accounted for that (Blackett & Gardette, 2008). Fallow land, which on the other hand, recorded the lowest number of trees per hectare, recorded the highest average tree DBH. The reason is that, this stratum is often an unproductive cropland (tree crops, annual crops and perennial crops) left uncultivated for a period of time to enhance the fertility of the soil.

Some farmers intentionally conserve some tree species (*Ceiba Petandra and Alstonia boonei*) on croplands to provide shades for the crops, particularly, in the traditional cocoa farms. As the parcels of the land are left uncultivated, the trees are also left behind to mature, resulting in trees with large DBH and higher AGC stock per hectare as compared to the other land cover types in the study area, irrespective of the lowest number of trees per hectare recorded in this stratum. This also explains why the average DBH of trees on cocoa plantation and croplands respectively were larger than the average DBH of trees found on the forest stratum. However, when the results were extrapolated at a landscape level (per hectare), forest recorded more above-ground carbon stock per hectare than cocoa and cropland. This may be due to the fact that, the tree density on forest stratum was found to be denser than cocoa and cropland. A similar observation was made by Mutanga (2012) in a study conducted in Ejisu Juabeng District of Ghana.

4.2. CPA extraction from the Worldview-2 image

4.2.1. Estimation of Scale Parameter

The ESP tool revealed different peaks of scale parameters at which the Worldview-2 image could be segmented. Among the peaks revealed by the ESP tool as the best scale for the segmentation, a scale parameter of 45 was found to be suitable for segmenting the whole image after a number of trial and error with different scales. The scale parameter of 45 resulted in object (tree crown) size close to the one observed on the field. This suggests that, a scale parameter for segmentation is instrumental in the accuracy of multi-resolution segmentation. Kim et al. (2008), described the scale parameter as the determinant of maximum heterogeneity in the image.

The scale parameter of 45 was however, found to be very huge as compared to the best scale parameters (19-25) selected by other studies for segmenting tree crowns from VHR image (Karna, 2012; Mutanga, 2012). This was expected because, the average DBH of the trees per stratum observed at the study area was found to be larger than the average DBH of the trees per stratum observed by Mutanga (2012) in Ejisu Juaben District of Ghana for instance. The observation made from the field was that, trees with larger DBH tend to have bigger CPA. According to Saha (2008), a scale parameter determines the average image object size. A higher scale parameter allows more merging and consequently bigger objects. Therefore, a higher scale parameter is used when a bigger CPA is expected and vice versa. The figure 7 below, shows the peaks of the scale parameter for the segmentation produced by the ESP tool.
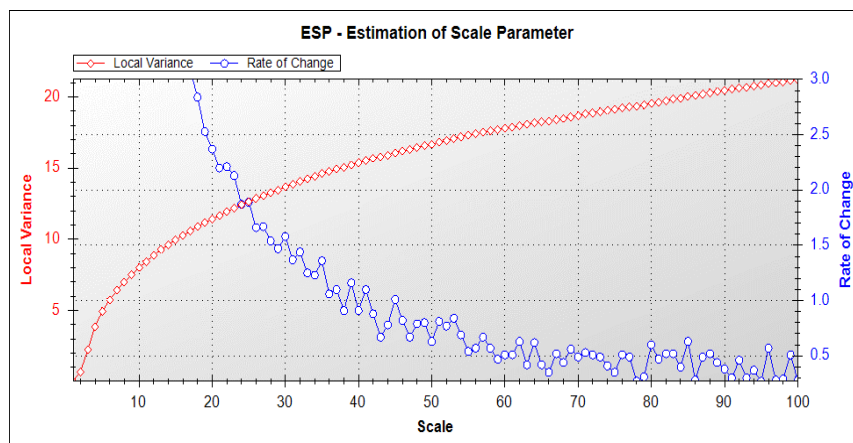

Figure 7: A graph showing different peaks of the scale parameter.

4.2.2. Multi-resolution segmentation

A combination of object scale 45, shape 0.8 and compactness 0.5 were found to be more appropriate for segmenting the Worldview-2 image, after a number of iterative processes. Masking of shadows was possible at a brightness value of less than or equal to 320. A simple ratio greater than 3.5 was able to split a contrast between tree crowns and other objects. A length factor of 72 pixels, which is 36 meters was able to split clusters of tree crowns (intermingled crowns).

Though "close image object algorithm" is often used over the "open image object algorithm", and it is recommended for smoothing (shaping) tree crowns and also to fill the holes created inside the segmented image, especially in a situation whereby removal of shadows, undesirable features and differences in spectral properties from the image objects have left spaces in the image, it was however observed that "close image object algorithm" was not suitable for smoothing tree crowns of a very huge image. Since its application was not successful in smoothing the whole Worldview-2 image. The morphological processes could not be completed when the algorithm was applied. Baral (2011), also applied "close image object algorithm" in smoothing tree crowns and attributed the failure of the algorithm to complete the morphological process to the inability of the eCognition software program to process a very huge image. Contrary, "open image object algorithm" was faster and more successful in smoothing the whole WorldView-2 image in this research.

It was also discovered that, a roundness value of 0.7 was able to get rid of most of the crowns of cocoa trees from the image. This procedure was also believed to remove pockets of oil palm crowns found on the image. Some other studies used vegetative indices such as red-edge band comparison (Digital Globe, 2008) and modified vegetative indices (Sims & Gamon, 2002) to automatically mask oil palm crowns from the segmented images. Nevertheless, the Worldview-2 image which was used for this study contained only four bands (the 3 visible bands and the near infrared). Also, the coastal blue and the red edge band needed for the calculation of the modified vegetative indices and the red edge comparison respectively were absent in this Worldview-2 image and hence it was not possible to use this approach.

Besides, the use of vegetative indices to automatically mask out oil palm in a similar study was found to affect tree crown delineation (Mutanga, 2012). Furthermore, a comparative study to mask oil palm manually and automatically conducted by the same author revealed that, oil palm masking by manual delineation yielded a better accuracy than automatic delineation using vegetative indices. This was attributed to the fact that, oil palm exhibits a homogenous distinct star shape which is obvious and explicitly different from tree crowns to facilitate manual masking.

It can be deduced from the findings that, automatic removal of the crowns of the oil palm and the cocoa trees from the image causes the removal of most of the crowns of the desirable tree crowns from the image. Therefore, when the shape condition decreases, the removal of the oil palm and cocoa tree crowns increases and vice versa and this was recognized to hinder the accuracy of the segmentation output. On the other hand, automatic tree crown delineation was very suitable for separating the crowns of vegetation from other objects such as shadows, water, clouds, bare land, settlements and roads. A length pixel of 20 and an area pixel of 20 were able to remove extremely tiny objects in addition to elongated objects from the image. Figure 8 and 9 depict the segmented image before and after separation of tree crowns from the other objects.
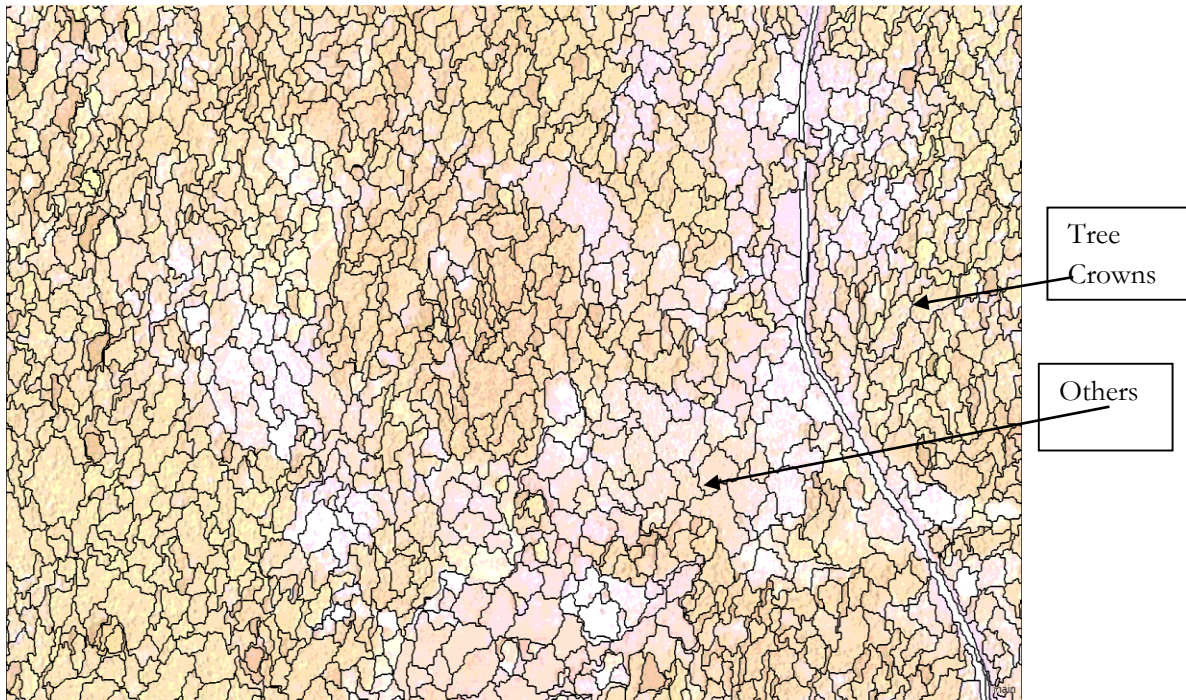
Figure 8: Segmented image before separation of other objects
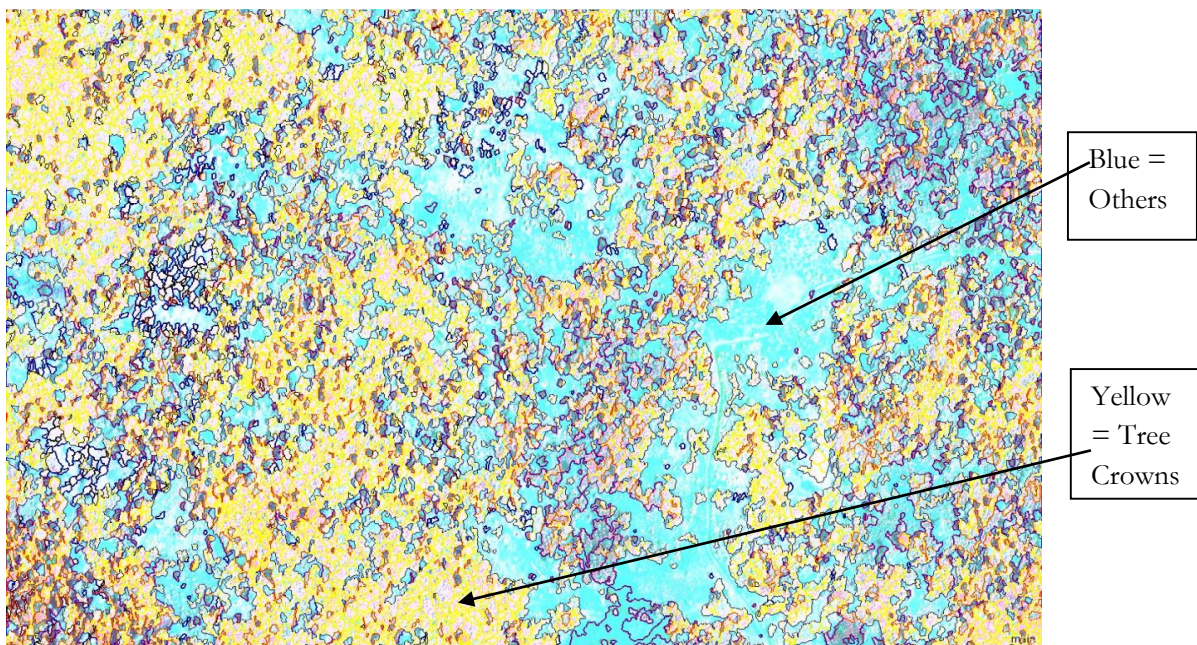
Figure 9: Segmented image after separation of other objects

4.2.3.   Segmentation accuracy

The worldview-2 image was covered by shadow, built up areas, dense forest with relatively closed canopy and intermingling crowns, cocoa trees also with elongated and intermingling crowns, oil palm plantation and other vegetation such as grass, shrubs and crops. All these, were capable of hindering the accuracy of the segmentation, yet the accuracy of the segmentation was found to be high. Out of the 1000 reference polygons (manually delineated tree crowns), about 808 (80.8%) were found to exhibit 1:1 matching with the automated tree crowns. This signifies that the accuracy of the segmented tree crowns was high.

This was not surprising, because the accuracy assessment of the segmentation is based on the positional accuracy of the manually delineated segments (reference polygons) with respect to the automated segments (Zhan et al., 2005). Mutanga (2012) also obtained segmentation accuracy between 72-83% when multi-resolution segmentation algorithm was applied for tree crown delineation in a similar setting (Ghana).

It can therefore be inferred that, the multi-resolution segmentation algorithm in the eCognition software program is an opportunity to extract biophysical parameters of trees from very high resolution satellite image, such as Worldview-2. A proven evidence to support the assertion that, high resolution image can offer the opportunity to extract very detailed information at the individual tree level (Leckie et al., 2003). Therefore, there is more hope for extraction of tree parameters for accurate AGC stock estimation in Ghana, irrespective of the complex ecosystem.

4.3.   Regression modelling

4.3.1.   Linear regression model between CPA and field calculated AGC stock

It was discovered from the results that, the DBH of the trees which were measured on the field and the CPA, delineated from the Worldview-2 image were not normally distributed. The results from a scatter diagram depicted that, the data were skewed. A linear regression model between 70% samples of the above-ground woody carbon stock of the trees, estimated from the DBH and the CPA extracted from the Worldview-2 image resulted in R^2 of 0.59 and multiple R of 0.77. Indicating that, the CPA was able to explain about 59% and 77% of variation in AGC stock estimated from the DBH respectively. The equation from the regression model is shown below:

Equation 8: Linear Regression Model between CPA & AGC Stock

Y=11.236 X -219.72

Where,

Y is the AGC Stock from the Worldview-2 image

X is the Segmented CPA

The validation model also predicted some negative AGC stock values as in the case of the estimation model, despite the very high R^2 (96%) which was recorded. Baral (2011) also obtained negative predicted AGC stock values from a linear relationship between CPA and field calculated AGC stock values in sub-tropical forest of Nepal. The negative carbon values predicted by the model was expected because, GFD is a complex ecosystem with DBH range (26.4-78.3cm), exceeding 50cm. As Hemery et al. (2005) pointed out, the DBH range exceeding 50cm may lead to distortion of the linear relationship between DBH and CPA due to the effect of senility and competition by the nearby trees.

Goaso forest reserve is a natural forest, very dense with closed canopies and intermingling tree crowns and hence competition with neighbouring trees and the problem of senility might have affected the growth of the tree crowns and this might have accounted for the negative values predicted by the linear regression model. The DBH of the trees in the cocoa plantation might also have contributed to this distortion, because the crowns of the cocoa trees were also found to be intermingling and might have caused competition with the other tree crowns. Furthermore, this model only works for trees with DBH above 10cm since trees with DBH below 10cm were not measured on the field and hence applying the model below 10cm of trees DBH may lead to distortion of the model.

Nonetheless, the removal of the outliers from the data set might have accounted for the high R² (96%) obtained by the validation model for instance, since more outliers were removed from the forest and cocoa strata. This observation is in support with the explanation presented by Mora et al. (2010) that, removal of outliers from a data set results in a good and a robust model. Figure 10 and Figure 11 illustrate the regression model between CPA and field calculated AGC stock for the estimation and the validation samples respectively. More details of the summary results can also be found in the Appendix 1 and Appendix 2.
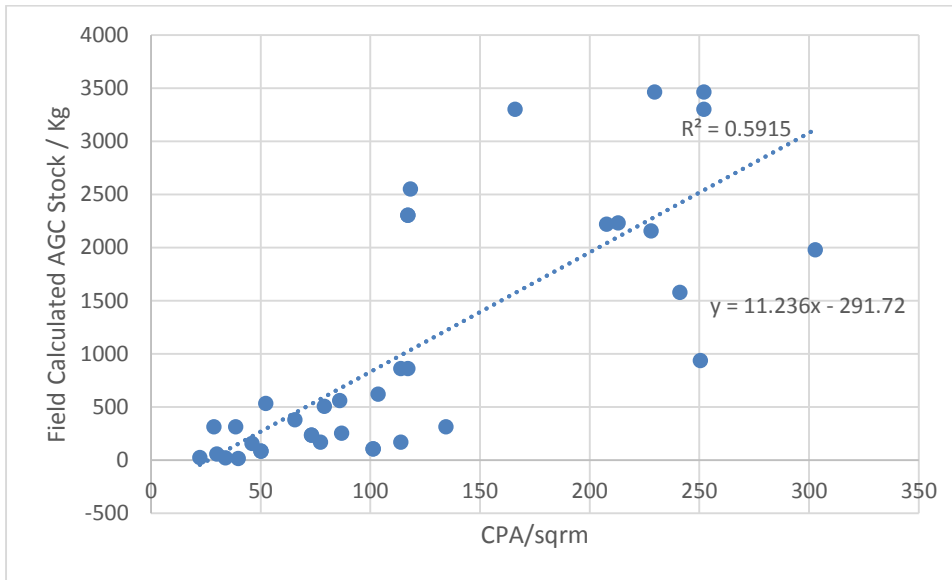
Figure 10: A graph showing the linear regression model between field calculated AGC stock and CPA
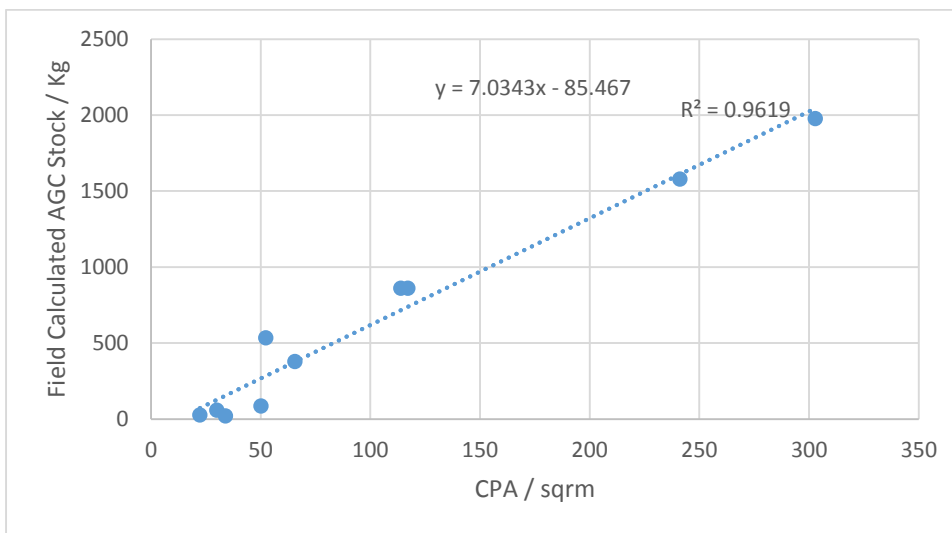
Figure 11: A graph showing validation of the linear regression model between field calculated AGC stock and CPA

4.3.2. Linear regression model between CPA^2 and field calculated AGC stock

Linear regression model between the AGC stock, estimated from the DBH and CPA^2 (transformed CPA) on the other hand, predicted only positive AGC stock of trees. The model yielded R² of 0.52 and multiple R of 0.72, indicating that the model explained about 52% and 72% of the variation in the AGC stock respectively. The Table 6 and Figure 12 below throw more light on the results from the model.

Table 6: Summary of the regression model between field calculated AGC stock and CPA^2

SUMMARY OUTPUT

Regression Statistics	
Multiple R	0.72
R Square	0.52
Adjusted R Square	0.50
Standard Error	810.74
Observations	37

ANOVA

	df	SS	MS	F	Significance F
Regression	1	245	24535702	37.33	5.54E-07
Residual	35	23005749	657307.1		
Total	36	47541451			

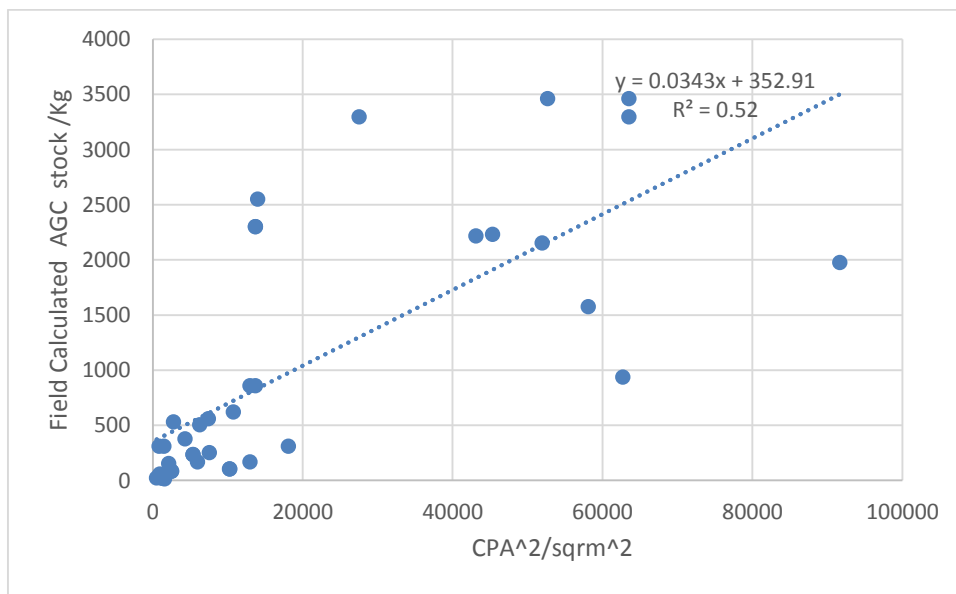|	Coefficients	Standard Error	t Stat	P-value	Lower 95%	Upper 95%
Intercept	352.91	175.21	2.01	0.05	-2.78	708.60
CPA^2	0.03	0.01	6.11	5.54E-07	0.02	0.05

Figure 12: A graph showing the linear regression between field calculated AGC stock and CPA^2

4.3.3. Validation of the AGC stock and CPA^2 Model

The R^2 (0.87) and the multiple R (0.94) obtained from the validation samples were higher than the ones obtained from the estimation samples. The values obtained were an indication that the model explained about 87% and 94% of the variation in AGC stock. The details of the results from the validation model are shown in Table 7, Figure 13 and Figure 14.

The positive AGC stock values predicted by the AGC stock and CPA^2 regression model confirm the claim made by Shimano (1997) that, CPA grows with the second power (square) relationship with the DBH, and the increase rate slows as DBH increases with transformation. This assertion holds because when the model was also fitted with second order polynomial equation, the model resulted in high R^2 and predicted only positive AGC stock. However, this approach was not used because when a polynomial is forced through a data, the implication of the imposed shape of the function is that, the range at which the model could be applied will be limited since errors may be extrapolated when the model is applied beyond the range of the model development as it was observed from the negative values predicted by the CPA and AGC stock model (Anderson et al., 2000).

Table 7: Summary of the validation of regression model between field calculated AGC stock and CPA^2

SUMMARY
OUTPUT

Regression Statistics	
Multiple R	0.94
R Square	0.87
Adjusted R Square	0.86
Standard Error	258.03
Observations	10

ANOVA

	df	SS	MS	F	Significance F
Regression	1	3720767.17	3720767	55.88	7.09E-05
Residual	8	532639.29	66579.91		
Total	9	4253406.46			

	Coefficients	Standard Error	t Stat	P-value	Lower 95%	Upper 95%
Intercept	246.21	96.97	2.54	0.03	22.60	469.83
CPA^2	0.02	0.003	7.48	7.09E-05	0.01	0.03
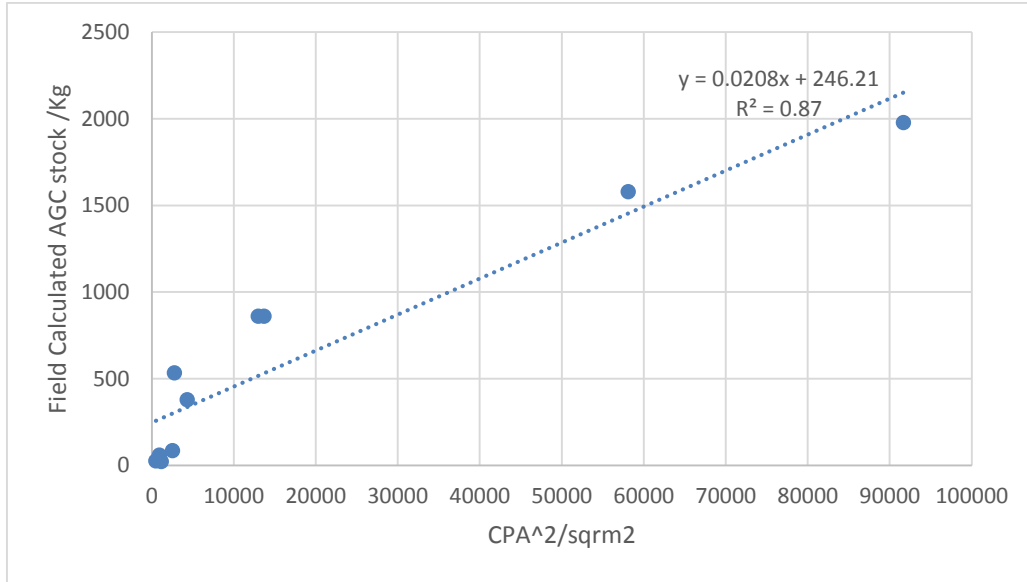
Figure 13: A graph showing validation of the linear regression between field calculated AGC stock and CPA^2
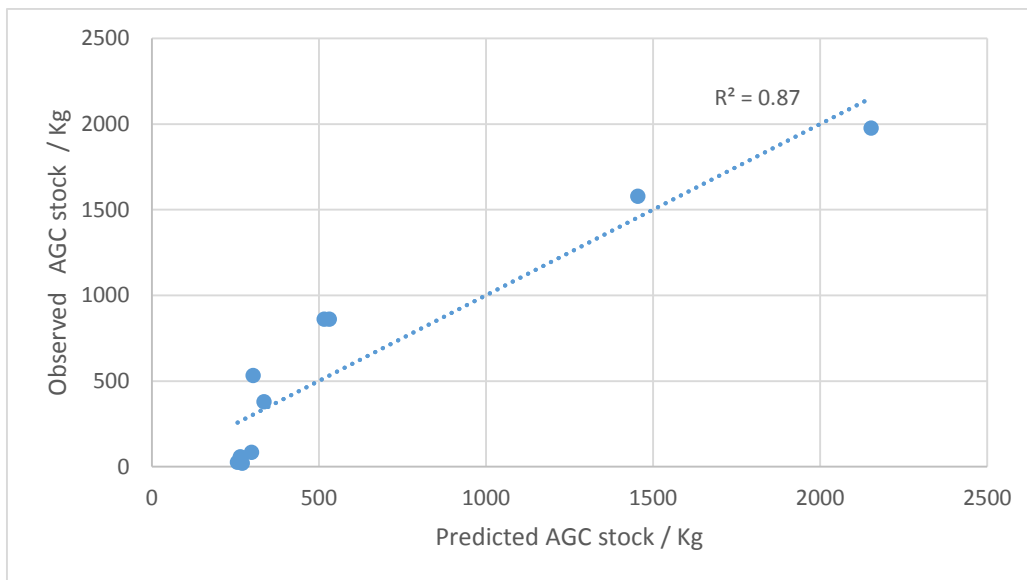
Figure 14: A graph showing the observed AGC stock against the predicted AGC stock from CPA^2 and AGC stock model

4.4. AGC stock estimation from the Worldview-2 image.

Approximately 210470 tree crowns were extracted from the Worldview-2 image. The equation 9 from the CPA^2 and the observed AGC model, yielded a total AGC stock of 157628003.4 Kg over the entire area (2894.339429 hectares) covered by the extent of the Worldview-2 image. This amount is equivalent to 54.5 tons per hectare. An average AGC stock of 761.54 Kg and standard deviation of 1688.96 Kg were also estimated from the Worldview-2 image.

Equation 9: CPA^2 & AGC Linear Regression

Y = 0.0343x+352.91

Where,

Y is AGC stock estimated from the Worldview-2 image

X is CPA^2

The uncertainty surrounding the total AGC stock estimate was found to be 0.0014 tons per hectare. Out of the total carbon density per hectare estimated for the whole area (GFD), the agro-ecosystem (off-forest reserve) recorded 28.0 tons per hectare and an uncertainty of 0.0020 tons per hectare, whilst the forest reserve also recorded 26.5 tons per hectare and an uncertainty of 0.0008 tons per hectare. Signifying that, without the trees in the agro-ecosystem, the carbon stock in the Forest District would have been only 26.5 tons per hectare. Figure 15 is a carbon map of the study area created from the final segmented tree crowns.
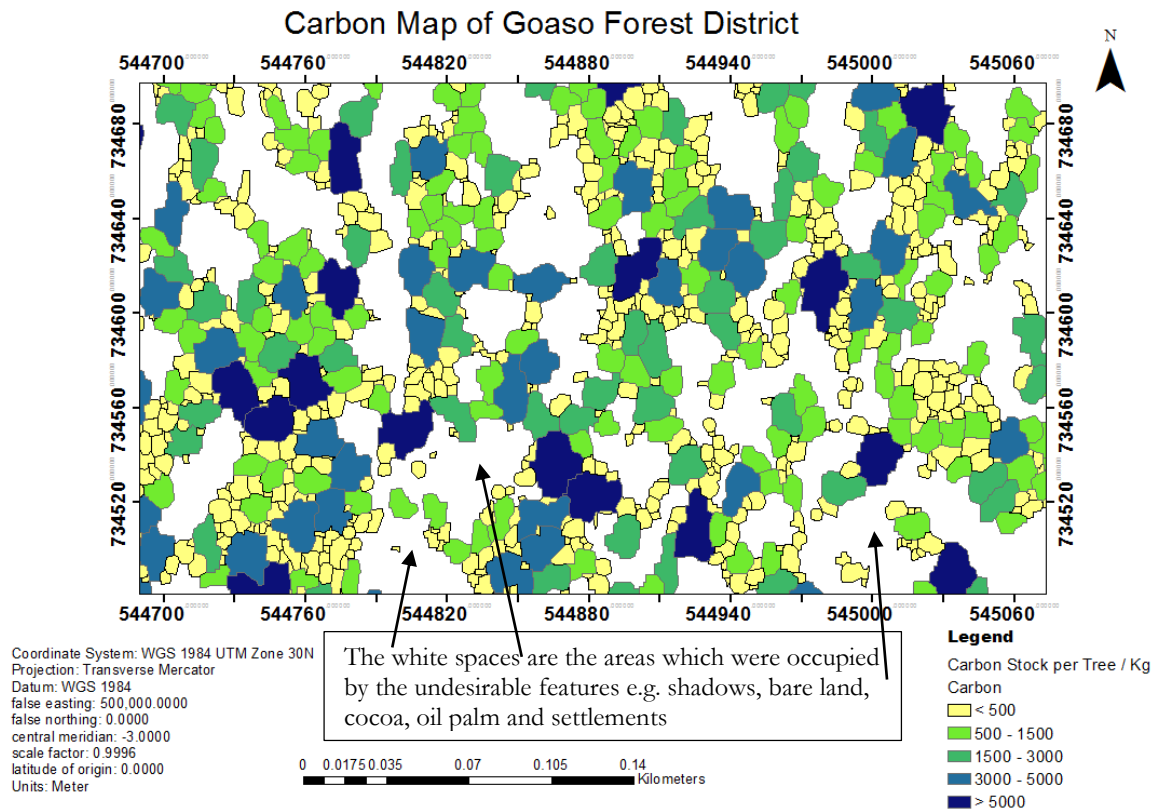
Figure 15: Carbon map of Goaso Forest District

Though it was expected that, the estimates in the agro-ecosystem would be higher than the forest reserve due to its bigger extent in terms of area coverage, other factors might have also contributed to the differences between the two estimates. One of the contributing factors is the tree size; the sizes of the trees in terms of DBH in the agro-ecosystem were found to be extremely bigger than the trees in the forest reserve. It was observed from the field that, DBH is correlated with the CPA. The bigger the DBH of a tree the wider the CPA, it was on some few instances when trees with huge DBH were found to have small CPA. *Ceiba*

pentandra is one of the tree species which exhibited such abnormality. Mutanga (2012) also came across the same finding on the field in Ghana.

Another factor which might have accounted for the higher AGC stock estimates in the agro-ecosystem as compared to the forest reserve was the presence of cocoa, oil palm, other vegetation and shadow on the image. Though, morphological operations were applied to get rid of crowns of the undesirable features (e.g. cocoa trees and oil palm) from the image, not all of them were removed. Particularly, the crowns of oil palm plantation. Effort to remove all of them also removed some of the desirable tree crowns. For instance, some of the threshold conditions used to remove the crowns of the cocoa tree were crown diameter and shape. Tree crowns with crown diameter less than 10m (20 pixels) and roundness greater than 0.7 were presumed to be the crowns of cocoa trees, owing to the fact that the crown diameter of cocoa trees are small and intermingling with elongated shape as compared to the natural trees.

However, some of the tree crowns in the forest reserve were also small in diameter, intermingling and elongated in shape and therefore many of such tree crowns in the forest reserve were also removed as undesirable features, thereby affecting the carbon estimates in the forest reserve. According to Preece et al. (2012), the contribution of small trees with stems <10cm to AGC stock estimates in plantings <20 years old is about 15%. Selective logging of desirable tree species in the forest reserve also attest to this fact since, annual allowable cuts in the forest reserves in Ghana have been increased from 1million to 2 million, cubic meter (Blackett& Gardette, 2008).

The carbon estimates from this research is not too different from the estimates published in scientific literature in tons per hectare for Ghana. In 1997, Brown hypothesized a potential AGB (without human intervention) of 182 tons per hectare equivalent to 85.54 tons per hectare AGC stock as well as 83 tons/hectare actual AGB (with human interventions) equivalent to 39.01 tons AGC stock per hectare from RS estimates for forest in Ghana (Brown, 1997). In 2000, Brown reviewed the AGB default values and published default values of 121.5 Mg /hectare and 68.3 Mg per hectare for closed and opened forest found in Ghana respectively, equivalent to 57.10 Mg C/hectare and 32 Mg C/hectare of AGC stock respectively. Carbon in Mg/hectare is in the same quantity and comparable to carbon in tons per hectare. Ministry of Land and Natural Resources (2012) also published an AGB of 275-400 Mg/hectare (129.3-188 Mg C/hectare) for forest reserve and 125-225 Mg/hectare (58.75- 105.75 Mg C/hectare) for the off-forest reserve. Furthermore, Mutanga (2012) also obtained an AGC stock of 45.9 Mg C/hectare for trees on farmlands in Ejisu-Juaben District of Ghana.

4.5. Pixel based image classification and accuracy assessment

The results from the pixel based classification of the Landsat-7, 2000 (initial land cover map) and Landsat-7, 2012 (final land cover map) as well as the accuracy assessment of the classification results are shown in Figure 16 and Table 8 respectively. The overall accuracy of the 2012 image classification was 71.69%, despite the fact that the image suffered from "line stripping". This is because, the classification result was improved by the field observations and World-view-2 image. Also, on the Landsat-7 imageries, there was a clear distinction between the various land cover types. The only constraint was the distinction between the natural trees and the tree crops (cocoa, oil palm). A major conversion of forest to cropland and the class "others" was observed on the 2012 final land cover map. Expansion of cocoa plantation in the Forest District was evident on the field. Bare land emanating from logging of trees was also observed on the field.
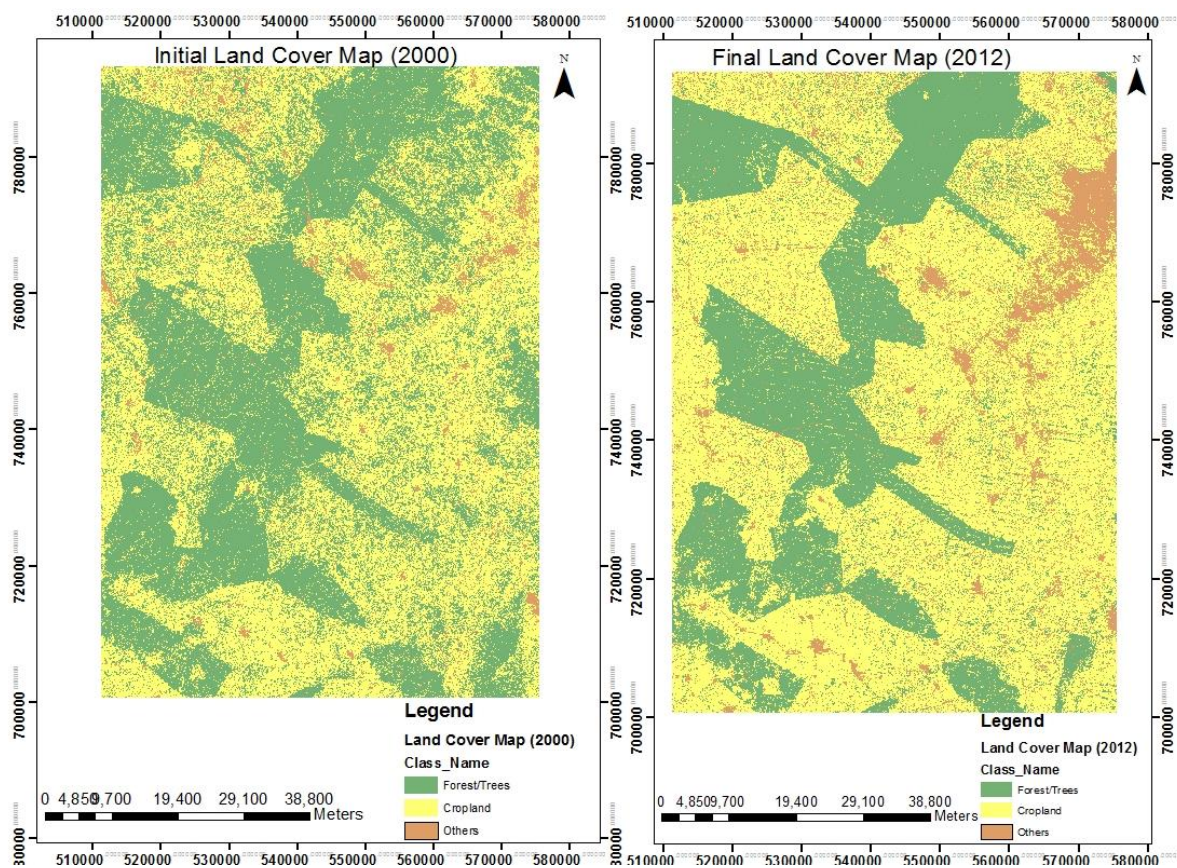
Figure 16: Initial (2000) and Final (2012) Land Cover Maps

Table 8: Error matrix from the accuracy assessment of the 2012 image classification

	Image Classification Results					
Reference	Forest/trees	cropland	others	Total	Error of Commission %	User Accuracy/%
Forest/Trees	37	25	3	65	43.08	56.92
Cropland	16	65	4	85	23.53	76.47
Others	2	10	50	62	19.36	80.64
Total	55	100	57	212		
Error of Omission %	32.72	35	12.28			
Producer Accuracy %	67.28	65	87.72			
Overall accuracy %	71.69					

4.6.   Modelling in Dinamica EGO software program

4.6.1.   Change Rate

The Table 9 and 10 give detailed account on the change rate from one land cover to another under BAU.

Table 9: Single transition matrix (overall change rate from 2000-2012 (12 years period))

Conversion From*	To*	Rate
Forest / Trees	Cropland	0.39
Forest / Trees	Others	0.04
Cropland	Forest	0.12
Cropland	Others	0.14
Others	Forest/Trees	0.08
Others	Cropland	0.45

Table 10: Multiple transition matrix (annual change rate from 2000-2012)

Conversion From*	To*	Annual Rate
Forest/Trees	Cropland	0.05
Forest/Trees	Others	-
Cropland	Forest	0.01
Cropland	Others	0.02
Others	Forest/ Trees	0.01
Others	Cropland	0.06

Analysis of the change rates revealed that, the forest district witnessed an unparalleled change rate of (39%) from forest/trees to cropland between the periods of 2000-2012. An annual conversion of 5% was also observed from forest/trees to cropland. The results also revealed that, on the annual basis, there was no conversion from forest/trees to the class "others". Suggesting that annual conversion from forest/trees to the class "others" was minimal. Over the entire period (2000-2012), forest/trees recorded a total loss of 43% and a total gain of 20% resulting in a net loss of 23%. The 20% gain in the forest/tree cover may be attributed to the re-introduction of tree planting (Agroforestry), popularly known as "Taungya" in the country by the Government of Ghana in 2002 (Kalame et al., 2011; Ros-tonen et al., 2013). A period (2000-2012) within which the change rate of this research was calculated. The tree planting exercise was a call in the right direction because, it had a positive effect on the deforestation rate which was reflected in the findings by Damnyag et al. (2013), when a comparison, was made between the rate of deforestation between 1986-2000 and 2000-2011. A faster rate was found within the period of 1986-2000 than within the period of 2000-2011.

Annually, 3% net decreased in forest/trees was recorded and it was found to be above the national deforestation rate which is approximately 2% annually (FAO, 2010). Damnyag et al. (2013), found an annual deforestation rate of 2% which was in line with the national estimate of Ghana as well as 39% deforestation rate for a period of 25 years in Ankasa Conservation Area of Ghana. The lump percentage of deforestation rate (39%) for the 25 years period is equal to the conversion from forest to cropland only over a period of 12 years in this research, implying that the situation in GFD calls for an urgent attention.

For the conversion from the class "others" to cropland, a very huge rate (44%) was observed from 2000-2012. A total loss of 53% and a total gain of 18% were recorded for the class "others", giving rise to a net loss of 35% in this class. These results were expected because, bare land is one of the constituents of the class "others" and some of the areas covered by the bare land may be a harvested cropland which could be easily converted back during the planting season. On the annual basis, there was a net loss of approximately 5% from the class "others" to forest/trees and cropland.

Cropland recorded an unprecedented total increase of 84% and a total loss of 26% leading to a net gain of 58% in land area between the periods of (2000-2012). A net annual increase of 8% was also recorded for the cropland. The results are indication that, crop expansion is booming in the Forest District. Most of the conversion from forest to cropland was found at the periphery of the forest reserve. Damnyag et al. (2013) also identified a higher rate of deforestation at the periphery of Ankasa Conservation Area of Ghana as compared to the core protected and the farthest areas.

4.6.2. Effect of the environmental variables on deforestation

Figure 17 and Figure 18 depict the effect of the environmental variables on deforestation and subsequently AGC stock. Figure 17 shows the effect of the environmental variables on the conversion of forest to the class "others", whilst the Figure 18 shows the effect of the environmental variables on the conversion of forest to cropland. It was discovered from the results that, the effect of distance to protected areas on deforestation was insignificant because, the weight of evidence contrast of zero was recorded at all the ranges (weight of evidence contrast = 0 means no significant effect, contrast > 0 means significant effect which favours deforestation, contrast < 0 means significant effect which inhibits deforestation). The effect of all the other spatial variables (distance to town, distance to road, distance to streams, digital elevation model), investigated in this study were found to exhibit a significant effect on deforestation.

The general trend was that, nearby distances favoured deforestation whilst distances farther away opposed it. The only exception to this trend was the effect of distance to town on deforestation. Though, distance within 0-3000m was found to favour conversion from forest to others, distances (2780-31000m), very far away from town, favoured more conversion of forest to the class "others". The intermediate distances (>3000<27800) were found to inhibit the conversion of forest to the class "others" but with some few pockets of distances which favoured the conversion. This trend could be attributed to the selective logging of trees and encroachment in the core area of the forest reserve. It was noticed from the 2025 projected BAU map that, most of the conversion from the forest to the class "others" will take place in the future around Kenyanse, one of the towns in the Forest District where Newmont Mining Company operates.

On the other hand, distances (100-2000m) nearby towns favoured more conversion of forest to cropland. The fact that farmers in Goaso prefer to have their farmlands not too far from their residence might have accounted for that (Gelens et al., 2010). Above 2000m, distance to town inhibited deforestation but was observed to favour deforestation again beyond a distance of 15200m. This could be explained as the degraded land in the core area of the forest reserve which was given to some farmers to practice agro-forestry (Kalame et al., 2011). The findings from the distance to towns on deforestation contradicts the findings by Gelens et al. (2010), when they examined the effect of distance parameters on deforestation from 1986-2004. Distance to town was found to favour more deforestation within a distance of 0-3000m. This discrepancy may be attributed to the fact that, they examined the effect of distance to town up to a maximum of 4000m, whilst this study examined the effect of distance to town on deforestation up to 31000m. The differences in the year of study (1986-2004) by Gelens et al. (2010) and (2000-2012) by this study might have also contributed to the differences in the findings. Apart from distance to town, all the other findings from the effect of the environmental variables on deforestation were found to be in agreement with the findings by Gelens et al. (2010).
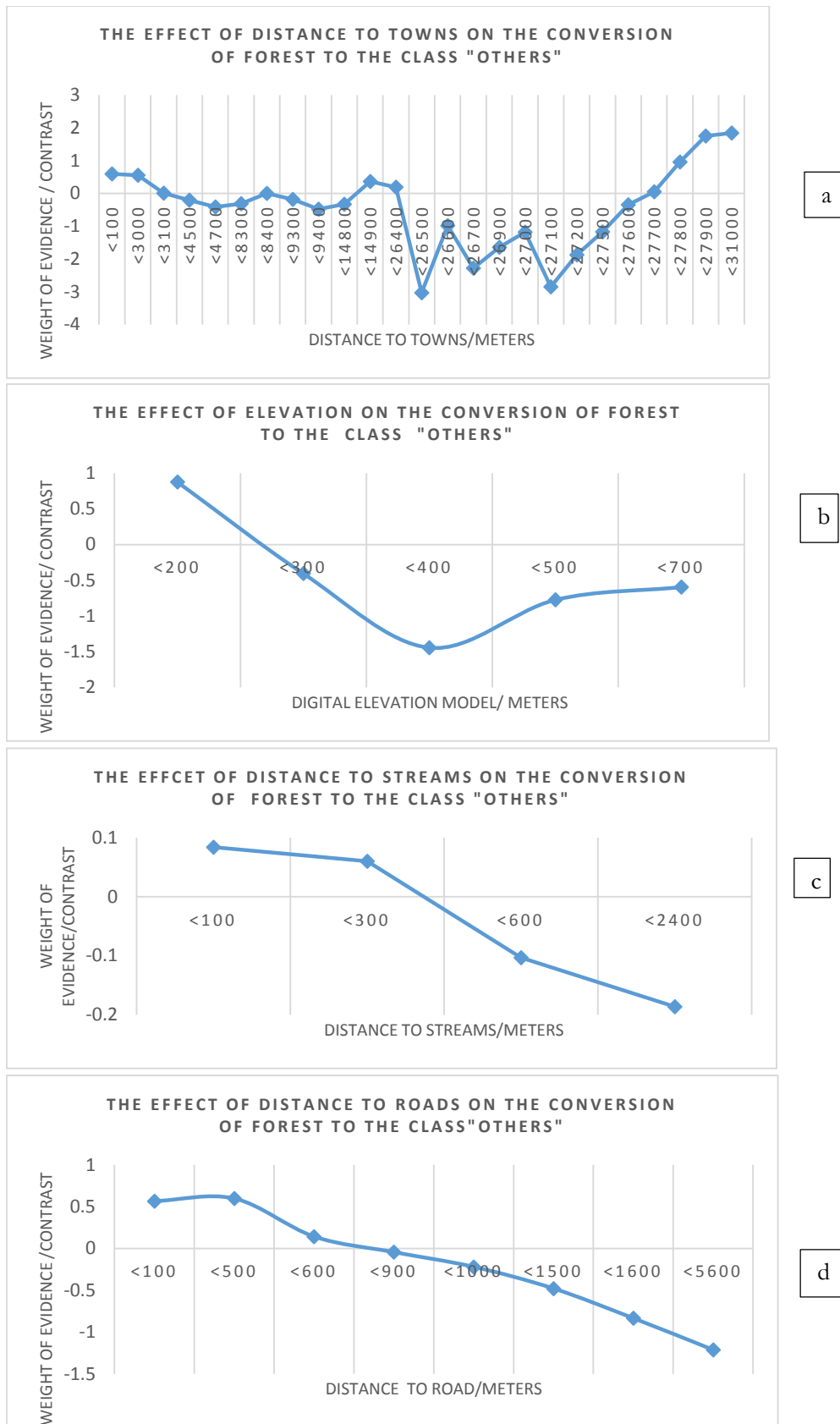
Figure 17: The effect of the environmental variables on the conversion of forest to the class "others"
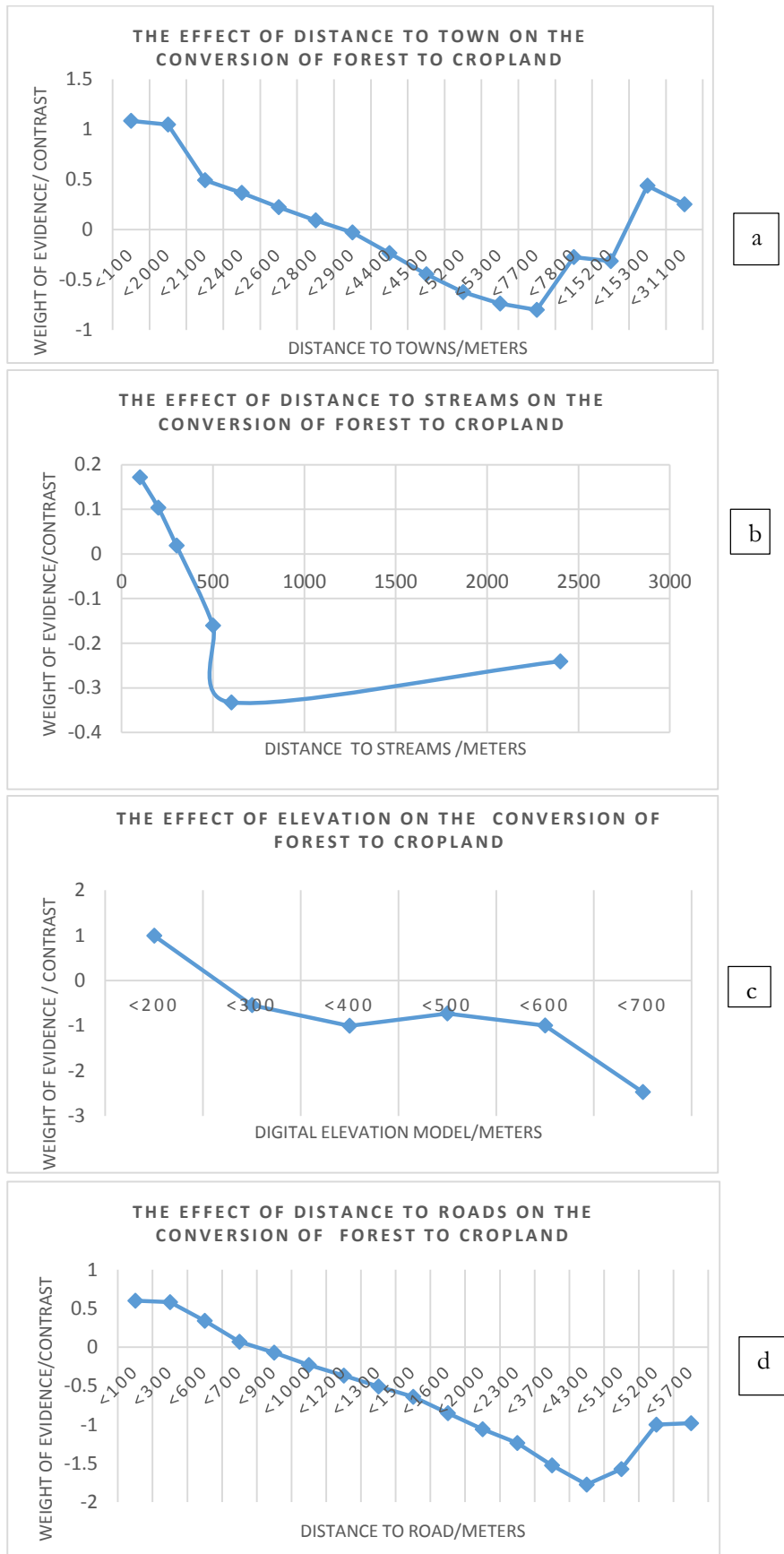
Figure 18: The effect of the environmental variables on the conversion of forest to cropland

In general, distance to town was found to exacerbate more deforestation than all the other spatial variables investigated in this study. Low elevation between (0-200m) was seen as the next to favour more conversion of forest to cropland after distance to town and this is attributed to the fact that, farmers in Ghana prefer farming on a low land, an observation which was made on the field. This is also due to the fact that, highlands may be prone to erosion when trees on them are cut and hence this may discourage the farmers from farming there. More details of the results from the effect of the environmental variables on deforestation, can be found in Appendix 4 to Appendix 8.

Figure 19 and Figure 20 also depict the most favourable areas of change from forest to the class "others" and forest to cropland respectively. The blue regions on the maps indicate areas with low probability of change. The yellow regions indicate areas with medium probability of change and the red regions also indicate areas with high probability of change. It can be observed from the maps that, the agro-ecosystem (off-forest reserve) has a higher probability of change than the forest reserve. This means that, enacting strict laws to protect the trees in the agro-ecosystem will help to boost the AGC stock in the Forest District. More details of other conversions can also be seen in the Appendix 14 to Appendix 17.

Figure 21 depicts changes in 2001, 2015 and 2025 under BAU scenario. It can be seen from the 2025 BAU map that, some of the core areas of the forest reserve would be depleted and converted to the class "others" in the future if the BAU trend continues. It can also be observed that more changes will occur closer to roads, rivers/streams and towns but some conversions of forest to the class "others" would also be seen far away from towns if the BAU trend persists. Another observable feature on the maps is that, the forest reserve looks more depleted under BAU scenario in 2025. Figure 22 on the other hand, is simulated land cover maps depicting changes from 2015-2025 under three different REDD⁺ scenarios. Whilst Figure 23 is a comparison between BAU simulated map in 2025 and the three different REDD⁺ scenarios. It can be observed from the map that, the forest looks greener under REDD⁺ scenario at 0% annual net deforestation rate in 2025.
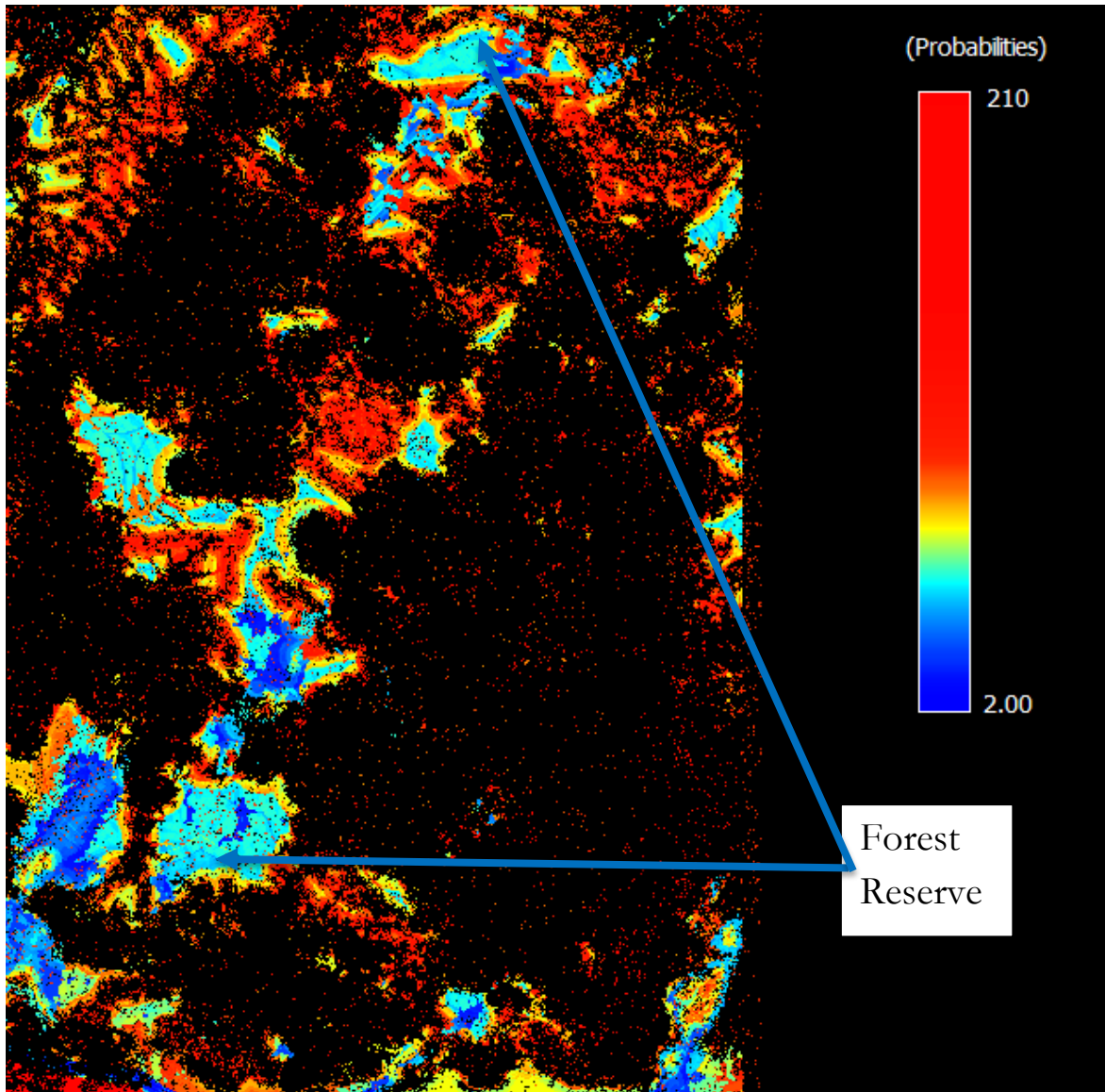
The blue indicates areas with low probability of change, the yellow indicates areas with medium probability of change and the red indicates areas with high probability of change whilst the black is not involved in the analysis.

Figure 19: Probability map depicting favourable areas of change from forest to the class "others".
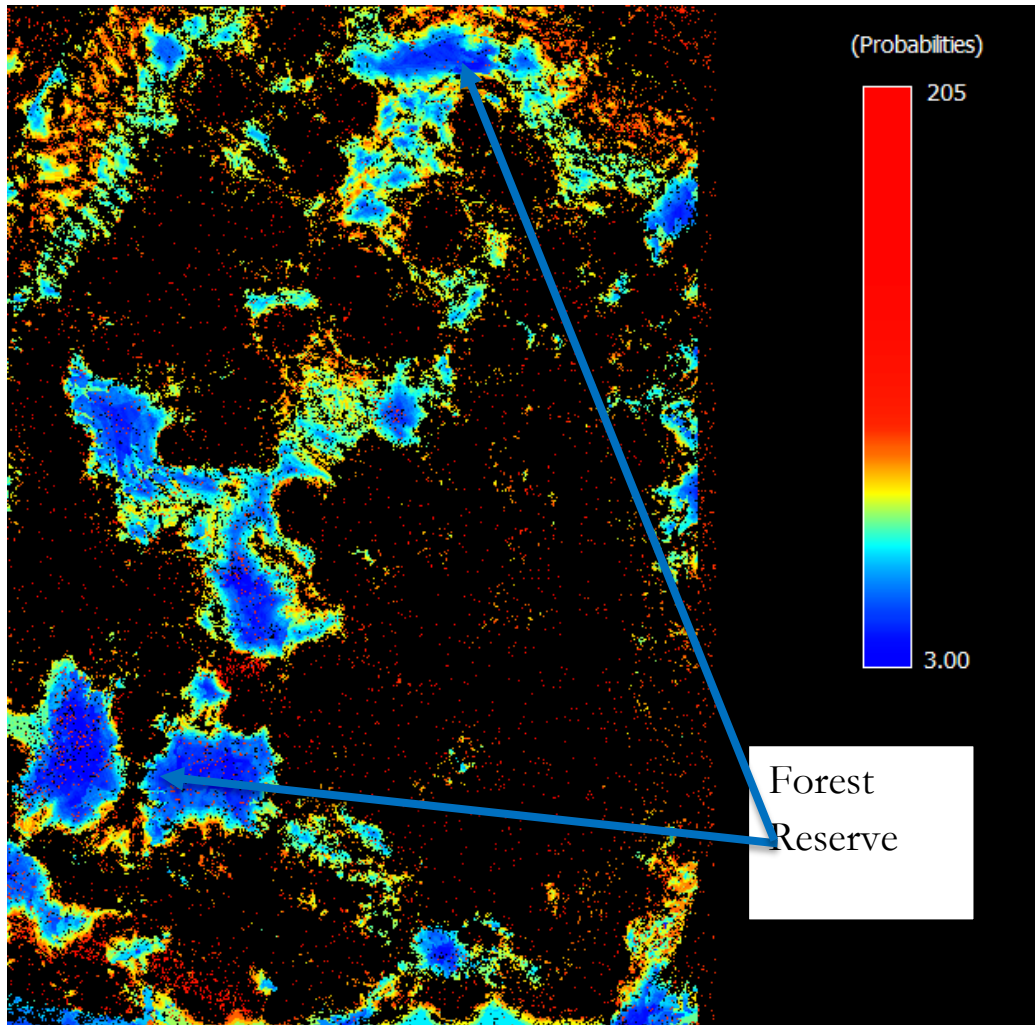
The blue indicates areas with low probability of change, the yellow indicates areas with medium probability of change and the red indicates areas with high probability of change whilst the black is not involved in the analysis.

Figure 20: Probability maps depicting favourable areas of change from Forest to Cropland
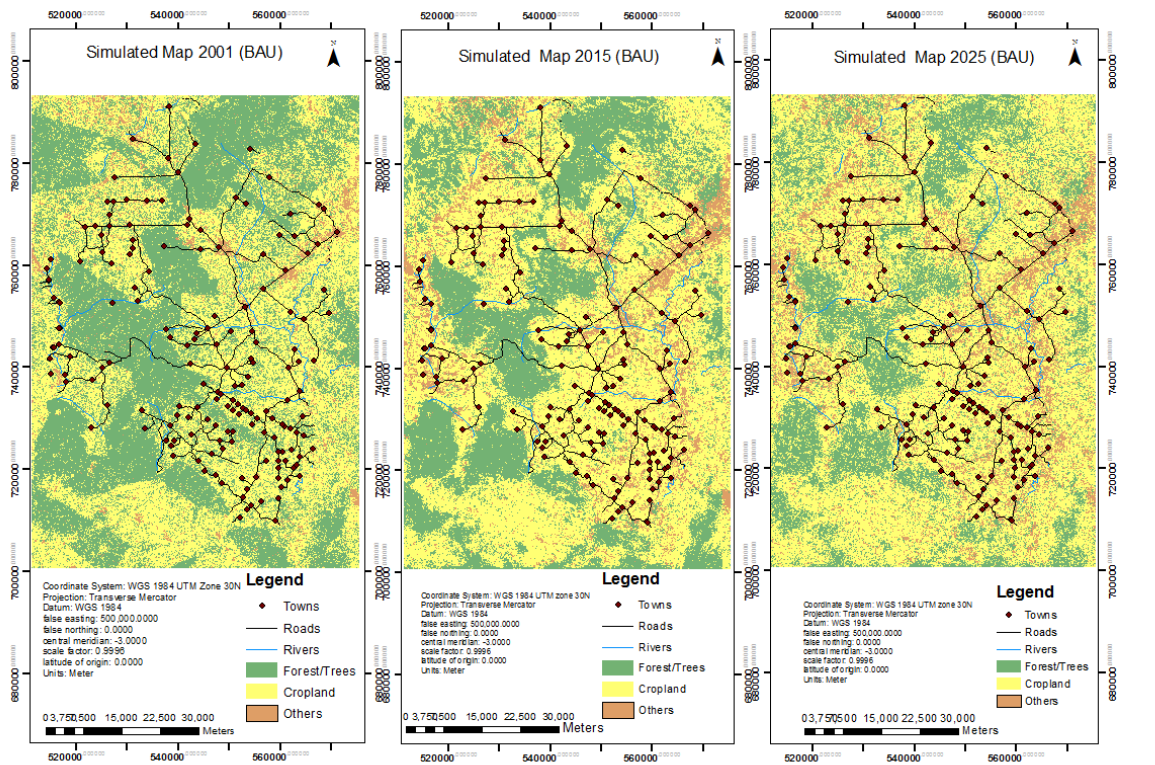
Figure 21: Simulated land cover maps 2001, 2015, 2025 under (BAU)
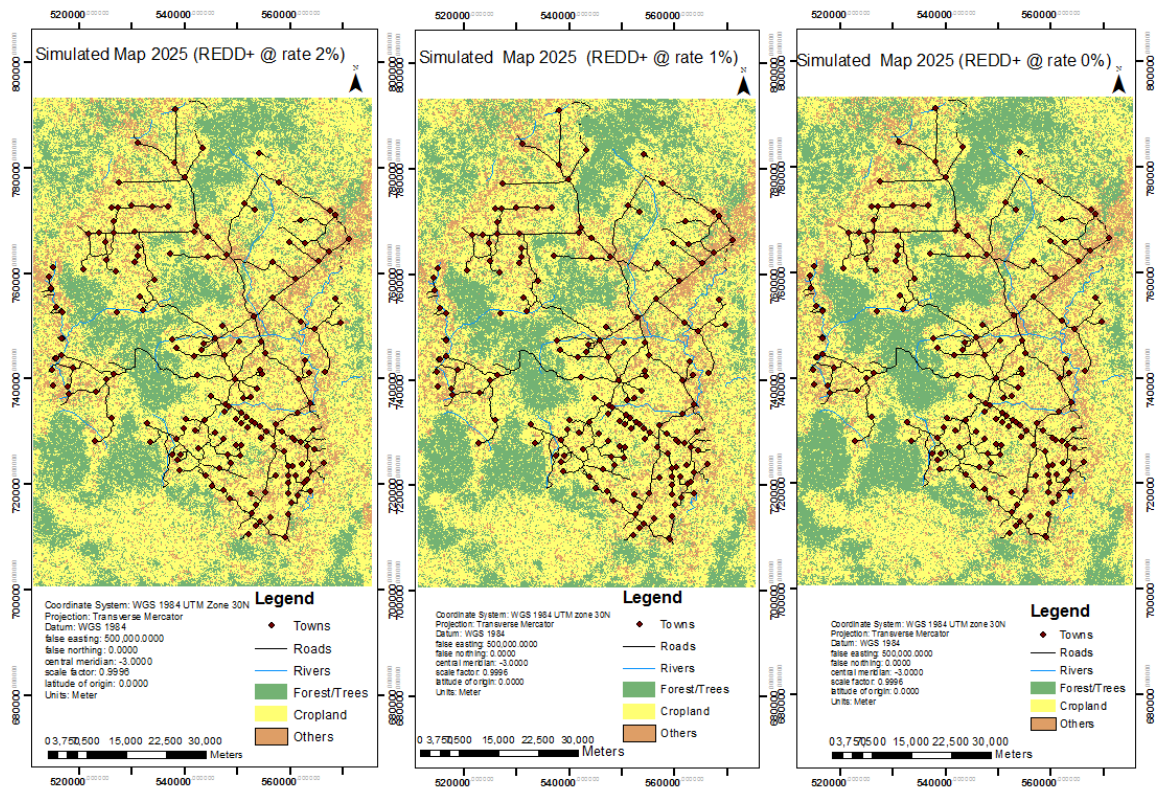
Figure 22: Comparison of 2025 simulated maps under three different REDD+ scenarios
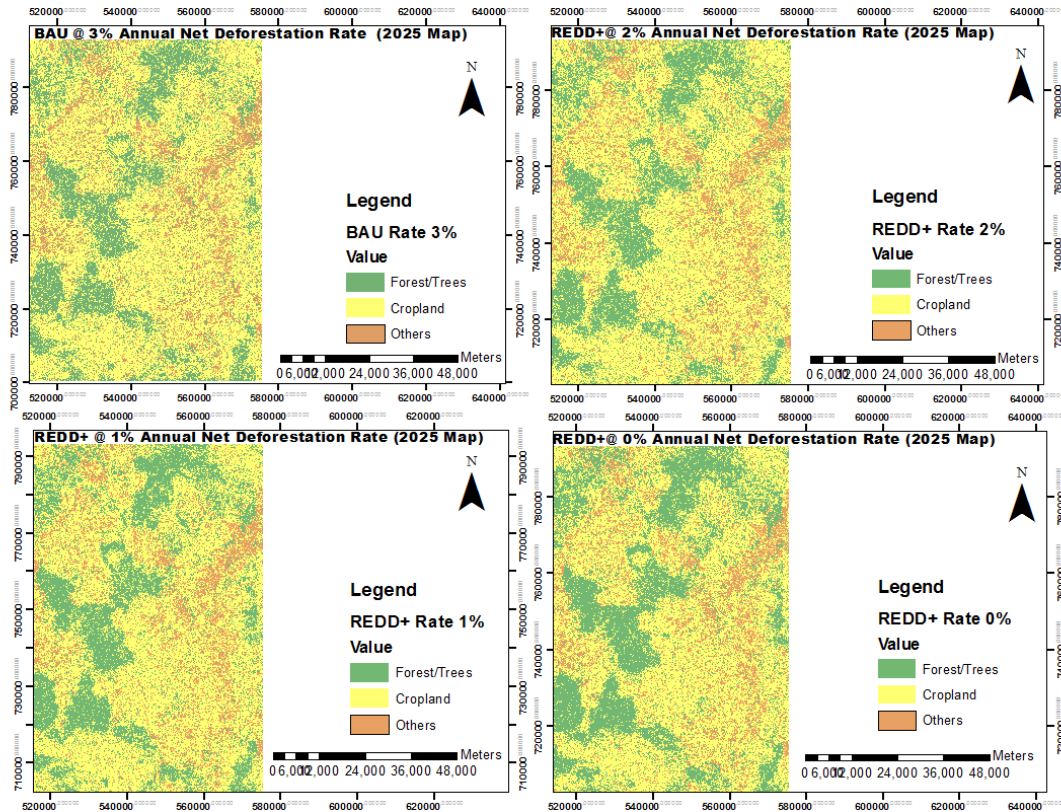
Figure 23: Comparison of simulated land cover maps (2025) under BAU and three different REDD+ scenarios

4.6.3. Carbon stock model under Business as Usual and REDD+ scenarios and uncertainties

The model predicted total AGC stock values of 15014811.36 tons, 9998535.78 tons and 8355896.51 tons for the past (2001), present (2015) and the future (2025) respectively under BAU scenario. A decline of about 33. 4 % in the forest carbon pool for the Forest District from 2001 to 2015 as well as 44.3% decrease in the forest carbon pool from 2001-2025 were projected by the model under the same scenario respectively. Implying that, the forest carbon pool will be shrinking at an alarming rate if this trend is allowed to continue in the future. Also, the model predicted a decline of about 16.4 % from 2015 to 2025 under BAU scenario as compared to 9.2 % and 1.4% decline in the forest carbon pool under REDD+ scenario whereby the annual net deforestation rates were assumed to be reduced to 2% and 1% respectively. In contrast, the model predicted about 7% gain in the forest carbon pool from 2015-2025 under the REDD+ scenario with an assumption that there will be no deforestation (net annual deforestation rate at 0%) but other conversions will continue. Details of the total AGC stock estimates and uncertainties under BAU and REDD+ can be found in the figure 24 and the Appendix 9 to Appendix 13.

Figure 24: Total AGC stock density in tons per year in Goaso Forest District under BAU and REDD+ scenarios

The corresponding uncertainties in the AGC stock estimates were 21471.18 tons, 14297.91 tons and 11948.93 tons for 2001, 2015 and 2025 respectively in the whole GFD under BAU scenario. The average uncertainty per hectare was found to be approximately 0.10 (10%) under the BAU scenario. This does not deviate from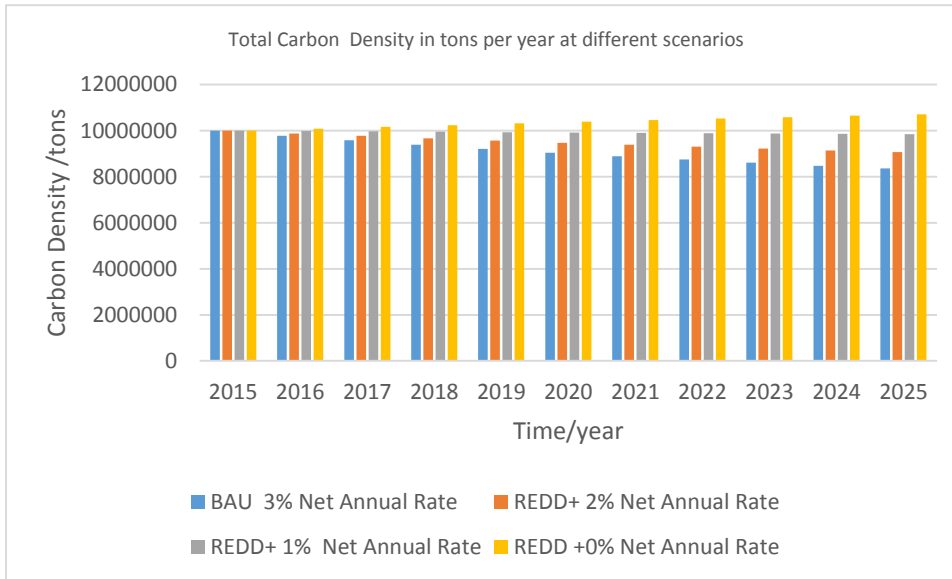 the uncertainties (10-15%) known to be involved in combining Remote Sensing data and field surveys for carbon measurement, in IPCC (2003) report. Though, it was highlighted that, this uncertainty range (10-15%) is low, this had a serious implication on the model because, the annual changes in the carbon stock in the model were controlled by a net annual deforestation rate of 3%, whilst the model was predicting with an error margin of 10%. This resulted in over-estimation of the available carbon stock per year. For instance, the observed carbon stock for 2012 was 54.5 tons C/hectare and the amount predicted by the model for 2012 when converted to hectare is equal to 70.9 tons C/hectare, resulting in relative error of 0.30 (30%). According to Alvarez et al. (2012), the relative error can be derived from the formula below:

Equation 10: Relative Error Equation

Relative Error = Predicted Carbon-Measured Carbon / Measured Carbon

Consequently, this led to a situation whereby the model predicted an initial (2001) carbon stock of 99.2 tons /hectare and a final (2025) carbon estimate of (55.2 tons C/hectare) in tons per hectare at the end of the simulation. This final amount is slightly more than the observed (2012) carbon estimate in tons per hectare (54.5 tons c/ ha) in the Forest District. Thus, such discrepancies may create confusion in the minds of users and policy makers if the software program is adopted for modelling, though, it can be used to mimic how the carbon stock is changing every year. The discrepancies in the carbon stock simulation can clearly be observed from the comparison between the original 2012 land cover map and the 2012 land cover map simulated by the model, displayed in Figure 25. The differences between the two maps are explicit.
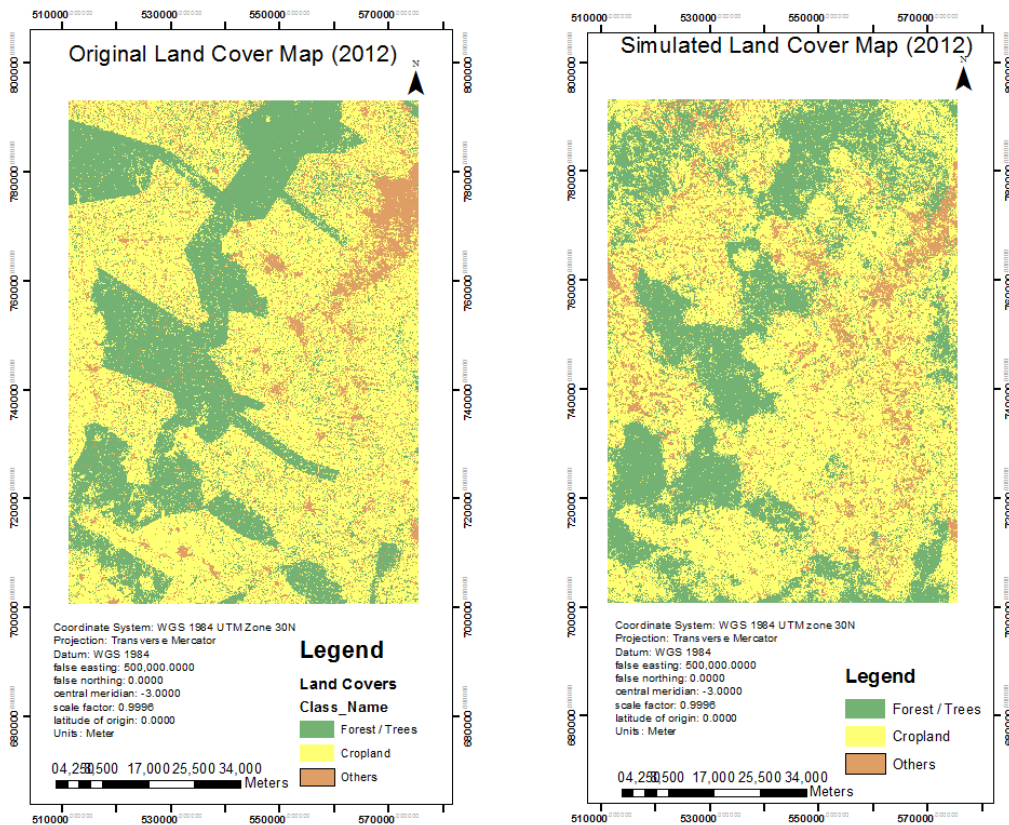
Figure 25: Comparison between the original and simulated land cover maps (2012)

Setting the number of iteration, a model in the Dinamica Ego software must run, without specifying the years within which the model simulation must start and end is a major drawback of the Dinamica EGO software program in future carbon stock modelling. This is because, in reality, the REDD+ scenario must run from the current date into the future. But this was seen as a challenge because, the Dinamica EGO software program does not allow the user to specify a particular year a simulation must start from and end. Users can only specify the number of iteration of a simulation. The software automatically count the beginning of the iteration from the date of the initial land cover map.

For instance, the carbon stock model required two land cover maps before changes in carbon stock as well as future projection could be simulated. However, in the model, if the acquisition date of the initial land cover map is 2000, and a projection in to 2012, 2015 2025 and so on are required by the user, the number of iterations are set to 12, 15 and 25 and so on respectively. Thus, the exact year within which a simulation is to be ran cannot be specified by the user. Starting the initial simulation beyond the acquisition date of the initial land cover map is impossible in the software. This resulted in a situation whereby a simulated 2015 land cover map from BAU scenario was used to represent the initial and final land cover maps under REDD+ scenarios since the actual or original 2015 land cover map of the study area was also unavailable at the time of the simulation.

The Dinamica EGO software program, may not be the only cause of the error propagation. Brown (2001) questioned the accuracy of carbon estimates and mentioned that "errors may come from sampling (variation among sampling units e.g. the number of plots within the population), measurement (parameter of interest

e.g. stem diameter), regression (error based on the regression equation) and so on". Another major factor, which might have accounted for the error propagation in this research is the exclusion of small trees (trees with diameter<10cm) from the analysis at the plot and the CPA extraction levels. AGC stock modelling in Dinamica EGO software program however, took into an account every tree in the forest class. According to Preece et al. (2012), the contribution of small trees with stems <10cm to above-ground carbon stock estimates in plantings <20 years old is about 15%. This amount is equivalent to the error propagation observed in the carbon stock model in the Dinamica EGO software program.

Also, the Landsat 7 imageries which were used for the modelling had some strips on them which were also capable of hindering the accuracy of the model. The result goes on to buttress the fact that, Landsat satellite imageries often lead to uncertainty in the carbon stock estimation (Thenkabail et al., 2004). It is also in line with the claim that, Landsat imageries are not effective in estimating carbon stock in dense canopy closure and have the tendency to underestimate or overestimate carbon stock results in tropical forest (Waring & Running, 2010).

4.6.4.   Validation of the Carbon Stock Model.

4.6.4.1.   Exponential Decay Function

The Table 11 below illustrates the minimum similarity of difference obtained for the carbon stock model. The minimum similarity of difference for the carbon stock model under BAU and REDD+ scenarios ranges between 0.697-0.740. This constituted about 69-74% validity. A minimum similarity difference of 1 or 100% represents a perfect fit. The similarity map in Figure 26 also places more emphasis on the validity of the model. The blue areas (0) indicate a poor fit, whereas red and yellow (1) areas demonstrate high to moderate fit.

Table 11: Exponential decay function

Type of Scenario	First Similarity Mean	Second Similarity Mean	Minimum Similarity Of Difference
Business As Usual	0.66	0.66-0.67	0.70
REDD+	0.66-0.71	0.67-0.71	0.70-0.74
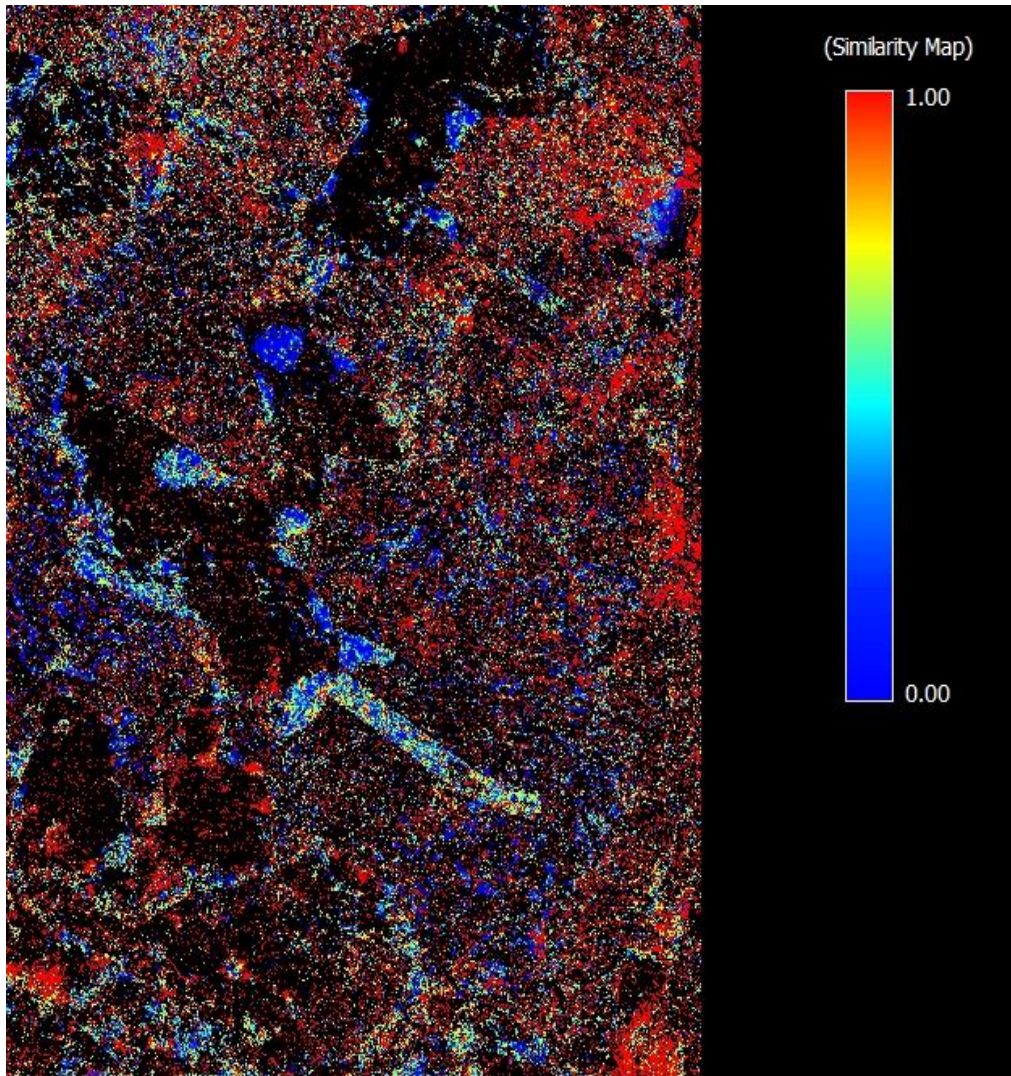
Figure 26: Similarity Map

4.6.4.2. Multiple Windows and Constant Decay Function

It can be seen from the Table 12 and Figure 27 that, the model went from 43% at 1 cell by 1 cell resolution to 87% at cell 11 by 11 cells resolution. Due to the fact that, the simulation received as an input, a fixed transition matrix (change rates), setting the quantity of changes, the model fitness was assessed with respect to location changes. The fact that the cell resolution of the Landsat-7 is 30m and the window search radius is half of the resolution, it can therefore be deduced from the graph of the model fitness per spatial resolution in Figure 27 that, the simulation reached a similarity fitness value of over 59% at a spatial resolution of 45 meters and 87% at a spatial resolution of 165m. The results from the two validation methods suggested that, the validity of the carbon stock model in Dinamica ranges from 74-87%. Signifying that, the model can predict with error margin between 13-26%.

Table 12: Multiple window decay function

Window Size/cells	Spatial Resolution/meters	Minimum Similarity	Percentage Minimum Similarity	Maximum Similarity
1	15	0.41	40.72	0.43
3	45	0.54	54.36	0.59
5	75	0.63	63.08	0.70
7	105	0.70	69.61	0.77
9	135	0.75	74.58	0.83
11	165	0.78	78.41	0.87

Figure 27: Model fitness

5. CONCLUSIONS AND RECOMMENDATIONS

5.1. Conclusions

The major conclusions from the research can be drawn from the answers to the following research questions:

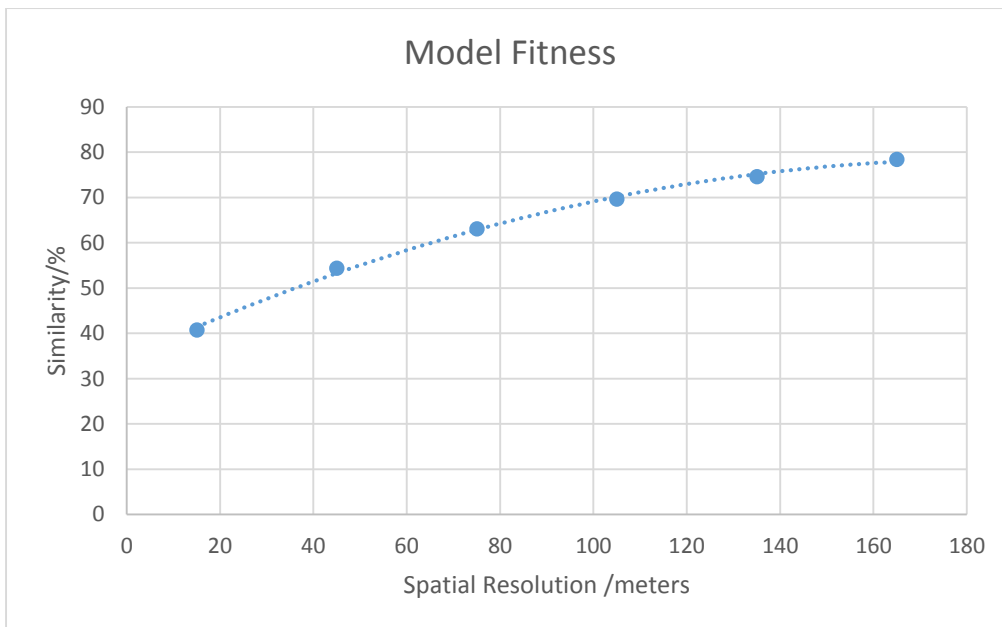**1. What are the AGC stock estimates of trees per hectare from VHR satellite image in the whole GFD and the agro-ecosystem only?**

The AGC stock in the Whole GFD was estimated at 54.5 tons per hectare with an uncertainty of 0.0014 tons per hectare. Out of the total, the agro-ecosystem (off-forest reserve) alone recorded an AGC stock of 28.0 tons per hectare and an uncertainty of 0.0020 tons per hectare, whilst the forest reserve also recorded an AGC stock of 26.5 tons per hectare and an uncertainty of 0.0008 tons per hectare. Signifying that, without the trees in the agro-ecosystem, the carbon stock in the Forest District would have been only 26.5 tons per hectare.

It can therefore be inferred from the results that, the contribution made by the trees in the agro-ecosystem into the AGC pool is more than that of the forest reserve. This is an evidence to support the claim that, conservation of trees in the Goaso agro-ecosystem by the farmers warrant carbon financial incentives. The Forest District can also serve as a priority area for REDD+ pilot project implementation.

2. What is the annual net deforestation/change rate from 2000-2012 in GFD?

GFD recorded 3% net annual deforestation/change rate from 2000-2012.

3. What are the effects of the major drivers (Explanatory/Environmental variables) of change in Goaso Forest District on deforestation?

The effect of the major spatial drivers: elevation, distance to protected areas, roads, streams and towns on deforestation in GFD were investigated. All the drivers were found to exhibit a significant effect on deforestation at all the weight of evidence ranges except the effect of distance to protected area, which recorded an insignificant effect on deforestation at all the weight of evidence ranges.

The general trend was that, nearby distances favoured deforestation whilst faraway distances opposed or inhibited deforestation. The only exception from this trend was distance to town which was found to favour and exacerbate more deforestation in faraway distances. It can also be concluded from the results that, the trees in the agro-ecosystem have the higher probability of changing to other covers than the trees in the forest reserve and hence enacting policies to protect the trees in the agro-ecosystem, as in the forest reserve may lead to conservation of trees and consequently carbon stock enhancement in the Forest District.

4. What are the expected effect of the BAU and REDD+ scenarios on the AGC stock in the whole GFD in the future?

The total carbon stock in the Whole GFD was simulated to be 15014811.36 tons, with an uncertainty of 21471.18 tons in 2001 and declined from 2001 to 9998535.78 tons with an uncertainty of 14297.91 tons in 2015 and further declined from 2015 to an amount of 8355896.506 tons with an uncertainty of 11948.93 tons in 2025 under BAU Scenario. The research revealed a decline of about 44.3% in the total AGC stock from 2001-2025 under BAU scenario for the whole Forest District. Also, the model predicted a decline of about 16.4 % from 2015 to 2025 under BAU scenario as compared to 9.2 % and 1.43% decline in the forest carbon pool under REDD+ scenario whereby the annual net deforestation rates were assumed to be reduced to 2% and 1% respectively. In contrast, the model predicted about 7% gain in the forest carbon pool from

2015-2025 under the REDD+ scenario with an assumption that there will be no deforestation (net annual deforestation rate at 0%) but other conversions will continue. The total simulated AGC stock in 2025 under REDD+ scenarios whereby the net annual deforestation rates were assumed to be reduced to 2%, 1% and 0% from the current year (2015) were: 9072937.45 tons, 9855275.57 tons, 10708367.73 tons with the corresponding uncertainties of 12974.30 tons, 14093.04 tons and 15312.97 tons respectively. The model was seen as a major improvement on the existing model because, the average uncertainty in tons per hectare under BAU scenario for the simulation over 25 years was very low (0.10 tons / hectare) as compared to the average uncertainty in tons per hectare (95.71 tons/hectare) for 12 years simulation recorded by the existing model.

5.2.   Recommendations

a. The research measured the AGC stock of trees only. A research which will estimate the carbon stock of all the land covers (shrubs, crops, grass, and water) is recommended.

b. Integration of socio-economic drivers such as population growth, income level, crop yield, food prices, government policies, land tenure issues into the carbon stock dynamic model in the Forest District is highly recommended since deforestation in the District is partly driven by such factors.

c. The assumption of the weight of evidence method is that, the input data must be spatially independent. Meaning that, correlated variables must be disregarded or combined before the model is ran. It is therefore recommended that, future research on correlation analysis of the environmental variables must be undertaken.

d. Practical implementation of the REDD+ scenario to explore the actual effect of this scenario on deforestation and carbon stock must be studied on a long term research to better understand whether the scenario will lead to a positive gain on the carbon stock of trees.

e. The use of other software programs for the carbon stock modelling must be explored in further research. The ideal situation will be the comparison of validity of two or more software programs.

LIST OF REFERENCES

Agterberg, F., & Bonham-Carter, G. (1990). Deriving weights of evidence from geo-science contour maps for the prediction of discrete events. In *: XXII International symposium AP-COM* (pp. 381–395).

Aguilar-Amuchastegui, N., & Forrest, J. (2013). *Assessing Risks to Forest Cover and Carbon Stocks :* (p. 18). Retrieved from http://wwf.panda.org/what_we_do/footprint/forest_climate2/publications/?209271/REDD-MRV-tools

Albrecht, A., & Kandji, S. T. (2003). Carbon sequestration in tropical agroforestry systems. *Agriculture, Ecosystems & Environment*, *99*(1-3), 15–27. doi:10.1016/S0167-8809(03)00138-5

Alcamo, J., & Ribeiro, T. (2001). *Scenarios as tools for international environmental assessments* (pp. 1–31).

Altrell, D., & Vuorinen, A. P. (2002). *National Forest Inventory Philippines Field Manual*. (M. Saket, D. Altrell, & A. . Vuorinen, Eds.) (p. 5).

Alvarez, E., Duque, A., Saldarriaga, J., Cabrera, K., De, G., Lema, A., … Rodríguez, L. (2012). Forest Ecology and Management Tree above-ground biomass allometries for carbon stocks estimation in the natural forests of Colombia. *Forest Ecology and Management*, *267*, 299. doi:10.1016/j.foreco.2011.12.013

Anderson, S. ., Kupfer, J. ., Wilson, R. ., & Cooper, R. (2000). Estimating forest crown area removed by selection cutting: a linked regression-GIS approach based on stump diameters. *Forest Ecology and Management*, *137*(1-3), 171–177. doi:10.1016/S0378-1127(99)00325-4

Antle, J. (2002). Sensitivity of carbon sequestration costs to soil carbon rates. *Environmental Pollution*, *116*(3), 413–422. doi:10.1016/S0269-7491(01)00218-4

Ardila, J. P., Bijker, W., Tolpekin, V. A., & Stein, A. (2011). Context -sensitve extraction of trees crown objects in urban areas using VHR satellite images. *International Journal of Applied Earth Observation and Geoinformation*, 15, 57–69.

Asner, G. P. (2001). Cloud cover in Landsat observations of the Brazilian Amazon. *International Journal of Remote Sensing*, *22*, 3855–3862. doi:10.1080/01431160010006926.

Bakker, W. H., Feringa, W., Gieseke, A. S. M., Goerte, B. G. H., Grabmaier, K. A., Hecker, C. A., … Woldai. (2009). *Principles of Remote Sensing : An introduction textbook*. (K. Tempfli, N. Kerle, G. C. Huurneman, & L. L. F. Janssen, Eds.) (Fourth.). Enschede, Netherlands: The International Institute for Geo-Information Science and Earth Observation.

Baral, S. (2011). *Mapping carbon stock using high resolution satellite images in sub-tropical Forest of Nepal*. ITC - University of Twente.

Basuki, T. M. (2012). *Quantifying tropical forest biomass* (p. 32).

Basuki, T. M., van Laake, P. E., Skidmore, A. K., & Hussin, Y. A. (2009). Allometric equations for estimating the above-ground biomass in tropical lowland Dipterocarp forests. *Forest Ecology and Management*, *257*(8), 1684–1694. doi:10.1016/j.foreco.2009.01.027

Bayat, A. T., van Gils, H., & Weir, M. (2012). Carbon Stock of European Beech Forest; A Case at M. Pizzalto, Italy. *APCBEE Procedia*, *1*, 159–168. doi:10.1016/j.apcbee.2012.03.026

Benz, U. C., Hofmann, P., Willhauck, G., Lingenfelder, I., & Heynen, M. (2004). Multi-resolution, object-oriented fuzzy analysis of remote sensing data for GIS-ready information. *ISPRS Journal of Photogrammetry and Remote Sensing*, *58*(3-4), 239–258. doi:10.1016/j.isprsjprs.2003.10.002

Bih, F. (2006). *methods for non-timber forest products inAssessment off-reserve forests Case study of Goaso district , Ghana*. Albert-Ludwigs-Universität Freiburg.

Blackett, H., & Gardette, E. (2008). *Cross-border flows of timber and wood products in West Africa*.

Blaschke, T. (2010). Object based image analysis for remote sensing. *ISPRS Journal of Photogrammetry and Remote Sensing*, *65*(1), 2–16. doi:10.1016/j.isprsjprs.2009.06.004

Bosetti, V., & Lubowski, R. (2010). *Deforestation and Climate Change : Reducing Carbon Emissions from Deforestation and Forest Degradation* (p. 1). Cheltenham: Edward Elgar Publishing.

Brown, S. (1997). *Estimating biomass and biomass change in tropical forests...* (No. 134) (p. 55). ROME, ITALY. Retrieved from http://www.fao.org/docrep/w4095e/w4095e00.HTM

Brown, S. (2002). Measuring carbon in forests: current status and future challenges. *Environmental Pollution*, *116*(3), 363–372. doi:10.1016/S0269-7491(01)00212-3

Bunting, P., Lucas, R. M., Jones, K., & Bean, A. R. (2010). Characterisation and mapping of forest communities by clustering individual tree crowns. *Remote Sensing of Environment*, *114*(11), 2536–2547. doi:10.1016/j.rse.2010.05.030

Chambers, J. Q., Santos, J. Dos, Ribeiro, R. J., & Higuchi, N. (2001). Tree damage, allometric relationships, and above-ground net primary production in central Amazon forest. *Forest Ecology and Management*, *152*(1-3), 73–84. doi:10.1016/S0378-1127(00)00591-0

Chave, J., Andalo, C., Brown, S., Cairns, M. A., Chambers, J. Q., Eamus, D., … Yamakura, T. (2005). Tree allometry and improved estimation of carbon stocks and balance in tropical forests. *Oecologia*, *145*(1), 87–99. doi:10.1007/s00442-005-0100-x

Chen, Q., Yang, X. L., Petriu, E. M., & ieee. (2004). Watershed segmentation for binary images with different distance transforms.

CIFOR. (2009). Carbon Accounting:Quick steps. In *Assessing the Implicationns of Climate Change for USAID Forestry Programs* (pp. 1–24).

Clinton, N., Holt, A., Scarborough, J., Yan, L., & P, G. (2010). Accuracy Assessment Measures for Object based Image Segmentation Goodness. *Photogrammetric Engineering and Remote Sensing*, *76(3)*, 289–299.

Costanza, R. (1989). Model goodness of fit: a multiple resolution procedure. *Ecological Modelling*, *47*, 199–215.

Damnyag, L., Saastamoinen, O., Blay, D., Dwomoh, F. K., Anglaaere, L. C. N., & Pappinen, A. (2013). Sustaining protected areas: Identifying and controlling deforestation and forest degradation drivers in the Ankasa Conservation Area, Ghana. *Biological Conservation*, *165*, 86–94. doi:10.1016/j.biocon.2013.05.024

Dawkins, H. C. (1963). Crown diameters: their relation to bole diameter in tropical forest trees. *Commonwealth Forestry Rev*, *42*, 318–333.

Definiens. (2009). *Definiens eCognition Developer 8 User Guide*.

Definiens. (2011). eCognition Developer 8.64.1. München, Germany: Trimble Germany GmbH, Trappentreustr. 1, D-80339 München, Germany.

Digital Globe. (2008). *WHITE PAPER The benefits of the 8 Spectral Bands of Worldview-2*.

Dragut, L., Tiede, D., & Levick, S. R. (2010). ESP: A tool to estimate scale parameter for multi-resolution image segmentation of remotely sensed data. *International Journal of Geographical Information Science*, *24(6)*, 859–871.

Drake, J. B., Knox, R. G., Dubayah, R. O., Clark, D. B., Condit, R., Blair, J. B., & Hofton, M. (2003). Above-ground biomass estimation in closed canopy Neotropical forests using lidar remote sensing : factors, 147–159.

FAO. (2010). *Global Forest Resources Assessment*. Rome.

Fehrmann, L., & Kleinn, C. (2006). General considerations about the use of allometric equations for biomass estimation on the example of Norway spruce in central Europe. *Forest Ecology and Management*, *236*(2-3), 412–421. doi:10.1016/j.foreco.2006.09.026

Feng, X., Liu, G., Chen, J. M., Chen, M., Liu, J., Ju, W. M., … Zhou, W. (2007). Net primary productivity of China's terrestrial ecosystems from a process model driven by remote sensing. *Journal of Environmental Management*, *85*(3), 563–73. doi:10.1016/j.jenvman.2006.09.021

FRA. (2010). *GLOBAL FOREST RESOURCES ASSESSMENT 2010 T ERMS AND D EFINITIONS* (No. 144/E) (pp. 9–15). ROME, ITALY.

Funder, M. (2009). *Reducing Emissions from Deforestation and Degradation (REDD). An overview of risks and opportunities for the poor* (pp. 1– 64). Copenhagen. Retrieved from www.diis.dk

Gao, Y., Mas, J. F., Kerle, N., & Navarrete Pacheco, J. A. (2011). Optimal region growing segmentation and its effect on classification accuracy. *International Journal of Remote Sensing*, *32*(13), 3747–3763. doi:10.1080/01431161003777189

Gelens, M. F., van Leeuwen, L., & Hussin, Y. A. (2010). Geo-information applications for off-reserve tree management, 1–77.

Ghana REDD+ R-PP. (2010). *Submitted to Forest Carbon Partnership*.

Gibbs, H. K., Brown, S., Niles, J. O., & Foley, J. A. (2007). Monitoring and estimating tropical forest carbon stocks: making REDD a reality. *Environmental Research Letters*, *2*(4), 8–10. doi:10.1088/1748-9326/2/4/045023

GloballomeTree. (n.d.). Assessing volume, biomass and carbon stocks of trees and forests. Retrieved from http://www.globallometree.org/

Goetz, S. J., Baccini, A., Laporte, N. T., Johns, T., Walker, W., Kellndorfer, J., … Sun, M. (2009). Mapping and monitoring carbon stocks with satellite observations: a comparison of methods. *Carbon Balance and Management*, *4*(1), 2. doi:10.1186/1750-0680-4-2

Hagen, A. (2003). Fuzzy set approach to assessing similarity of categorical maps. *International Journal of Geographical Information Science*, *17*(3), 235–249. doi:10.1080/13658810210157822

Hemery, G. E., Savill, P. S., & Pryor, S. N. (2005). Applications of the crown diameter–stem diameter relationship for different species of broadleaved trees. *Forest Ecology and Management*, *215*(1-3), 285–294. doi:10.1016/j.foreco.2005.05.016

Horowitz, J. (2010). The forest consensus. *Carbon Balance and Management*, 203–206.

Houghton, R. A. (2001). The spatial distribution of forest biomass in the Brazilian Amazon : a comparison of estimates.

Houghton, R. A. (2005). Aboveground Forest Biomass and the Global Carbon Balance. *Global Change Biology*, *11*(6), 945–958. doi:10.1111/j.1365-2486.2005.00955.x

Husch, B., Kershaw, J. A., & Beers, T. W. (2003). *Forest Mesuration*. UK: John Wiley & Sons Inc.

IPCC. (2003). *Intergovernmental Panel on Climate Change Good Practice Guidance for Land Use , Land-Use Change and Forestry*. (K. T. and F. W. Jim Penman, Michael Gytarsky, Taka Hiraishi, Thelma Krug, Dina Kruger, Riitta Pipatti, Leandro Buendia, Kyoko Miwa, Todd Ngara & IPCC, Eds.) (pp. 66–67). JAPAN. Retrieved from the Institute for Global Environmental Strategies (IGES) for the IPCC ©

Jia, S., & Akiyama, T. (2005). A precise, unified method for estimating carbon storage in cool-temperate deciduous forest ecosystems. *Agricultural and Forest Meteorology*, *134*(1-4), 70–80. doi:10.1016/j.agrformet.2005.08.014

Jindal, R., Kerr, J. M., & Carter, S. (2012). Reducing Poverty Through Carbon Forestry? Impacts of the N'hambita Community Carbon Project in Mozambique. *World Development*, *40*(10), 2123–2135. doi:10.1016/j.worlddev.2012.05.003

Kalame, F. B., Aidoo, R., Nkem, J., Ajayie, O. C., Kanninen, M., Luukkanen, O., & Idinoba, M. (2011). Modified taungya system in Ghana: a win–win practice for forestry and adaptation to climate change? *Environmental Science & Policy*, *14*(5), 519–530. doi:10.1016/j.envsci.2011.03.011

Kamusoko, C., Oono, K., Nakazawa, A., Wada, Y., Nakada, R., Hosokawa, T., … Isobe, T. (2011). Spatial Simulation Modelling of Future Forest Cover Change Scenarios in Luangprabang Province, Lao PDR, (1993), 707–729. doi:10.3390/f2030707

Karna, Y. K. (2012). *Mapping above ground carbon using worldview satellite image and Lidar data in relationship with tree diversity of forests*. ITC-University of Twente.

Ke, Y., Quackenbush, L. J., & Im, J. (2010). Remote Sensing of Environment Synergistic use of QuickBird multispectral imagery and LIDAR data for object-based forest species classi fi cation. *Remote Sensing of Environment*, *114*(6), 1141–1154. doi:10.1016/j.rse.2010.01.002

Keller, M., Palace, M., & Hurtt, G. (2001). Biomass estimation in the Tapajos National Forest , Brazil Examination of sampling and allometric uncertainties, *154*.

Kim, S.-R., Kwak, D.-A., Lee, W.-K., oLee, W.-K., Son, Y., Bae, S.-W., … Yoo, S. (2010). Estimation of carbon storage based on individual tree detection in Pinus densiflora stands using a fusion of aerial photography and LiDAR data. *Science China. Life Sciences*, *53*(7), 885–97. doi:10.1007/s11427-010-4017-1

Kuuluvainen, T. (1991). Relatioships between crown projected area and components of above-ground biomass in Norway spruce trees in even-aged stands: Empirical results and their interpretation. *Forest Ecology and Management*, *40*(3-4), 243–260.

Lamonaca, A., Corona, P., & Barbati, A. (2008). Exploring forest structural complexity by multi-scale segmentation of VHR imagery, *112*, 2849. doi:10.1016/j.rse.2008.01.017

Leboeuf, A., Beaudoin, A., Fournier, R., Guindon, L., Luther, J., & Lambert, M. (2007). A shadow fraction method for mapping biomass of northern boreal black spruce forests using QuickBird imagery. *Remote Sensing of Environment*, *110*(4), 488–500. doi:10.1016/j.rse.2006.05.025

Leckie, D. G., Gougeon, F. A., Hill, D. A., Quinn, R., Armstrong, L., & Shreenan, R. (2003). Combined high-density lidar and multispectral imagery for individual tree crown analysis. Retrieved from https://cfs.nrcan.gc.ca/publications?id=22833

Leica Geosystems. (2011). User Manual: Atcor for ERDAS IMAGINE 2011, Haze reduction , Atmospheric and Topographic correction.

Liddell, M. J., Nieullet, N., Campoe, O. C., & Freiberg, M. (2007). Assessing the above-ground biomass of a complex tropical rainforest using a canopy crane. *Austral Ecology*, *32*(1), 43–58. doi:10.1111/j.1442-9993.2007.01736.x

Liu, J., & Yang, Y. H. (1994). Multiresolution color image segmentation. *Pattern Analysis and Machine Intelligence, IEEE Transactions on*, *16(7)*, 689–700.

Lu, D. (2006). The potential and challenge of remote sensing-based biomass estimation. *International Journal of Remote Sensing*, *27*(7), 1297–1328. doi:10.1080/01431160500486732

Luther, J. E., Fournier, R. A., Piercey, D. E., Guindon, L., & Hall, R. J. (2006). Biomass mapping using forest type and structure derived from Landsat TM imagery. Retrieved from https://cfs.nrcan.gc.ca/publications?id=26349

Maeda, E. E., de Almeida, C. M., de Carvalho Ximenes A., A., Formaggio, A. R., Shimabukuro, Y. E., & Pellikka, P. (2011). Dynamic modeling of forest conversion: Simulation of past and future scenarios of rural activities expansion in the fringes of the Xingu National Park, Brazilian Amazon. *International Journal of Applied Earth Observation and Geoinformation*, *13*(3), 435–446. doi:10.1016/j.jag.2010.09.008

Mckenzie, E., Rosenthal, A., Bernhardt, J., Girvetz, E., Kovacs, K., Olwero, N., & Toft, J. (2012). *Developing Scenarios to Assess Ecosystem Service Tradeoffs : Guidance and Case Studies for InVEST Users* (pp. 5–20). Washington-USA: World Wildlife Fund.

Miksys, V., Varnagirytekabasinskiene, I., Stupak, I., Armolaitis, K., Kukkola, M., & Wojcik, J. (2007). Above-ground biomass functions for Scots pine in Lithuania. *Biomass and Bioenergy*, *31*(10), 685–692. doi:10.1016/j.biombioe.2007.06.013

Ministrry of Land and Natural Resources. (2012). *Ghana Investment Plan for the Forest Investment Program (FIP).* Retrieved from http://www.fcghana.org/assets/file/

Möller, M., Lymburner, L., & Volk, M. (2007). The comparison index: A tool for assessing the accuracy of image segmentation. *International Journal of Applied Earth Observation and Geoinformation*, *9*(3), 311–321. doi:10.1016/j.jag.2006.10.002

Mora, B., Wulder, M. A., & White, J. C. (2010). Segment-constrained regression tree estimation of forest stand height from very high spatial resolution panchromatic imagery over a boreal environment. *Remote Sensing of Environment, In Press, Corrected Proof*.

Morales, R. M., Miura, T., & Idol, T. (2008). An assessment of Hawaiian dry forest condition with fine resolution remote sensing. *Forest Ecology and Management*, *255*(7), 2524–2532.

Mutanga, E. (2012). *Assessment of carbon stock for tree resources on farmlands using an object based image analysis of a very high resolution sattellite image : A case study in EJISU- Juaben District , Ghana*. University Of Twente.

Muukkonen, P., & Heiskanen, J. (2007). Biomass estimation over a large area based on standwise forest inventory data and ASTER and MODIS satellite data: A possibility to verify carbon inventories. *Remote Sensing of Environment*, *107*(4), 617–624. doi:10.1016/j.rse.2006.10.011

Olander, L. P., Galik, C. S., & Kissinger, G. A. (2012). Operationalizing REDD+: scope of reduced emissions from deforestation and forest degradation. *Current Opinion in Environmental Sustainability*, *4*(6), 661– 669. doi:10.1016/j.cosust.2012.07.003

Padwick, C., Scientist, P., Deskevich, M., Pacifici, F., & Smallwood, S. (2010). Worldview-2 pan-sharpening.

Patenaude, G., Milne, R., & Dawson, T. P. (2005). Synthesis of remote sensing approaches for forest carbon estimation: reporting to the Kyoto Protocol. *Environmental Science & Policy*, *8*(2), 161–178. doi:10.1016/j.envsci.2004.12.010

Pohl, C., & Van Genderen, J. L. (1998). *Review article Multisensor image fusion in remote sensing: Concepts, methods and applications*. *International Journal of Remote Sensing* (Vol. 19, pp. 823–854). doi:10.1080/014311698215748

Pontius, R. O. (2002). Statistical Methods to Partition Effects of Quantity and Location During Comparison of Categorical Maps at Multiple Resolutions, *01610*(October), 1041–1049.

Pouliot, D. ., King, D. ., Bell, F. ., & Pitt, D. (2002). Automated tree crown detection and delineation in high-resolution digital camera imagery of coniferous forest regeneration. *Remote Sensing of Environment*, *82*(2-3), 322–334. doi:10.1016/S0034-4257(02)00050-0

Power, C., Simms, A., & White, R. (2001). Hierarchical fuzzy pattern matching for the regional comparison of Land Use Maps. *International Journal of Geographical Information Science*, *15*, 77–100.

Preece, N. D., Crowley, G. M., Lawes, M. J., & van Oosterzee, P. (2012). Comparing above-ground biomass among forest types in the Wet Tropics: Small stems and plantation types matter in carbon accounting. *Forest Ecology and Management*, *264*, 228–237. doi:10.1016/j.foreco.2011.10.016

Qureshi, A., Badola, R., & Hussain, S. A. (2012). A review of protocols used for assessment of carbon stock in forested landscapes. *Environmental Science & Policy*, *16*, 83–87. doi:10.1016/j.envsci.2011.11.001

Rosenqvist, Å., Milne, A., Lucas, R., Imhoff, M., & Dobson, C. (2003). A review of remote sensing technology in support of the Kyoto Protocol. *Environmental Science & Policy*, *6*(5), 441–455. doi:10.1016/S1462-9011(03)00070-4

Rossillo - Calle, F., de Groot, P., Henstock, S. ., & Woods, J. (2007). *The biomass assessment Handbook*. *Eartth Scan*. London.

Ros-tonen, M. A. F., Insaidoo, T. F. G., & Acheampong, E. (2013). Forest Policy and Economics Promising start , bleak outlook : The role of Ghana ' s modi fi ed taungya system as a social safeguard in timber legality processes ☆. *Forest Policy and Economics*, *32*, 57–67. doi:10.1016/j.forpol.2012.11.011

Roy, P. S., & Ravan, S. a. (1996). Biomass estimation using satellite remote sensing data—An investigation on possible approaches for natural forest. *Journal of Biosciences*, *21*(4), 535–561. doi:10.1007/BF02703218

Saha, R. R. S. K. (2008). Multi-resolution Segmentation for Object-based Classifi cation and Accuracy Assessment of Land Use / Land Cover Classifi cation using Remotely Sensed Data, (June), 189–201.

Samalca, I. K., Gier, A. De, & Hussin, Y. A. (2007). Estimation of tropical forest biomass for assessment of carbon sequestration using regression models and remote sensing in Berau, East Kalimantan-Indonesia. *Unpublished*.

Sampaio, G., Nobre, C., Costa, M. H., Satyamurty, P., Soares-filho, B. S., & Cardoso, M. (2007). Regional climate change over eastern Amazonia caused by pasture and soybean cropland expansion, *34*. doi:10.1029/2007GL030612

Schneider, E. K., Fan, M., Kirtman, B. P., & Dirmeyer, P. (2006). Potential effects of Amazon deforestation on tropical Climate. *Cola Technical Report*, *226*, 1–41.

Schoemaker, P. J. H., & Ph, D. (1993). *Scenario Planning Scenario Planning* (pp. 1–11).

Shafri, H. Z. M., Hamdan, N., & Saripan, M. I. (2011). Semi-automatic detection and counting of oil plam trees from high spatial resolution airborne imagery. *International Journal of Remote Sensing*, *32 (8)*, 2095–2115.

Shimano, K. (1997). Analysis of the relationship between DBH and crown projection area using a new model. *Journal of Forest Research*, *2*(4), 237–242. doi:10.1007/BF02348322

Sims, D. A., & Gamon, J. A. (2002). Relationships between leaf pigment content and spectral reflectance across a wide range of species, leaf structures and developmental stages. *Remote Sensing of Environment*, *81*(2-3), 337–354. doi:10.1016/S0034-4257(02)00010-X

Soares-Filho, B. ., Alencar, A., Nepstad, D., Cerqueira, G., Diaz, M. C., Rivero, S., … Voll, E. (2004). Simulating the response of land-cover changes to Road paving and governance along a major Amazon highway: the Santarém–Cuiabá corridor. *Global Change Biology*, *10*(5), 745–764.

Soares-Filho, B. S., Corradi, L., Cerqueira, & Araujo, W. (2003). Simulating the spatial patterns of change through the use of the dinamica model. *Simposio Brasileiro de Sensoriamento Romoto*, *11*(BH, INPE), 721–728.

Soares-Filho, B. S., Coutinho Cerqueira, G., & Lopes Pennachin, C. (2002). dinamica—a stochastic cellular automata model designed to simulate the landscape dynamics in an Amazonian colonization frontier. *Ecological Modelling*, *154*(3), 217–235. doi:10.1016/S0304-3800(02)00059-5

Soares-filho, B. S., Coutinho, G., & Lopes, C.-P. (2002). DINAMICA - a new model to simulate and study landscape dynamics. *Forests*, 1–39.

Soares-Filho, B. S., Garcia, R. A., Rodrigues, H. O., Moro, S., & Nepstad, D. (2007). Coupling socioeconomic and demographic dimensions to a spatial simulation model of deforestation for the Brazilian Amazon. In *In: LBA-ECO 11th Science Team Meeting.*

Soares-Filho, B. S., Nepstad, D. C., Curran, L. M., Cerqueira, G. C., Ramos, C. A., Voll, E., … Schlesinger, P. (2006). Modelling conservation in the Amazon Basin. *Nature*, *440*(23), 520–523.

Soares-Filho, B. S., Rodrigues, H. O., Costa, W. L., & Schlesinger, P. (2009). *M o d e l i n g E n v i r o n m e n t a l D y n a m i c s w i t h D i n a m i c a E G O*. (B. S. Soares-Filho, Ed.) (pp. 56–80). Belo Horizonte / MG- Brazil.

Suganuma, H., Abe, Y., Taniguchi, M., Tanouchi, H., Utsugi, H., Kojima, T., & Yamada, K. (2006). Stand biomass estimation method by canopy coverage for application to remote sensing in an arid area of Western Australia. *Forest Ecology and Management*, *222*(1-3), 75–87. doi:10.1016/j.foreco.2005.10.014

Takimoto, A., Nair, P. K. R., & Nair, V. D. (2008). Carbon stock and sequestration potential of traditional and improved agroforestry systems in the West African Sahel. *Agriculture, Ecosystems & Environment*, *125*(1-4), 159–166. doi:10.1016/j.agee.2007.12.010

Thenkabail, P. S., Enclona, E. a, Ashton, M. S., Legg, C., & De Dieu, M. J. (2004). Hyperion, IKONOS, ALI, and ETM+ sensors in the study of African rainforests. *Remote Sensing of Environment*, *90*(1), 23–43. doi:10.1016/j.rse.2003.11.018

Tomppo, E., Nilsson, M., Rosengren, M., Aalto, P., & Kennedy, P. (2002). Simultaneous use of Landsat-TM and IRS-1C WiFS data in estimating large area tree stem volume and aboveground biomass. *Remote Sensing of Environment*, *82*(1), 156–171. doi:10.1016/S0034-4257(02)00031-7

Tucker, C. J. (1979). Red and photographic infrared linear combinations for monitoring vegetation. *Remote Sensing of Environment*, *8*(2), 127–150. doi:10.1016/0034-4257(79)90013-0

UN-REDD. (2009). The United Nations Collaborative Programme on Reducing Emissions from Deforestation and Forest Degradation in Developing Countries. Retrieved May 23, 2014, from http://www.un-redd.org/AboutREDD/tabid/102614/Default.aspx

Veldkamp, A., & Lambin, E. F. (2001). Predicting land-use change, *85*, 1–6.

Wang, L., Gong, P., & Biging, G. S. (2004). Individual Tree-Crown Delineation and Treetop Detection in High-Spatial-Resolution Aerial Imagery, *3114*(March), 351–358.

Waring, R. H., & Running, S. W. (2010). *Forest Ecosystems : Analysis at Multiple Scales*. Burlington: Elsevier Science.

Wei, W., Chen, X., & Ma, A. (2005). *Object-oriented information extraction and application in high-resolution remote sensing image*. *paper presented at the 2005 IEEE International Geoscience and Remote Sensing Symposium, IGARSS 2005, July 25, 2005 July 29, 2005*. Seoul, Republic of Korea.

Wiggins, S., Marfo, K., & Anchirinah, V. (2004). Protecting the Forest or the People?Environmental Policies and Livelihoods in the Forest Margins of Southern Ghana. *World Development*, *32(11)*, 1939–1955.

Wollenberg, E., Edmunds, D., & Buck, L. (2000). Using scenarios to make decisions about the future: anticipatory learning for the adaptive co-management of community forests. *Landscape and Urban Planning*, *47*(1-2), 65–77. doi:10.1016/S0169-2046(99)00071-7

Yi, W., Gao, Z., Li, Z., & Chen, M. (2012). Land-use and land-cover sceneries in China: an application of Dinamica EGO model. *Spie*, *8513*, 1–7. doi:10.1117/12.927782

Zhan, Q., Molenaar, M., Tempfli, K., & Shi, W. (2005). Quality assessment for geo-spatial objects derived from remotely sensed data. *International Journal of Remote Sensing*, *26*(14), 2953–2974. doi:10.1080/01431160500057764

Zhang, J. (2010). Multi-source remote sensing data fusion: status and trends. *International Journal of Image and Data Fusion*, *1*(1), 5–24. doi:10.1080/19479830903561035

Zheng, D., Rademacher, J., Chen, J., Crow, T., Bresee, M., Le Moine, J., & Ryu, S.-R. (2004). Estimating aboveground biomass using Landsat 7 ETM+ data across a managed landscape in northern Wisconsin, USA. *Remote Sensing of Environment*, *93*(3), 402–411. doi:10.1016/j.rse.2004.08.008

Zheng, G., Chen, J. M., Tian, Q. J., Ju, W. M., & Xia, X. Q. (2007). Combining remote sensing imagery and forest age inventory for biomass mapping. *Journal of Environmental Management*, *85*(3), 616–23. doi:10.1016/j.jenvman.2006.07.015

APPENDICES

Appendix 1: A summary of the regression analysis between CPA and field calculated carbon

SUMMARY OUTPUT

Regression Statistics	
Multiple R	0.77
R Square	0.59
Adjusted R Square	0.58
Standard Error	744.91
Observations	37

ANOVA

	df	SS	MS	F	Significance F
Regression	1	28120353	28120353	50.677	2.69E-08
Residual	35	19421098	554888.5		
Total	36	47541451			

	Coefficients	Standard Error	t Stat	P-value	Lower 95%	Upper 95%
Intercept	-291.716	224.497	-1.299	0.202295	-747.47	164.038
CPA	11.23604	1.578	7.119	2.69E-08	8.032	14.440

Appendix 2 : A Summary of the regression analysis between (CPA) and validation samples of field calculated carbon

SUMMARY OUTPUT

Regression Statistics	
Multiple R	0.98
R Square	0.96
Adjusted R Square	0.96
Standard Error	142.28
Observations	10

ANOVA

	df	SS	MS	F	Significance F
Regression	1	4091444.797	4091445	202.0945	5.8383E-07
Residual	8	161961.6577	20245.21		
Total	9	4253406.455			

	Coefficients	Standard Error	t Stat	P-value	Lower 95%	Upper 95%
Intercept	-85.46675	67.92462324	-1.25826	0.243778	-242.10121	71.167712
CPA	7.03428238	0.494814666	14.21599	5.84E-07	5.89323771	8.175327

Appendix 3: Total area per land cover type

Land Cover Type	Area/ Cells	Area/Hectares	Area/Sqrm
Forest/ Trees	1603999	151336.4988	1513364988
Cropland	3763071	355043.856	3550438560
Others	926488	87413.67677	874136767.7

Appendix 4: Effect of digital elevation model (DEM) on the model

Conversion	Range	Possible Change	Executed Change	Weight Coefficient	Contrast	Significant?
Forest to Cropland	0-200	646484	3833530	0.75	1.00	yes
Forest to Cropland	200-300	1927348	706155	-0.17	-0.55	Yes
Forest to Cropland	300-400	147964	30816	-0.96	-1.01	Yes
Forest to Cropland	400-500	43958	11015	-0.72	-1.73	Yes
Forest to Cropland	500-600	18519	3759	-1.00	-1.00	Yes
Forest to Cropland	600-700	328	18	-2.47	-2.47	Yes
Forest to Others	0-200	294203	31249	0.67	0.88	Yes
Forest to Others	200-300	1286616	65423	-0.12	-0.41	Yes
Forest to Others	300-400	118917	1769	-1.39	-1.44	Yes
Forest to Others	400-500	33872	929	-0.76	-0.78	yes
Forest to Others	500-700	15575	505	-0.59	-0.60	Yes

Appendix 5: Effect of distance to roads on the model

Changes	Range	Possible Changes	Executed Changes	Weight Coefficient	Contrast	Significant?
Forest to Cropland	0-100	326470	174443	0.52	0.60	yes
Forest to Cropland	100-300	569266	294589	0.457	0.58	Yes
Forest to Cropland	300-600	622024	291476	0.26	0.34	Yes
Forest to Cropland	600-700	136357	57349	0.07	0.07	Yes
Forest to Cropland	700-900	223672	86970	-0.65	-0.07	Yes
Forest to Cropland	900-1000	81035	28556	-0.22	-0.23	Yes
Forest to Cropland	1000-1200	140071	45367	-0.35	-0.37	Yes
Forest to Cropland	1200-1300	55128	16095	-0.50	-0.51	Yes
Forest to Cropland	1300-1500	97127	25952	-0.62	-0.64	Yes
Forest to Cropland	1500-1600	43753	9919	-0.84	-0.85	yes
Forest to Cropland	1600-2000	138699	27378	-1.01	-1.06	Yes
Forest to Others	0-100	166951	14924	0.50	0.57	Yes
Forest to Others	100-500	555149	44105	0.37	0.60	yes
Forest to Others	500-600	100610	6429	0.13	0.14	Yes
Forest to Others	600-900	228113	12403	-0.04	-0.04	yes
Forest to Others	900-1000	55011	2532	-0.21	-0.22	Yes
Forest to Others	1000-1500	212879	7967	-0.43	-0.48	Yes
Forest to Others	1500-1600	34722	888	-0.83	-0.83	Yes
Forest to others	1600-5600	360875	7421	-1.05	-1.21	yes

Appendix 6: Effect of distance to stream on the model

Changes	Range	Possible Changes	Executed Changes	Weight Coefficient	Contrast	Significant?
Forest to Cropland	0-100	630080	275814	0.13	0.17	yes
Forest to Cropland	100-200	620946	263991	0.08	0.10	Yes
Forest to Cropland	200-300	511485	209469	0.02	0.02	Yes
Forest to Cropland	300-500	652082	245786	-0.12	-0.16	Yes
Forest to Cropland	500-600	115636	38375	-0.32	-0.33	Yes
Forest to Cropland	600-2400	121525	42764	-0.23	-0.24	Yes
Forest to Others	0-100	377051	22785	0.06	0.084	Yes
Forest to Others	100-300	700110	41139	0.03	0.06	yes
Forest to Others	300-600	510677	27120	-0.07	-0.10	Yes
Forest to Others	600-2400	82737	3976	-0.18	-0.19	yes

Appendix 7: Effect of distance to towns on the model

Changes	Range	Possible Changes	Executed Changes	Weight Coefficient	Contrast	Significant?
Forest to Cropland	0-100	1903	1276	1.08	0.11	yes
Forest to Cropland	100-2000	533687	328166	0.84	1.05	Yes
Forest to Cropland	200-2100	41667	22002	0.49	0.49	Yes
Forest to Cropland	2100-2400	125084	61841	0.35	0.37	Yes
Forest to Cropland	2400-2600	81918	37799	0.22	0.23	Yes
Forest to Cropland	2600-2800	81033	34793	0.09	0.09	Yes
Forest to Cropland	2800-2900	41244	16557	-0.03	-0.03	Yes
Forest to Cropland	2900-4400	515057	186627	-0.19	-0.23	Yes
Forest to Cropland	4400-4500	29219	8960	-0.44	-0.45	Yes
Forest to Cropland	4500-5200	187700	52003	-0.59	-0.62	yes
Forest to Cropland	5200-5300	23617	5878	-0.73	-0.74	Yes
Forest to Cropland	5300-7700	392418	100090	-0.70	-0.80	Yes
Forest to Cropland	7700-7800	10436	3587	-0.27	-0.27	yes
Forest to Cropland	7800-15200	500706	173757	-0.26	-0.31	Yes
Forest to cropland	15200-15300	2986	1542	0.44	0.44	yes
Forest to Cropland	15300-31100	215871	100383	0.23	0.25	Yes
Forest to Others	0-100	696	69	0.60	0.60	Yes
Forest to Others	100-3000	465107	37892	0.38	0.56	Yes
Forest to others	3000-3100	24940	1432	0.01	0.01	No
Forest to Others	3100-4500	316791	15350	-0.17	-0.21	Yes
Forest to Others	4500-4700	40994	1592	-0.40	-0.41	Yes
Forest to Others	4700-8300	467931	21343	-0.24	-0.31	Yes
Forest to Others	8300-8400	7161	409	0.00	0.00	No
Forest to Others	8400-9300	60346	2912	-0.18	-0.18	Yes
Forest to Others	9300_9400	6441	234	-0.47	-0.48	Yes
Forest to Others	9400-14800	226559	9797	-0.29	-0.33	Yes
Forest to Others	14800-14900	1805	145	0.37	0.37	Yes
Forest to Others	14900-26400	126702	8542	0.18	0.19	Yes
Forest to Others	26400_26500	345	1	-3.04	-3.04	Yes

Appendix 8: Effect of distance to towns on the model (Continued)

Forest to Others	26500-26600	316	7	-0.98	-0.98	Yes
Forest to Others	26600-26700	325	2	-2.28	-2.28	Yes
Forest to Others	26700-26900	690	8	-1.64	-1.64	Yes
Forest to Others	26900-27000	330	6	-1.85	-1.87	Yes
Forest to Others	27000-27100	288	1	-2.86	-2.85	Yes
Forest to Others	27100-27200	217	2	-1.87	-1.87	Yes
Forest to Others	27200-27500	600	11	-1.18	-1.177	yes
Forest to Others	27500-27600	97	4	-0.34	-0.34	Yes
Forest to Others	27600-27700	50	3	0.05	0.05	No
Forest to Others	27700-27800	44	6	0.96	0.96	Yes
Forest to Others	27800-27900	27	7	1.75	1.75	Yes
Forest to Others	27900-31000	357	99	1.85	1.85	Yes

Appendix 9: Simulated carbon density and uncertainty under BAU from 2001-2025

Time/year	Total Carbon Stock in tons	Carbon Density in tons /hectare	Total Uncertainty in tons	Uncertainty in tons /hectare
2001	15014811.36	99.21	21471.18	0.142
2002	14489145.41	95.74	20719.48	0.137
2003	13996215.41	92.48	20014.59	0.132
2004	13553955.76	89.43	19353.56	0.128
2005	13100419.07	86.56	18733.6	0.124
2006	12693801.79	83.88	18152.14	0.120
2007	12312403.15	81.36	17606.74	0.116
2008	11954640.57	78.99	17095.14	0.113
2009	11619023.96	76.78	16615.2	0.110
2010	11304165.97	74.70	16164.96	0.107
2011	11008766.62	72.74	15742.54	0.104
2012	10731613.28	70.91	15346.21	0.101
2013	10471554.97	69.19	14974.32	0.099
2014	10227528.08	67.58	14625.37	0.097
2015	9998535.78	66.07	14297.91	0.094
2016	9783642.90	64.65	13990.61	0.092
2017	9581960.52	63.32	13702.2	0.091
2018	9392681.94	62.06	13431.54	0.089
2019	9215026.13	60.89	13177.49	0.087
2020	9048278.87	59.79	12939.04	0.085
2021	8891756.78	58.75	12715.21	0.084
2022	8744832.99	57.78	12505.11	0.083
2023	8606916.57	56.87	12307.89	0.081
2024	8477442.37	56.02	12122.74	0.080
2025	8355896.51	55.21	11948.93	0.090

Appendix 10: Simulated carbon density and uncertainty under BAU 3% rate from 2015-2025

Time/year	Total Carbon Stock in tons	Carbon Density in tons/hectare	Total Uncertainty in tons	Uncertainty in tons /hectare
2015	9998535.78	66.07	14297.906	0.094
2016	9783642.90	64.65	13990.609	0.092
2017	9581960.52	63.32	13702.204	0.091
2018	9392681.94	62.06	13431.535	0.089
2019	9215026.13	60.89	13177.487	0.087
2020	9048278.87	59.79	12939.039	0.085
2021	8891756.78	58.75	12715.212	0.084
2022	8744832.99	57.78	12505.111	0.083
2023	8606916.57	56.87	12307.891	0.081
2024	8477442.37	56.02	12122.743	0.080
2025	8355896.51	55.21	11948.932	0.079

Appendix 11: Simulated carbon density and uncertainty under REDD+ 2% rate from 2015-2025

| Time/year	Total Carbon Stock in tons	Carbon Density in tons / hectare	Uncertainty in tons	Uncertainty in tons/ hectare
2015	9998535.78	66.07	14297.906	0.094
2016	9883628.57	65.31	14133.589	0.093
2017	9774332.35	64.59	13977.295	0.092
2018	9670390.21	63.90	13828.658	0.091
2019	9571550.38	63.25	13687.317	0.090
2020	9477576.50	62.63	13552.934	0.090
2021	9388232.19	62.04	13425.172	0.089
2022	9303301.67	61.47	13303.721	0.088
2023	9222579.39	60.94	13188.289	0.087
2024	9145854.69	60.43	13078.572	0.086
2025	9072937.45	59.95	12974.301	0.086

Appendix 12: Simulated carbon density and uncertainty under REDD+ 1% rate 2015-2025

Time /year	Total Carbon Stock in tons	Carbon Density in tons /hectare	Uncertainty in tons	Uncertainty in tons /hectare
2015	9998535.78	66.07	14297.906	0.095
2016	9983614.234	65.97	14276.568	0.094
2017	9968702.964	65.87	14255.245	0.094
2018	9953863.63	65.77	14234.025	0.094
2019	9939147.614	65.68	14212.981	0.094
2020	9924590.885	65.58	14192.165	0.094
2021	9910224.272	65.48	14171.621	0.094
2022	9896088.881	65.39	14151.407	0.094
2023	9882205.27	65.30	14131.553	0.093
2024	9868599.12	65.21	14112.097	0.093
2025	9855275.57	65.12	14093.044	0.093

Appendix 13 : Simulated carbon density and uncertainty under REDD+ 0% rate from 2015-2025

Time/year	Total Carbon Stock in tons	Carbon Density in tons/hectare	Uncertainty in tons	Uncertainty in tons /hectare
2015	9998535.78	66.07	14297.906	0.094
2016	10083594.76	66.63	14419.541	0.095
2017	10165062.09	67.17	14536.039	0.096
2018	10243143.30	67.68	14647.695	0.097
2019	10318013.08	68.18	14754.759	0.097
2020	10389835.87	68.65	14857.465	0.098
2021	10458765.81	69.11	14956.035	0.099
2022	10524957.05	69.55	15050.689	0.099
2023	10588532.91	69.97	15141.602	0.100
2024	10649632.12	70.37	15228.974	0.101
2025	10708367.73	70.76	15312.966	0.101

Appendix 14: Probability map depicting favourable area of change from Cropland to the class "Others"
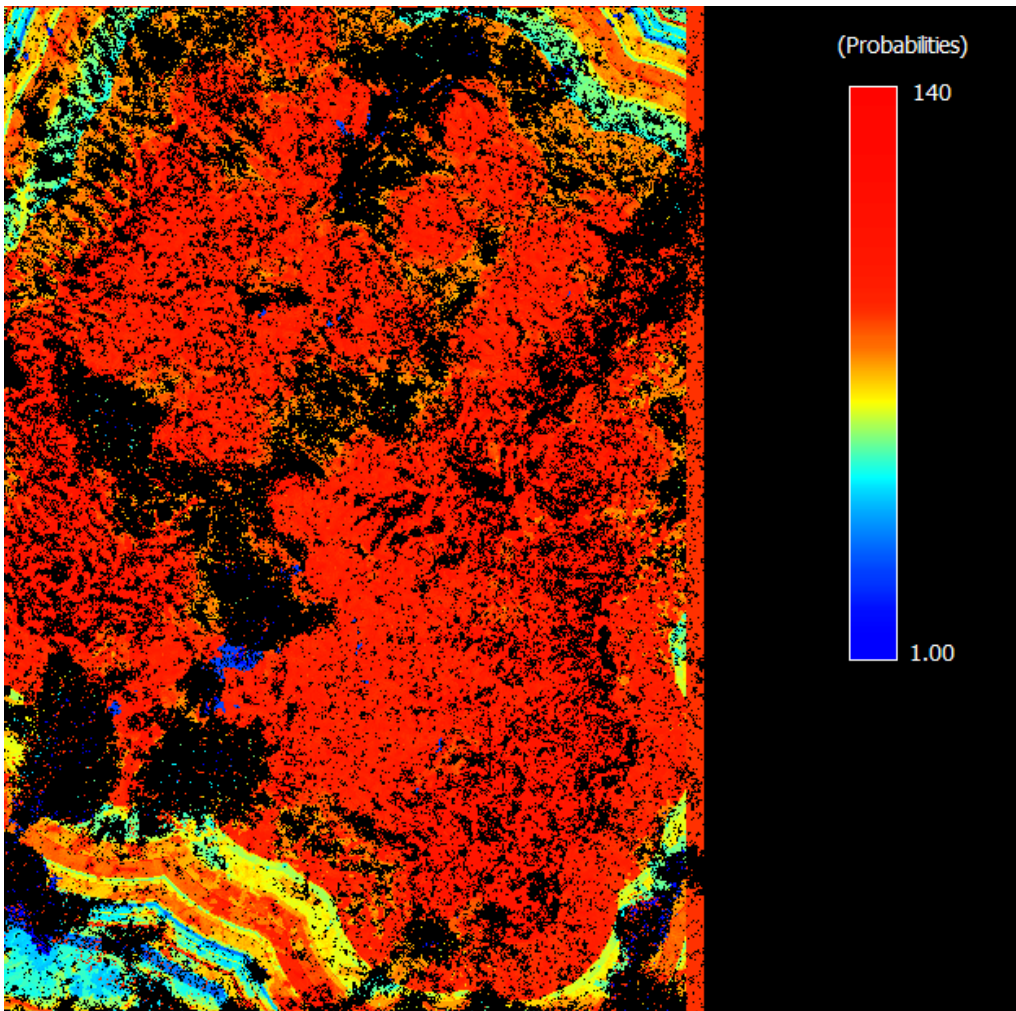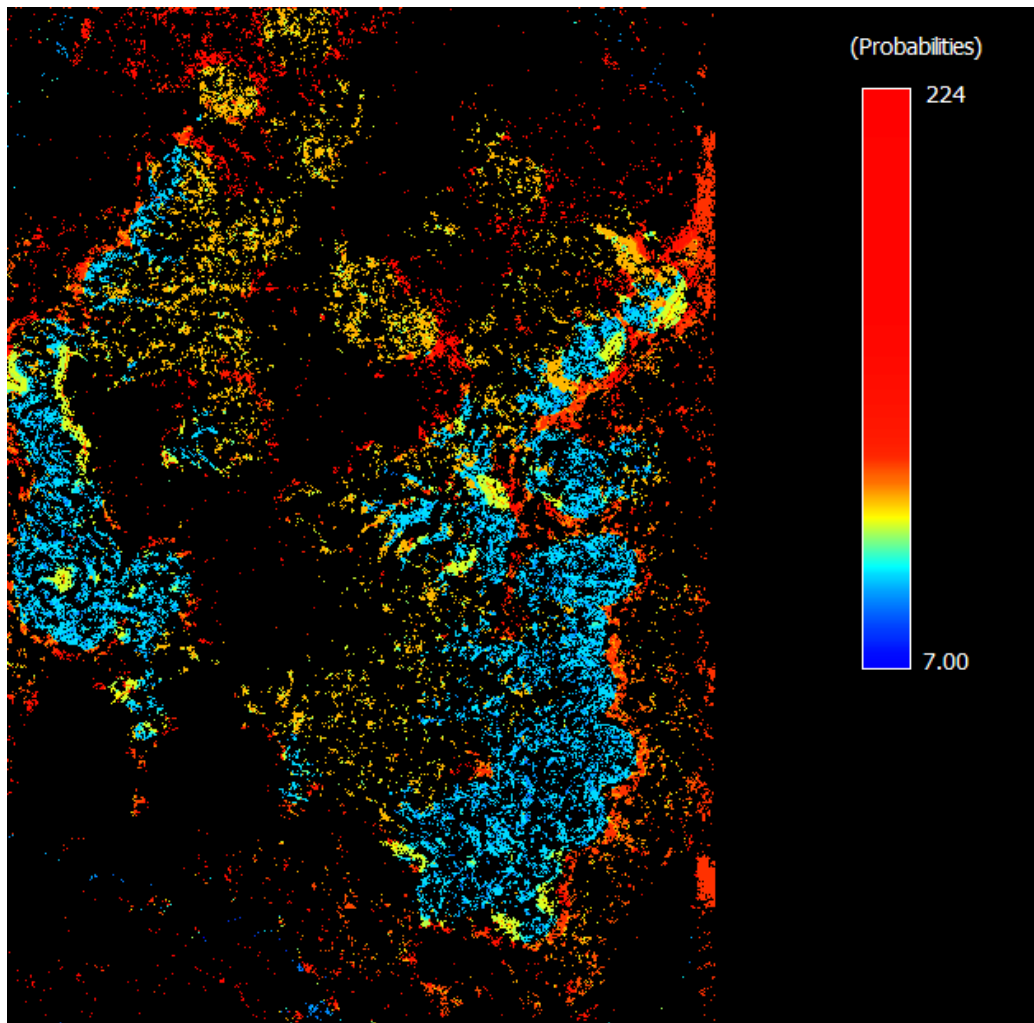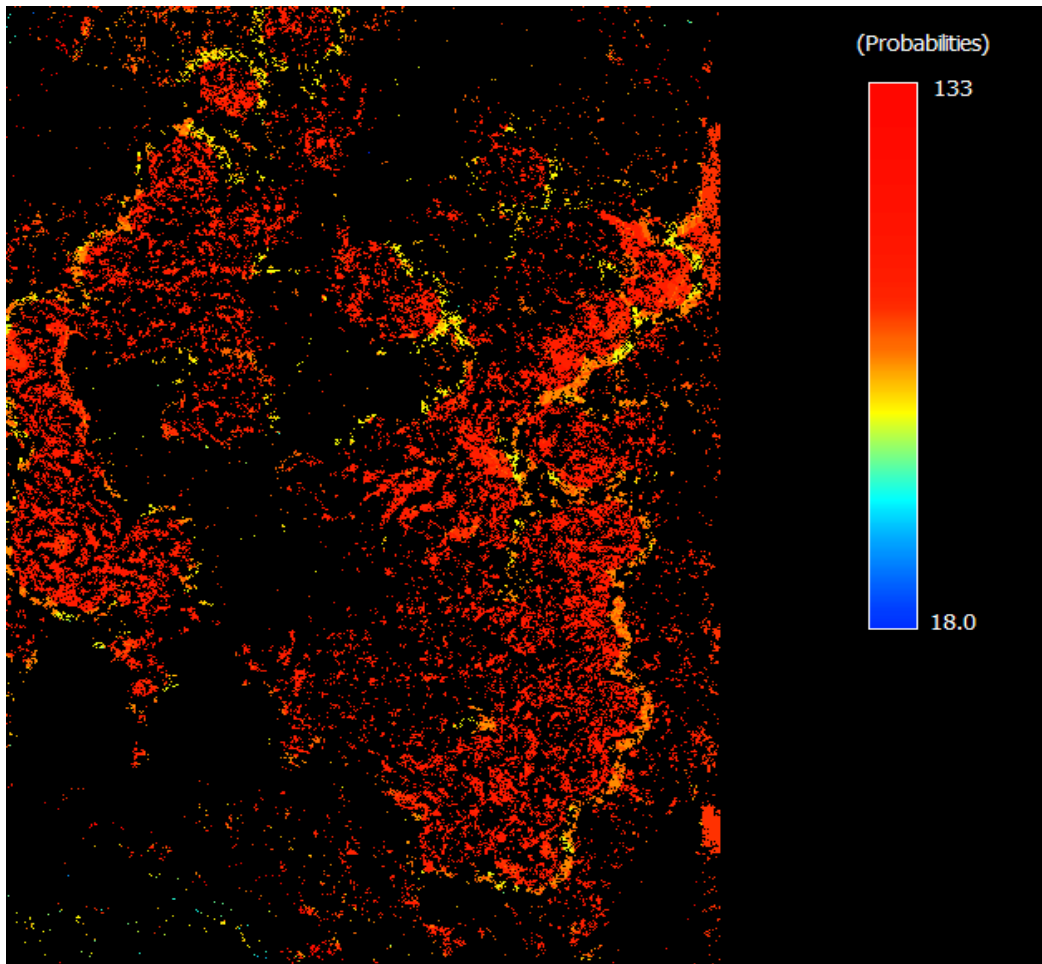

The blue indicates areas with low probability of change, the yellow indicates areas with medium probability of change and the red indicates areas with high probability of change whilst the black is not involved in the analysis.

Appendix 15: Probability map depicting favourable area of change from Cropland to Forest
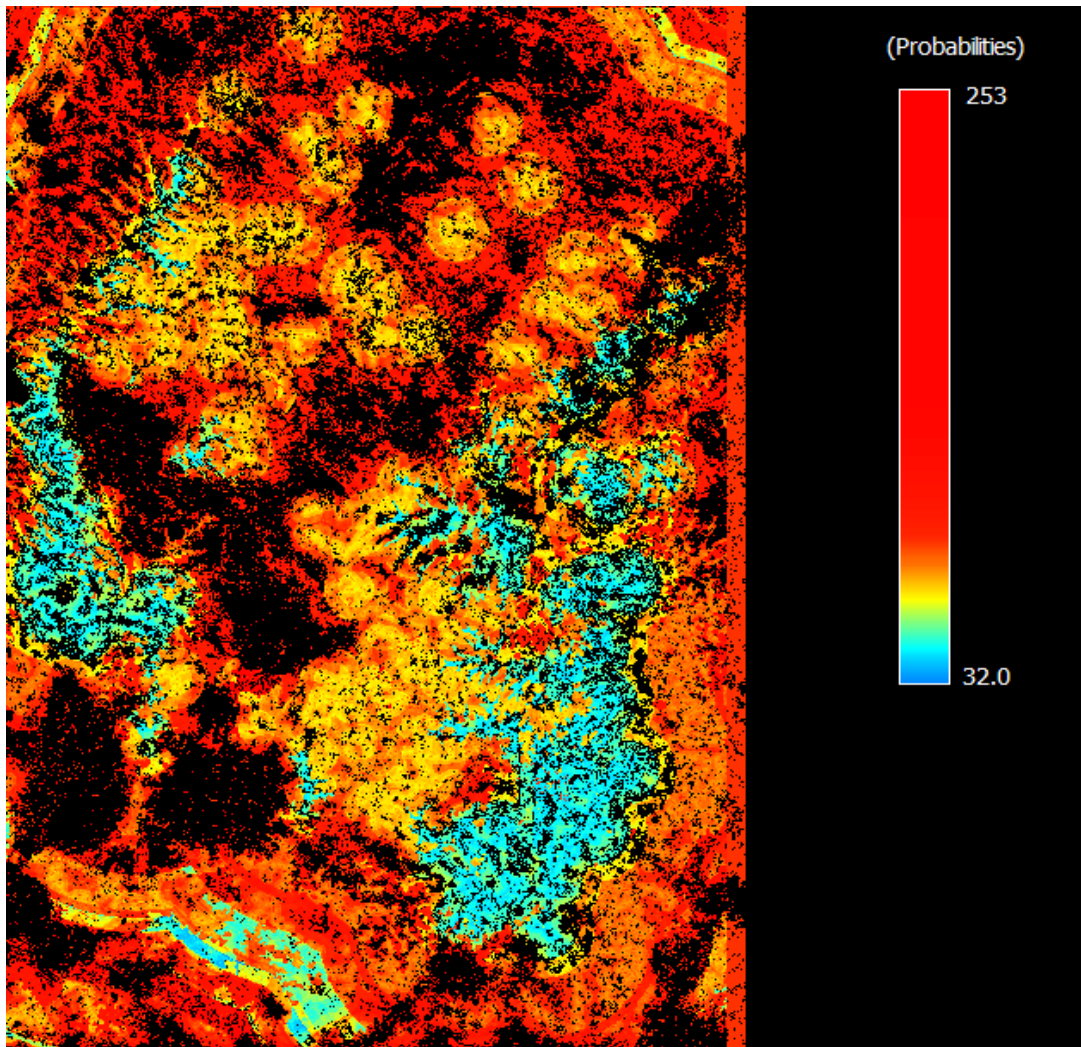
The blue indicates areas with low probability of change, the yellow indicates areas with medium probability of change and the red indicates areas with high probability of change whilst the black is not involved in the analysis.

Appendix 16 : Probability Map depicting favourable area of change from the class "Others" to Forest

The blue indicates areas with low probability of change, the yellow indicates areas with medium probability of change, and the red indicates areas with high probability of change whilst the black is not involved in the analysis.

Appendix 17: Probability Map depicting favourable area of change from the Class "Others" to Cropland

The blue indicates areas with low probability of change, the yellow indicates areas with medium probability of change and the red indicates areas with high probability of change whilst the black is not involved in the analysis.

Appendix 18: Diversity of tree species identified from the field

Local Name	Scientific Name	Number of trees
Afena	*Strombosis pustulata*	6
Akasa	*Chrysophyllum alb.*	2
Akata	*Bombax buonopozense*	9
Akuakuo_Ninsuo	*Spathodea campanulata*	6
Akumaba	*Unknown*	1
Akyere	*Blighia sapida*	4
Apro	*Unknown*	3
Aprofita	*Aprofita*	1
Aprokuma	*Antrocaryon micraster*	6
Atabene	*Chrysophyllum per*	15
Awiemfosamina	*Albizia ferruginea*	1
Beko	*Unknown*	2
Cashew	*Unknown*	1
Celtis zenkeri	*Celtis zenkeri*	1
Dahoma	*Piptadeniastrum africanum*	6
Danta	*Nesogordonia papaverifera*	4
Duasika	*Annickia polycarpa*	1
Dwene	*Unknown*	1
Edinam	*Entandrophragma utile*	11
Emire	*Terminalia ivorensis*	4
Enoko	*Unknown*	1
Esa	*Celtis mildbraedii*	84
Esa_Fufuo	*Unknown*	3

Appendix 19: Diversity of tree species identified from the field (continued)

Local Name	Scientific Name	Number of Trees
Esakosua	Celtis adolfi friederici	13
Esamfra	Pouteria spp	5
Esia	Petersianthus quadrialatus	2
Fotor	Glyphaea brevis	8
Fruntum	Funtumia elastica	8
Hyedua	Daniella ogea	8
Kakapenpen	Rauvolfia vomitoria	4
Koto	Bussea accidentalis	13
Kroma	Klainedoxa gabonesis	2
Kumanyine	Lanea welwitschii	5
Kusia	Nauclea diderrichii	4
Kweku_aduaba	unknown	1
Kyenkyen	Antiaris toxicaria	12
Mahogany	Khaya angolensis	1
Mango	Mangifera indica	1
Nakwa	Holoptela grandis	7
Nwaduaba	Ficus sur	2
Nwama	Ricinodendron heudelotii	3
Nwonekyene	Cleistopholis patens	11
Nyamedua	Alstonia boonei	15
Nyankyere	Ficus exasperata	21
Odum	Milicia excelsa	9
Ofram	Terminalia superba	15
Ohaa	Terminalia oblonga	13
Okoro	Albizia zygia	20
Otwisi	Vitex ferruginea	3
Onyina	Ceiba pentandra	12
Onyinakoben	Rhodognaphalon brevicuspe	3
Opam	Unknown	2

Appendix 20: Diversity of tree species identified from the field (continued)

Local Name	Scientific Name	Number of Trees
Oprono	*Mansonia altissima*	10
Orange	*Citrus*	3
Otia	*Pycananthus angolensis*	6
Pampenama	*Corynanthe pachyceras*	5
Pear	*Persea americana*	1
Pepea	*Maragaritaria discoidea*	2
Sapele	*Entandrophragma cylindricum*	1
Sesramonso	*Unknown*	2
Sesea	*Trema orientalis*	3
Susromasa	*Unknown*	1
Tamatama	*Unkown*	12
Tanuro	*Trichilia monadelpha*	3
Wama	*Ricinodendron heudelotii*	6
Watapuro	*Cola gigantea*	7
Wawa	*Triplochiton scleroxylon*	20
Wawabema	*Sterculia rhinopetala*	3
Woetea	*Unknown*	1
Wonton	*Morus mesozygia*	4
Wotrowotro	*Unknown*	1
Yaya	*Amphimas pterocarpoides*	6
Not given	*Zanthoxylum leprieurii*	1
Unclassified		13

Appendix 21: A typical cropland with felled Trees

Appendix 22: A typical cropland with standing trees

Appendix 23: A typical cocoa plantation with intermingling crown